

## Distribution Agreement

In presenting this thesis or dissertation as a partial fulfillment of the requirements for an advanced degree from Emory University, I hereby grant to Emory University and its agents the non-exclusive license to archive, make accessible, and display my thesis or dissertation in whole or in part in all forms of media, now or hereafter known, including display on the world wide web. I understand that I may select some access restrictions as part of the online submission of this thesis or dissertation. I retain all ownership rights to the copyright of the thesis or dissertation. I also retain the right to use in future works (such as articles or books) all or part of this thesis or dissertation.

Signature:

---

Eric Maltbie

---

Date

**The effects of ketamine on functional brain networks in awake nonhuman primates and the therapeutic potential for treatment of substance abuse**

By **Eric Maltbie**

Doctor of Philosophy

Graduate Division of Biological and Biomedical Sciences  
Neuroscience

---

Leonard L. Howell, Ph.D.

Advisor

---

Jocelyne Bachevalier, Ph.D.

Committee Member

---

Kaundinya Gopinath, Ph.D.

Committee Member

---

Shella Keilholz, Ph.D.

Committee Member

---

Michael Owens, Ph.D.

Committee Member

Accepted:

---

Lisa A. Tedesco, Ph.D.

Dean of the James T. Laney School of Graduate Studies

---

Date

**The effects of ketamine on functional brain networks in awake nonhuman primates and the therapeutic potential for treatment of substance abuse**

By

Eric Maltbie

B.S., University of North Carolina at Chapel Hill

Advisor: Leonard Howell, Ph.D.

An abstract of a dissertation submitted to the Faculty of the James T. Laney School of Graduate Studies of Emory University in partial fulfillment of the requirements for the degree of Doctor of Philosophy in Neuroscience

2017

## **Abstract**

### **The effects of ketamine on functional brain networks in awake nonhuman primates and the therapeutic potential for treatment of substance abuse**

By Eric Maltbie

At present, there is considerable interest in improving the understanding of the unique effects of the N-methyl-D-aspartate (NMDA) glutamate receptor antagonist, ketamine. Sub-anesthetic infusions of ketamine induce acute psychotomimetic effects, but also produce prolonged neurobiological changes with therapeutic efficacy for treating depression in human subjects. However, the underlying mechanisms mediating these effects remain poorly understood. Building on the recent development of methodology allowing for the collection of quality pharmacological MRI (phMRI) data in awake nonhuman primates (NHPs), this dissertation examines the neural circuitry underlying both the psychotomimetic and therapeutic effects of ketamine. Ketamine induced robust and extensive brain activation and strengthened functional connectivity (FC) in several brain networks, including fronto-striatal circuitry known to be disrupted by cocaine. Subsequently, the efficacy of ketamine for the treatment of cocaine abuse was investigated. Ketamine pretreatment attenuated both the effects of cocaine on fronto-striatal (and whole-brain) FC and cocaine-seeking behavior. In conclusion, phMRI in awake NHPs enables valuable, behaviorally relevant translational imaging models. Ketamine increases FC in fronto-striatal circuits responsible for executive control over reward-based decision making and attenuates the effects of cocaine on both FC and behavior. These findings support the therapeutic potential of ketamine in the treatment of substance use disorders.

**The effects of ketamine on functional brain networks in awake nonhuman primates and the therapeutic potential for treatment of substance abuse**

By

Eric Maltbie

B.S., University of North Carolina at Chapel Hill

Advisor: Leonard Howell, Ph.D.

A dissertation submitted to the Faculty of the James T. Laney School of Graduate Studies of Emory University in partial fulfillment of the requirements for the degree of  
Doctor of Philosophy in Neuroscience

2017

## **Acknowledgements**

This dissertation was made possible due to the incredible support and mentorship of my advisor Dr. Leonard Howell. His thoughtful guidance was critical to my intellectual growth and development. I learned more during my few short years of work in the Howell Lab than I ever could have imagined before coming to Emory and I will be forever grateful for the chance to learn from Dr. Howell.

I would also like to thank my committee members for investing time and energy in helping me to design the framework of this dissertation and to critically assess the details of each experiment. I want to thank Dr. Kaundinya Gopinath in particular, for working so closely with me on the original ketamine project and teaching me all of the finer details of image analysis.

I am also thankful for the exceptional research technicians, Marisa Olsen and Juliet Brown, whom I had the privilege to work with in the Howell Lab. I deeply appreciate the impressive surgical skills displayed by Juliet in implanting all of the indwelling catheters and I will never cease to be grateful for having the pleasure to work daily with Marisa to train and scan all of these monkeys. We made a great team.

I also must acknowledge all of my friends in the Emory Neuroscience PhD training program for making the last few years so enjoyable. My lab-mates Dr. Elizabeth Pitts and Dr. Maylen Perez-Diaz and my buddy, and soon to be doctor, Travis Rotterman, will always be among my closest friends.

Finally, I have to thank my family. Without their unwavering support I would never have been in this position.

## **Table of Contents**

---

<b>Chapter 1: Ketamine and pharmacological imaging: use of functional magnetic resonance imaging to evaluate mechanisms of action</b>	<b>1</b>
<b>1.1 Context, Author's Contribution, and Acknowledgement of Reproduction</b>	<b>2</b>
<b>1.2 Abstract</b>	<b>2</b>
<b>1.3 Introduction</b>	<b>3</b>
<i>1.3.1 - Neural Mechanisms</i>	4
<b>1.4 Pharmacological Imaging Methods</b>	<b>6</b>
<i>1.4.1 - Brain Activation</i>	7
<i>1.4.2 - Functional Connectivity</i>	8
<b>1.5 Pharmacological Imaging and the Behavioral Effects of Ketamine</b>	<b>10</b>
<i>1.5.1 - Psychotomimetic effects</i>	10
<i>1.5.2 - Antidepressant effects</i>	19
<b>1.6 Discussion</b>	<b>21</b>
<b>1.7 Future Directions</b>	<b>23</b>
<i>1.7.1 - phMRI and ketamine mechanism of action</i>	23
<i>1.7.2 - phMRI and translational models</i>	25
<b>1.8 Conclusions</b>	<b>27</b>
<b>1.9 Dissertation Overview</b>	<b>28</b>
<b>Chapter 2: Ketamine-induced effects on brain activation in conscious nonhuman primates</b>	<b>35</b>
<b>2.1 Context, Author's Contribution, and Acknowledgement of Reproduction</b>	<b>36</b>
<b>2.2 Abstract</b>	<b>36</b>
<b>2.3 Introduction</b>	<b>37</b>
<b>2.4 Materials and Methods</b>	<b>40</b>
<i>2.4.1 - Subjects</i>	40
<i>2.4.2 - MRI data acquisition</i>	41
<i>2.4.3 - Drug infusion protocols</i>	42

2.4.4 - Pharmacological MRI data analysis	43
2.4.5 - Clinical ratings of behavior	50
<b>2.5 Results</b>	<b>51</b>
2.5.1 - Blood plasma drug levels	51
2.5.2 - Ketamine-induced BOLD activation	51
2.5.3 - Reduction in ketamine-induced activation by risperidone pretreatment	52
2.5.4 - Ketamine-induced effects within a priori ROIs	52
2.5.5 - ROI-averaged Group-mean Time Courses	53
2.5.6 - Clinical ratings of behavior	53
<b>2.6 Discussion</b>	<b>53</b>

## **Chapter 3: Ketamine-induced effects on functional connectivity in conscious nonhuman primates** **69**

<b>3.1 Context, Author's Contribution, and Acknowledgement of Reproduction</b>	<b>70</b>
<b>3.2 Abstract</b>	<b>70</b>
<b>3.3 Introduction</b>	<b>71</b>
<b>3.4 Materials and Methods</b>	<b>74</b>
3.4.1 - Subjects	74
3.4.2 - Drug infusion protocols	75
3.4.3 - fMRI Data Analysis	76
<b>3.5 Results</b>	<b>79</b>
3.5.1 - Blood plasma drug levels	79
3.5.2 - Ketamine-induced changes in FC to dlPFC	79
3.5.3 - Ketamine-induced changes in FC to SgC	80
3.5.4 - Ketamine-induced changes in FC to Amygdala	80
3.5.5 - Ketamine-induced changes in FC to Nucleus Accumbens	81
3.5.6 - Ketamine-induced changes in FC to other ROIs	81
3.5.7 - Ketamine-induced inter-hemispheric asymmetry in FC networks	82
<b>3.6 Discussion</b>	<b>83</b>



3.6.1 - Insights into the results of the ketamine drug infusion	
<i>phMRI study</i>	86
3.6.2 - Limitations	86
<b>3.7 Conclusions</b>	88

**Chapter 4: Effects of ketamine treatment on cocaine-induced changes to functional connectivity in conscious nonhuman primates** 107

<b>4.1 Context, Author's Contribution, and Acknowledgement of Reproduction</b>	108
<b>4.2 Abstract</b>	108
<b>4.3 Introduction</b>	110
<b>4.4 Methods</b>	112
4.4.1 - Subjects	112
4.4.2 - Surgery and habituation to MRI	112
4.4.3 - MRI data acquisition	113
4.4.4 - Drug infusion protocol	113
4.4.5 - fMRI Data Quality Control	114
4.4.6 - Ketamine treatment	114
4.4.7 - fMRI preprocessing and spatial normalization	114
4.4.8 - FC analysis	115
4.4.9 - Data Analysis	116
4.4.10 - Cocaine Self-administration	116
4.4.11 - Experimental timeline	116
<b>4.5 Results</b>	117
4.5.1 - Acute cocaine administration robustly decreased FC	117
4.5.2 - Ketamine pretreatment attenuated cocaine-induced changes in FC	118
4.5.3 - The effects of cocaine on FC predicted response rates during self-administration	119
4.5.4 - Chronic cocaine self-administration robustly decreased FC	119
4.5.5 - Acute effects of cocaine on FC following chronic self-administration	120

4.5.6 - <i>Effects of ketamine pretreatment on FC after self-administration</i>	121
4.5.7 - <i>Individual subject results for dlPFC-NAcc FC</i>	122
<b>4.6 Discussion</b>	<b>123</b>
4.6.1 - <i>Limitations</i>	126
<b>4.7 Conclusions</b>	<b>127</b>
<b>Chapter 5: Investigating the effects of ketamine treatment on reinstatement and reacquisition of cocaine self-administration in rhesus monkeys</b>	<b>138</b>
<b>5.1 Context, Author's Contribution, and Acknowledgement of Reproduction</b>	<b>139</b>
<b>5.2 Abstract</b>	<b>139</b>
<b>5.3 Introduction</b>	<b>140</b>
<b>5.4 Methods</b>	<b>142</b>
5.4.1 - <i>Subjects</i>	142
5.4.2 - <i>Surgery</i>	142
5.4.3 - <i>Cocaine self-administration</i>	143
5.4.4 - <i>Ketamine treatment</i>	144
5.4.5 - <i>Reinstatement</i>	144
5.4.6 - <i>Reacquisition</i>	145
5.4.7 - <i>Data analysis</i>	146
<b>5.5 Results</b>	<b>146</b>
5.5.1 - <i>Self-administration</i>	146
5.5.2 - <i>Reinstatement</i>	147
5.5.3 - <i>Reacquisition</i>	148
<b>5.6 Discussion</b>	<b>149</b>
<b>Chapter 6: Clinical use of ketamine, future directions, and limitations</b>	<b>158</b>
<b>6.1 - Results Summary</b>	<b>159</b>
<b>6.2 - Clinical use of sub-anesthetic ketamine treatment</b>	<b>163</b>
<b>6.3 - Future directions for translational models using phMRI in awake NHPs</b>	<b>164</b>

<b>6.4 - Limitations</b>	165
<b>6.5 - Conclusions</b>	167

<b>Appendix: Complete list of publications to which the author has contributed during his graduate training</b>	<b>168</b>
---	------------

<b>References</b>	<b>169</b>
-------------------	------------

## **Index of Tables and Figures**

---

**Table 1-1** \_\_\_\_\_ 31

**Table 1-2** \_\_\_\_\_ 32

**Figure 1-1** \_\_\_\_\_ 34

---

**Table 2-1** \_\_\_\_\_ 59

**Table 2-2** \_\_\_\_\_ 60

**Table 2-3** \_\_\_\_\_ 61

**Table 2-4** \_\_\_\_\_ 63

**Figure 2-1** \_\_\_\_\_ 65

**Figure 2-2** \_\_\_\_\_ 66

**Figure 2-3** \_\_\_\_\_ 67

**Figure 2-4** \_\_\_\_\_ 68

---

**Table 3-1** \_\_\_\_\_ 89

**Table 3-2** \_\_\_\_\_ 93

**Figure 3-1** \_\_\_\_\_ 97

**Figure 3-2** \_\_\_\_\_ 98

**Figure 3-3** \_\_\_\_\_ 99

**Figure 3-4** \_\_\_\_\_ 100

**Figure 3-5** \_\_\_\_\_ 101

**Figure 3-6** \_\_\_\_\_ 102

**Figure 3-7** \_\_\_\_\_ 103

**Figure 3-8** \_\_\_\_\_ 104

**Figure 3-9** \_\_\_\_\_ 105

**Figure 3-10** \_\_\_\_\_ 106

---

**Table 4-1** \_\_\_\_\_ 129

**Table 4-2** \_\_\_\_\_ 130

**Figure 4-1** \_\_\_\_\_ 131

**Figure 4-2** \_\_\_\_\_ 132

**Figure 4-3** \_\_\_\_\_ 133

**Figure 4-4** \_\_\_\_\_ 134

**Figure 4-5** \_\_\_\_\_ 135

**Figure 4-6** \_\_\_\_\_ 136

**Figure 4-7** \_\_\_\_\_ 137

---

**Table 5-1** \_\_\_\_\_ 153

**Table 5-2** \_\_\_\_\_ 154

**Figure 5-1** \_\_\_\_\_ 155

**Figure 5-2** \_\_\_\_\_ 156

**Figure 5-3** \_\_\_\_\_ 157

---

**Chapter 1: Ketamine and pharmacological imaging: use of functional magnetic resonance imaging to evaluate mechanisms of action**

## **1.1 Context, Author's Contribution, and Acknowledgement of Reproduction**

The following introductory chapter provides background on ketamine and the pharmacological imaging methods used in this dissertation, and reviews the current literature on the study of ketamine using pharmacological imaging methods. The review highlights the studies that provide the rationale for investigating the therapeutic potential of ketamine as a treatment for cocaine abuse. Under the guidance of Dr. Leonard Howell and with the help of substantive advice from Dr. Kaundinya Gopinath, the dissertation author designed, researched, and wrote this, now published, review. The chapter is reproduced with minor edits from:

Maltbie E, Gopinath K, Howell L (2017). Ketamine and pharmacological imaging: use of functional magnetic resonance imaging to evaluate mechanisms of action. *Behavioural Pharmacology*. Epub ahead of print.

## **1.2 Abstract**

**Rationale:** Ketamine has been used as a pharmacological model for schizophrenia as sub-anesthetic infusions have been shown to produce temporary schizophrenia-like symptoms in healthy humans. More recently, ketamine has emerged as a potential treatment for multiple psychiatric disorders, including treatment-resistant depression and suicidal ideation. However, the mechanisms underlying both the psychotomimetic and therapeutic effects of ketamine remain poorly understood.

**Objective:** This review provides an overview of what is known of the neural mechanisms underlying the effects of ketamine and details what pharmacological magnetic resonance imaging studies have revealed at a systems-level focused on brain circuitry.

**Results:** Multiple analytic approaches show that ketamine produces robust and consistent effects at the whole-brain level. These effects are highly conserved across human and nonhuman primates, validating the use of nonhuman primate models for further investigations with ketamine. Regional analysis of brain functional connectivity suggests that the therapeutic potential of ketamine may be derived from a strengthening of executive control circuitry.

**Conclusions:** There are still important questions about ketamine's mechanism of action and therapeutic potential that can be addressed using appropriate pharmacological neuroimaging techniques. The unique effects of ketamine make it an intriguing candidate for the treatment of drug abuse.

### **1.3 Introduction**

Ketamine is a non-competitive N-methyl-D-aspartate (NMDA) glutamate receptor antagonist with a complex profile of pharmacological effects that has made it an important target in biomedical and neuroscience research. High doses of ketamine have long been used medically to produce anesthesia (Haas and Harper, 1992) and the recreational use of ketamine as a dissociative drug of abuse has a lengthy history as well (Lodge and Mercier, 2015). For the past two and a half decades, ketamine has been used as a pharmacological model for schizophrenia as sub-anesthetic doses have been shown to produce temporary schizophrenia-like symptoms in healthy humans (Krystal et al., 1994; Olney and Farber, 1995). In rodents and nonhuman primates, sub-anesthetic doses of ketamine induce deficits in the startle response and working memory that have translational relevance to schizophrenia (Skoblenick and Everling, 2012; Verma and Moghaddam, 1996; Yang et al., 2010). While ketamine can be administered through



several routes, including intramuscular, intranasal and oral, most investigations have utilized intravenous infusions due to the precise dosing and ability to adjust rapidly if unwanted side effects occur. The strength of these models has helped lead to new hypotheses of glutamatergic system dysfunction in schizophrenia (Frohlich and Van Horn, 2014).

In addition to its utility for modeling schizophrenia, ketamine has emerged as a potential treatment for multiple psychiatric disorders. Sub-anesthetic doses of ketamine in the same range as those used for modeling schizophrenia have shown efficacy for treating postoperative pain (Schmid et al., 1999), neuropathic pain (Schwartzman et al., 2009), treatment-resistant depression (Berman et al., 2000; Krystal et al., 2013), and suicidal ideation (Ballard et al., 2014; Price and Mathew, 2015). Indeed, the rapid onset of improvement in suicidal ideation induced by ketamine, reported to emerge as quickly as 40 minutes post-infusion (DiazGranados et al., 2010), provides a major advantage for treating this psychiatric emergency as other effective treatments are slower acting (Reinstatler and Youssef, 2015). Ketamine also exerts rapid antidepressant effects in treatment resistant depression with peak response reported within 24 hours after a single sub-anesthetic dose (Murrough et al., 2013; Zarate et al., 2006). Additionally, recent studies have begun to investigate the potential use of ketamine as a treatment for psychostimulant abuse (Dakwar et al., 2016; Dakwar et al., 2014).

### 1.3.1 Neural Mechanisms

The discovery of the remarkable behavioral effects of sub-anesthetic ketamine has led to a great deal of research investigating its underlying neural mechanisms. High doses of ketamine result in general suppression of the central nervous system and produce general

anesthesia (**Table 1-1**). However, at sub-anesthetic doses that produce psychotomimetic and rapid antidepressant effects (**Table 1-1**), ketamine administration leads to enhancement of excitatory glutamatergic transmission (Duncan et al., 1998; Moghaddam et al., 1997). There is growing evidence that sub-anesthetic doses of ketamine predominantly block the NMDA receptors on inhibitory interneurons (Homayoun and Moghaddam, 2007; Wang et al., 2013), resulting in a disinhibition of excitatory projection neurons (Maeng et al., 2008). The reason for ketamine to primarily inhibit interneurons remains unknown. It has been proposed that the tonic firing pattern displayed by many cortical interneurons likely removes the magnesium block from NMDA receptors, allowing ketamine to block the channel. Meanwhile, burst firing pyramidal neurons likely spend more time in magnesium block, reducing the probability that ketamine will block NMDA receptor channels on these excitatory neurons (Wang and Gao, 2009; Wang and Gao, 2012).

Ketamine-induced enhancement of glutamatergic function can have significant downstream effects on mesocortical and mesolimbic dopamine pathways (Adams and Moghaddam, 1998; Lorrain et al., 2003; Moghaddam et al., 1997; Vollenweider et al., 2000). Specifically, there is evidence that disinhibition of pyramidal projection neurons in the prefrontal cortex leads to downstream activation of dopaminergic neurons (Carr and Sesack, 2000; Del Arco et al., 2008; Takahata and Moghaddam, 2003). Moreover, sub-anesthetic ketamine infusions increase blood flow and metabolic activity in the prefrontal cortex, striatum and thalamus (Holcomb et al., 2001; Vollenweider et al., 1997) and these effects correlate with the emergence of dissociative and schizophrenia-like symptoms (Driesen et al., 2013a; Holcomb et al., 2001; Vollenweider et al., 1997). Thus,

while sub-anesthetic ketamine induces excitation in many brain areas, its effects on prefrontal circuitry may be of particular importance for the induction of psychotomimetic and antidepressant effects (Arnsten et al., 2012; Del Arco and Mora, 2009; Opler et al., 2016). In this regard, the homology of the human prefrontal cortex to that of other primates (Phillips et al., 2014) might add significant translational value to the use of nonhuman primate models for investigating the effects of ketamine. Indeed, even the micro-circuitry within the prefrontal cortex appears to be well conserved across human and nonhuman primates with NMDA receptors playing an important role in local processing that may not be present in rodents (Wang and Arnsten, 2015). Accordingly, the current review focuses on pharmacological imaging and ketamine effects on brain circuitry with an emphasis on human and nonhuman primate studies.

#### **1.4 Pharmacological Imaging Methods**

The neuronal signaling changes induced by administration of sub-anesthetic ketamine can be measured using pharmacological magnetic resonance imaging (phMRI). Increases in neuronal signaling lead to increases in metabolic rate as well as cerebral blood flow (CBF) to deliver more oxygen and glucose to meet the increased demand. The increases to CBF and anaerobic glucose metabolism are greater than the increase in oxidative metabolic rate (Fox et al., 1988), leading to a higher blood oxygen concentration and resultant changes in the blood-oxygenation-level dependent (BOLD) signal (Simon and Buxton, 2015). Measurement of the BOLD signal is utilized in phMRI to quantify the effects of drugs on neuronal signaling (Leslie and James, 2000). Previous work has shown that during sub-anesthetic infusion of ketamine, increases to regional CBF (Langsjo et al., 2003) remain coupled with increases to regional glucose metabolic rate (Langsjo et al.,

2004). This provides strong evidence that ketamine-induced changes to the BOLD signal accurately reflect underlying changes to neuronal signaling, making phMRI an effective tool for measuring the effects of ketamine on neural networks in the brain. Indeed, phMRI is particularly well-suited for investigating the effects of ketamine at the regional and network level given its high spatial and temporal resolution compared to other whole-brain imaging modalities such as positron emission tomography (PET) and single-photon emission computed tomography (SPECT) (Buxton, 2002). This review will discuss key findings from phMRI studies that have contributed to understanding the effects of ketamine on brain function at the whole-brain, regional, and network levels. All of the phMRI studies reviewed (**Table 2-1**) utilized measurements of BOLD signal, however, multiple data analysis methods were employed. Brain activation studies examined regional changes in neuronal firing induced by ketamine, while functional connectivity studies examined changes to functional connections between discrete brain regions.

#### 1.4.1 Brain activation

Several studies have used phMRI to characterize regional changes in neuronal activity induced by sub-anesthetic ketamine infusion by measuring the BOLD activation response. Data acquisition begins prior to the administration of ketamine to establish a baseline signal and continues for at least several minutes beyond the start of ketamine infusion. Various ketamine infusion protocols have been used (**Table 1-2**) in human (Deakin et al., 2008), nonhuman primate (Maltbie et al., 2016), and rat (Chin et al., 2011) studies with each showing a significant ketamine-induced BOLD-response that appears to be proportional to the ketamine dose (De Simoni et al., 2013) and highly robust across species (Maltbie et al., 2016). Sub-anesthetic ketamine induces a reliable pattern of

regional increases in BOLD signal indicative of neuronal excitation, which is consistent with the ketamine-induced increases observed in regional glucose metabolism (Duncan et al., 1998; Langsjo et al., 2004). This acute regional BOLD-response to sub-anesthetic ketamine may be linked to ketamine's psychotomimetic effects.

#### 1.4.2 Functional connectivity

The BOLD signal exhibits spontaneous fluctuations associated with temporal patterns of neuronal network activity during rest. Correlations in these spontaneous signal fluctuations between discrete regions are termed functional connectivity and are thought to underlie communication within brain networks (Fox et al., 2005). Functional connectivity has been used in many different clinical applications (Fox and Greicius, 2010), including studies to evaluate the effects of sub-anesthetic ketamine. Functional connectivity analysis can offer some advantages compared to brain activation studies. Meaningful dynamic alterations in the strength of coupling between discrete regions may be independent from any corresponding increases in overall signal strength (Buckner et al., 2013), and network connectivity patterns within individual subjects are highly consistent across scanning sessions (Braga and Buckner, 2017). This allows for quantitative resting-state comparisons between different scanning sessions that are not possible using BOLD activation, such as the investigation of sub-anesthetic ketamine treatment for major depressive disorder (Abdallah et al., 2016). Although there are many different ways to perform functional connectivity analysis, the two types of functional connectivity analysis that have been most commonly used to study the effects of ketamine infusion are seed-based analysis and global brain connectivity (GBC).

#### *Seed-based functional connectivity*

Seed-based functional connectivity analysis utilizes a region-of-interest approach to calculate functional connectivity between specific regions. This technique compares the average time course of the BOLD signal within a specified seed region with the BOLD time course of every brain voxel outside of the seed region (or within a specified target region) usually by means of the cross-correlation coefficient (CC) between respective time courses (Fox and Raichle, 2007). This is the most common type of functional connectivity analysis used for determining brain networks. Changes to seed-based functional connectivity observed during acute ketamine administration (Dandash et al., 2015; Gopinath et al., 2016) may be related to psychotomimetic effects, while persistent changes observed 24-hours post-infusion (Abdallah et al., 2016; Lv et al., 2016) may be more closely related to antidepressant effects.

### *Global brain connectivity*

GBC is a measure of how connected a given brain area is to every other area in the brain. High values of GBC (at rest) occur in brain areas that are involved in many different brain functions, and are hence connected with multiple brain networks or are strongly connected to most of the other brain regions within one network. GBC is calculated by taking the average correlation between the BOLD time course in a given voxel and the BOLD time course of every other voxel in the brain (Cole et al., 2010). GBC can also be compartmentalized to global connectivity within large brain areas (e.g. frontal cortex) as done by Anticevic et al. (2015). Alterations in GBC have been associated with both schizophrenia (Cole et al., 2011) and acute ketamine administration (Driesen et al., 2013a) and have been investigated in relation to the psychotomimetic effects of ketamine infusion. Further, Abdallah et al. (2016) observed alterations in GBC in subjects with

major depressive disorder that were normalized 24-hours after ketamine infusion in responders.

### *Other functional connectivity analysis methods*

Independent component analysis and graph network analysis (Joules et al., 2015; Lv et al., 2016) have also been used to investigate the effects of sub-anesthetic ketamine. These analysis methods use algorithms to automatically segment the brain into intrinsic, functionally connected networks (Braga and Buckner, 2017). This allows for data-driven investigation of functional brain networks, which has both advantages and disadvantages compared to more directly hypothesis driven methods (Buckner et al., 2013). At present, there is smaller body of literature utilizing these methods, making them more difficult to correlate with the behavioral effects of ketamine.

## **1.5 Pharmacological Imaging and the Behavioral Effects of Ketamine**

### 1.5.1 Psychotomimetic effects

Several pHMRI studies have investigated associations between the changes to neuronal signaling and changes to subjective ratings of behavior induced by ketamine. Various subjective ratings scales have been utilized for this purpose. In order to measure psychosis-like symptoms, the Brief Psychiatric Rating Scale (BPRS) (Kopelowicz et al., 2008), Rating Scale for Psychotic Symptoms (RSPS) (Chouinard and Miller, 1999), Psychotomimetic States Inventory (PSI) (Mason et al., 2008), and positive dimension of the Positive and Negative Syndrome Scale (PANSS) (Kay et al., 1987) have been employed. Meanwhile, the negative dimension of PANSS (Kay et al., 1987) has been used to measure the schizophrenia-like blunted affect and social withdrawal, and the Clinician

Administered Dissociative States Scale (CADSS) (Bremner et al., 1998) has been used to assess the dissociative symptoms evoked by ketamine.

### *Brain activation*

Deakin et al. (2008) were the first to examine the effects of sub-anesthetic ketamine infusion on BOLD activation (in healthy control subjects). They found an extensive cortical BOLD signal response with peak signal changes occurring 3-5 minutes after the start of infusion in all regions. This timing corresponds very well with the peak ketamine concentration in the blood, and with the onset of behavioral effects (see below). BOLD activation was quite extensive, with multiple frontal, parietal, temporal, and limbic regions showing increased signal. However, when subjects were pretreated with the sodium channel blocker lamotrigine to reduce enhancement of glutamate release, there was significant attenuation of ketamine-induced BOLD activation throughout the brain. This provides evidence that enhancement of glutamatergic signaling is involved in the BOLD-response to ketamine and agrees with previous work showing that the behavioral effects of ketamine can also be attenuated by lamotrigine (Anand et al., 2000).

Deakin et al. (2008) further found several regions in which changes in BOLD were correlated with ratings of dissociative state (CADSS) or psychotic symptoms (BPRS), thus establishing the relevance of BOLD activation to the psychotomimetic effects of ketamine. Deactivation in the subgenual cingulate and medial orbitofrontal cortex (OFC) was correlated with increased CADSS ratings in the subjects, while deactivation in the medial OFC also correlated with increases in both CADSS ratings and BPRS ratings for psychosis. Activation of the posterior cingulate cortex and frontal pole (BA10) were also correlated with increased BPRS ratings, but not CADSS ratings.



The test-retest reliability of ketamine-induced BOLD activation was later established by De Simoni et al. (2013). They found the BOLD response to ketamine to be very robust, featuring a consistent magnitude and time course across different sessions, and both within and across healthy control subjects. Further, De Simoni et al. (2013) investigated the dose dependence of ketamine-induced BOLD activation and found that a higher dose (producing a 75 ng/mL ketamine blood serum concentration compared to 50 ng/mL at the lower dose) of ketamine corresponded to greater changes in BOLD signal and greater effect sizes. However, a full ketamine dose-response function has yet to be established with BOLD activation. While De Simoni et al. (2013) also collected behavioral ratings for psychotomimetic (PSI) and dissociative states (CADSS), they did not find any correlations with BOLD activation. They infer that the lack of correlation with behavior may be due to the low doses they were using for the ketamine infusion. Indeed, the higher of their two doses only produced an average plasma concentration of 73 ng/mL, a concentration that is on the low end of what has been used in pHMRI studies of ketamine (**Table 1-2**). Despite the low dosing, they still found robust BOLD activation, indicating pHMRI is highly sensitive to the effects of ketamine.

Doyle et al. (2013) were the first to test the interaction of an antipsychotic drug with the ketamine-induced BOLD response. They evaluated pretreatment with risperidone or lamotrigine on ketamine-induced brain activation in healthy control subjects. Clinically, risperidone is one of the most commonly prescribed antipsychotics, featuring similar efficacy and tolerability to other second-generation (“atypical”) antipsychotics used for the treatment of schizophrenia (Komossa et al., 2011). Risperidone is an antagonist at both dopamine D2 and serotonin 5-HT<sub>2A</sub> receptors, but with no affinity for any

glutamate receptor (Muly et al., 2012). Doyle et al. (2013) showed that risperidone attenuated the BOLD response to ketamine globally, blunting signal changes in frontal, insular, striatal, and thalamic regions. Despite this attenuation, ketamine still induced significant BOLD activation compared to saline in each of these areas following risperidone pretreatment. The magnitude of the activation was simply reduced. This indicates that glutamatergic signaling is not the only pathway involved in the BOLD response to ketamine and that dopamine D2 and serotonin 5-HT<sub>2A</sub> receptors may also be involved. Among these alternatives, 5-HT<sub>2A</sub> receptors are a more likely candidate in attenuating the effects of ketamine, given that the dopamine D2 antagonist haloperidol was ineffective in preventing the psychotomimetic effects of ketamine (Krystal et al., 1999). Note that neurons expressing 5-HT<sub>2A</sub> in the prefrontal cortex project to the ventral tegmental area and local antagonism of these receptors blocks dopamine overflow in the prefrontal cortex (Bortolozzi et al., 2005). Hence, 5-HT<sub>2A</sub> receptors are well positioned anatomically to modulate the psychotomimetic effects of ketamine.

Preclinical animal studies have also used phMRI to characterize the effects of ketamine on brain activation. Careful consideration is required for designing phMRI studies in animals (Steward et al., 2005). In particular, drugs used to anesthetize the animals may interact with the compound of interest (Haensel et al., 2015), as seen with both ketamine (Hodkinson et al., 2012) and phenylcyclidine (Gozzi et al., 2008). These complications can make studies in anesthetized animals difficult to interpret. However, methods have been developed for performing phMRI in awake rodents (King et al., 2005). Chin et al. (2011) studied ketamine-evoked BOLD activation in awake rats and found extensive activation in the cortex and hippocampus. This result aligns well with observations

reported in human subjects, indicating ketamine-induced BOLD activation is well conserved across species. Indeed, further preclinical phMRI studies could prove invaluable, particularly when conducted in awake subjects.

Given the homology of the human prefrontal cortex to that of other primates (Preuss, 1995; Wang and Arnsten, 2015), nonhuman primates provide a more translational model for studying the BOLD response to ketamine. Importantly, methods have been developed that enable rhesus monkeys to undergo MRI scanning without the use of anesthesia and with minimal restraint stress (Murnane and Howell, 2010). A recent study has shown that awake rhesus monkeys display ketamine-induced BOLD activation (Maltbie et al., 2016) that corresponds closely in both magnitude and extent to what has been reported in humans (De Simoni et al., 2013; Deakin et al., 2008; Doyle et al., 2013). Moreover, pretreatment with risperidone attenuated the ketamine-induced changes in BOLD in rhesus monkeys (Maltbie et al., 2016), again to a similar extent as reported in humans (Doyle et al., 2013). These data suggest that the pharmacological effects of ketamine are well conserved across species and attests to the validity of using ketamine in nonhuman primates as an animal model for schizophrenia, and as a potential model for evaluating novel antipsychotics.

### *Global brain connectivity*

Functional connectivity has been shown reliably to be disrupted in schizophrenia (Guo et al., 2013; Meyer-Lindenberg et al., 2001; Meyer-Lindenberg et al., 2005; Rotarska-Jagiela et al., 2010; Woodward et al., 2011). Further, there is evidence that functional connectivity may predict response to treatment with antipsychotics (Sarpal et al., 2016)

and that functional connectivity changes are correlated with alleviation of symptoms following successful treatment (Sarpal et al., 2015).

The first paper to use functional connectivity analysis to study ketamine infusion was published by Driesen et al. (2013a). They examined the effects of ketamine on GBC in healthy control subjects. Ketamine infusion increased the GBC of voxels throughout the brain, illustrating a global increase in functional connectivity. This finding is consistent with coherent neural activity across the brain seen during psychosis (Hakami et al., 2009; Wood et al., 2012). Additionally, Driesen et al. (2013a) found many brain regions (they reported several significant clusters including one extending from the OFC to the cerebellum) in which increased GBC correlated with increased positive schizophrenia symptom scores (PANSS), implying that increased connectivity in many brain networks is associated with the psychotomimetic effects of ketamine. However, they found that stable or reduced GBC in the dorsal and medial anterior striatum was correlated with increased negative psychotomimetic symptoms (PANSS).

Anticevic et al. (2015) compared the effects of ketamine in healthy control subjects to baseline measures from schizophrenic patients at different stages of treatment. They utilized a variant of GBC in which only voxels within the prefrontal cortex were considered. The restricted GBC was shown to increase after ketamine administration and this prefrontal-specific GBC was also significantly elevated in patients who were within one-year of the onset of schizophrenia symptoms. This finding may suggest that elevated functional connectivity in the prefrontal cortex could be a biomarker for schizophrenia. However, other than benefitting from decreased processing time, it is unclear why GBC should be restricted to prefrontal regions. Even if prefrontal regions are of primary

interest, these areas receive inputs from many other brain areas outside the prefrontal cortex and are part of highly integrative brain circuits (Arnsten et al., 2012; Del Arco and Mora, 2009). Furthermore, Anticevic et al. (2015) performed global signal regression to remove the average brain signal from every voxel in the brain. Given that ketamine increases global signal, as reported previously, the effects of this regression will be different for ketamine than for baseline or vehicle conditions and could confound any between-condition comparisons (Saad et al., 2012). Thus, while the results of this study are intriguing, they are somewhat difficult to interpret.

Recent studies in awake rhesus monkeys has demonstrated that ketamine-induced changes in functional connectivity are also well conserved across primate species (Gopinath et al., 2016). GBC analysis (**Figure 1-1**) shows that ketamine causes global hyperconnectivity in rhesus monkeys that is similar in both magnitude and regional pattern to what Driesen et al. (2013a) observed in human subjects. Thus, there are data from multiple imaging modalities documenting that nonhuman primates provide a highly translational model for evaluating the effects of ketamine on brain function.

Joules et al. (2015) investigated the effects of sub-anesthetic ketamine infusion on whole-brain functional connectivity in healthy control subjects using a graph theory analysis. The measures of whole-brain connectedness they considered are similar to GBC but, rather than being calculated on every voxel, they are calculated between anatomical regions within a whole-brain parcellation map. Joules et al. (2015) found a shift in whole-brain functional connectivity with ketamine infusion that is consistent with the reported increase in GBC (Driesen et al., 2013a). They further showed that a pattern recognition algorithm could be used consistently to classify the pattern of functional connectivity

induced by ketamine infusion as different than placebo infusion. This finding demonstrates the robustness of the effects of ketamine infusion on whole-brain functional connectivity.

### *Seed-based functional connectivity*

In addition to their GBC study, Driesen et al. (2013b) conducted an investigation in healthy control subjects of the effects of ketamine on functional connectivity to a seed region in the dorsolateral prefrontal cortex (dlPFC). The dlPFC is a region strongly implicated in schizophrenia because of its important role in working memory (Wang et al., 2013) and the group hypothesized that ketamine-induced changes in connectivity to the dlPFC would be associated with impaired performance on a working memory task. Unfortunately, they used a global signal regression that may have confounded their results for the reasons mentioned previously. Accordingly, while they found that ketamine reduced connectivity to the dlPFC seed, this possibly resulted from a greater impact of global signal regression under the ketamine condition than the control condition.

Dandash et al. (2015) used a regional seed-based analysis with seeds placed in the dorsal and ventral putamen, dorsal caudate, and nucleus accumbens. They reported that functional connectivity to the striatum was enhanced in healthy control subjects. While they did not find differences in connectivity to the putamen, they found increased connectivity from the midbrain and thalamus to the dorsal caudate and from the ventromedial prefrontal cortex to the nucleus accumbens. These results may have been limited by relatively low and highly variable ketamine plasma levels ( $68.6 \pm 43.6$  ng/ml) producing less robust drug effects. Nevertheless, they found that increases in connectivity between the medial prefrontal cortex and ventral striatum were correlated with ratings of

both psychosis-like behavior (RSPS) and dissociative state (CADSS). Further, they found that increases in connectivity between the midbrain and dorsal caudate were associated with increases in ratings of positive schizophrenia symptoms (BPRS) while the observed increases in connectivity between the ventrolateral thalamus and dorsal caudate were associated with *lower* ratings of psychosis (RSPS) and dissociative state (CADSS). The latter negative association could be important for differentiating the mechanisms underlying the psychotomimetic effects from the therapeutic effects of ketamine. Their finding of increased connectivity between the medial prefrontal cortex and ventral striatum may also inform the study of ketamine as a potential treatment for drug addiction, a condition in which fronto-striatal connectivity has been found to be impaired (Hu et al., 2015; Murnane et al., 2015).

Another study by Grimm et al. (2015) investigated ketamine-induced changes in functional connectivity specifically between the dlPFC and hippocampus. They found that acute ketamine administration increased dlPFC-hippocampus connectivity in both healthy human subjects and in rats. The generality of their results is limited, given that only a single connection was examined. However, abnormal dlPFC-hippocampus connectivity has been observed in schizophrenia (Meyer-Lindenberg et al., 2005) and a similar finding of robust ketamine-induced increases in dlPFC functional connectivity has been observed in awake rhesus monkeys (Gopinath et al., 2016). Overall, these data provide strong evidence that the effects of ketamine on functional connectivity are well conserved across species.

A recent study employed a regional seed-based analysis of changes in functional connectivity induced by ketamine in awake rhesus monkeys (Gopinath et al., 2016). As

reported previously in humans (Dandash et al., 2015), ketamine increased connectivity to a seed region in the nucleus accumbens, although the increases observed were considerably more extensive. In addition to the accumbens seed, the analysis also featured seed regions in the amygdala, posterior and subgenual cingulate, orbitofrontal cortex, and dlPFC. Among these seed regions, the greatest ketamine-induced changes in functional connectivity were seen in dlPFC projections. This may be a key finding for explaining both the psychotomimetic and antidepressant effects of ketamine (see Discussion).

### 1.5.2 Antidepressant effects

In addition to healthy control subjects, two phMRI studies have investigated the neuronal effects of ketamine infusion in patients with major depressive disorder (MDD). Each of these two studies used a different clinical ratings scale for quantifying changes to symptoms of depression following ketamine infusion. The Beck Depression Inventory (BDI) (Beck et al., 1961) was utilized by Downey et al. (2016), while Abdallah et al. (2016) employed the Montgomery–Asberg Depression Rating Scale (MADRS) (Montgomery and Asberg, 1979).

#### *Brain Activation*

Downey et al. (2016) used phMRI to investigate the acute effects of ketamine infusion in patients with MDD. They performed the phMRI scans during ketamine treatment and correlated the acute effects of ketamine with the alleviation of depression symptoms (BDI) 24-hours post infusion. They found a similar pattern of acute ketamine-evoked BOLD activation in subjects with MDD to what has been shown previously in healthy control subjects (De Simoni et al., 2013; Deakin et al., 2008; Doyle et al., 2013) as well as



in nonhuman primates (Maltbie et al., 2016). Further, they found that ketamine-induced BOLD activation in the rostral anterior cingulate cortex (rACC) correlated strongly ( $r=0.61$ ) with alleviation of depression symptoms (measured by BDI). While, to the author's knowledge, this is the only published phMRI paper to examine the effects of ketamine infusion on BOLD activation in subjects with MDD findings in task-based MRI suggest aberrant processing in the rACC may predict ketamine treatment outcomes (Salvadore et al., 2009; Salvadore et al., 2010).

### *Global brain connectivity*

Abdallah et al. (2016) investigated the prolonged effects of ketamine treatment on GBC in major depression. Prior to treatment, patients with MDD displayed reduced GBC within the prefrontal cortex (responders and non-responders) compared to healthy controls. Following sub-anesthetic ketamine treatment (24 hours post-infusion), responders displayed normalized prefrontal GBC, while non-responders maintained significantly reduced prefrontal GBC. The increase in GBC in lateral PFC and in the caudate correlated with the alleviation of symptoms (MADRS). The data correspond very well with the acute effects of ketamine on GBC observed in healthy control subjects (Driesen et al., 2013a) and awake nonhuman primates (**Figure 1-1**), including increased GBC throughout the brain with the most prominent increases seen in the prefrontal cortex. The study by Abdallah et al. (2016), featured a relatively small sample (N=18 MDD patients, with 10 responders), however the results provide evidence that MDD may feature prefrontal dysconnectivity as measured by GBC and that the increased GBC reliably induced acutely by ketamine could be related to its antidepressant effects. Further investigation is certainly warranted.

### *Seed-based functional connectivity*

In the same study that examined GBC after ketamine treatment in major depression, Abdallah et al. (2016) investigated the prolonged effects of ketamine (24 hours after infusion) on seed regions in the dlPFC, subgenual cingulate, and posterior cingulate cortex. These regions play an important role in cortico-limbic networks (Mayberg, 2003) responsible for affective processing and may be important for the antidepressant effects of ketamine (Johansen-Berg et al., 2008). Abdallah et al. (2016) reported that subjects with MDD displayed higher connectivity between prefrontal regions and the dlPFC and subgenual cingulate seeds, but lower connectivity between more distant cortical and subcortical regions. They further reported these regional connectivity differences to be normalized following ketamine treatment. They speculate that in MDD, within-region connectivity over short distances may be increased, while between-region connectivity over longer distances may be disrupted and that ketamine normalizes connectivity within and between brain regions. While further work is needed to establish better the prolonged effects of ketamine on functional connectivity, these initial results imply that the extensive increases in cortical and subcortical connectivity to dlPFC induced acutely by ketamine (Gopinath et al., 2016) may persist following drug clearance and may contribute to the antidepressant effects of the drug.

## **1.6 Discussion**

Whether or not the dissociative and psychotomimetic effects of ketamine are separable from the therapeutic effects remains an open question. Ratings for ketamine-induced CADSS have been correlated with improvement in depression symptoms following treatment (Luckenbaugh et al., 2014). However, the same study found the schizophrenia-

like symptoms (BPRS) induced by ketamine were not correlated with treatment outcome. phMRI studies of ketamine indicate that the psychotomimetic effects may not be entirely distinguishable from the therapeutic effects. Abdallah et al. (2016) found that increases in prefrontal and striatal GBC 24 hours post-ketamine treatment were correlated with antidepressant efficacy, while Driesen et al. (2013a) found extensive increases in GBC (including a cluster in OFC) induced acutely by ketamine infusion that correlated with positive psychotomimetic symptoms (PANSS). Thus, these phMRI studies indicate that the same neurocircuitry involved in the acute psychotomimetic effects of ketamine is also important for the therapeutic effects.

The effects of ketamine on specific brain regions, particularly the dlPFC, suggest that similar mechanisms underlie psychotomimetic and therapeutic effects. The dlPFC is a region strongly implicated in schizophrenia because of its important role in working memory (Wang et al., 2013). The hyperconnectivity induced by ketamine could be related to improper processing in the dlPFC leading to aberrant downstream signaling and resulting psychotomimetic effects, as hypothesized by Driesen et al. (2013b). Further, the dlPFC plays an essential role in the executive control of emotion (Ochsner and Gross, 2005), which has been shown to be dysfunctional in major depression (Fales et al., 2008). Direct activation of the dlPFC using repeated transcranial magnetic stimulation is an effective treatment for depression (Concerto et al., 2015), speculatively because of a resultant strengthening of network connections responsible for executive control of emotion (Fox et al., 2012; Koenigs and Grafman, 2009; Ma, 2015). Thus, the ketamine-induced increases in dlPFC connectivity may be a key indicator of psychotomimetic

effects present during ketamine infusion as well as the neuroplastic changes thought to underlie the delayed antidepressant effects that follow ketamine administration.

There is also evidence from phMRI studies to suggest differences in the mechanisms underlying the psychotomimetic and therapeutic effects. While Abdallah et al. (2016) found that ketamine-induced increases to GBC in the caudate were correlated with alleviation of depression symptoms (MADRS) in MDD patients, Dandash et al. (2015) observed that increases in functional connectivity between dorsal caudate and ventrolateral thalamus were associated with *lower* ratings of psychosis (RSPS) and dissociative state (CADSS) induced by ketamine in healthy control subjects. Driesen et al. (2013a) likewise found that healthy controls exhibiting greater increases to GBC in both dorsal caudate and ventrolateral thalamus displayed fewer increases in negative schizophrenia symptom scores (PANSS). Hence, while the psychotomimetic and therapeutic effects of ketamine may have convergent mechanisms within the prefrontal cortex (and dlPFC in particular) there appear to be differences in effects on striatal processing that influence the behavioral effects.

While these phMRI studies have provided significant insight into the brain circuitry mediating the behavioral effects of ketamine, the extent to which the therapeutic effects of ketamine can be isolated from the psychotomimetic and dissociative effects remains an open question that requires further investigation.

## **1.7 Future Directions**

### **1.7.1 phMRI and ketamine mechanism of action**

While ketamine-induced BOLD activation has been a useful first step for studying the whole-brain effects of ketamine, functional connectivity may prove to be more informative for understanding the mechanism of action of ketamine in the brain. It is important to note that when neural activity increases, metabolic activity (and therefore BOLD signal) is primarily enhanced at the synapses and not at the cell bodies (Buxton, 2002). Thus, in the case of localized disinhibition of pyramidal neurons, as presumed with ketamine, the downstream areas receiving projections from the disinhibited region(s) may show the greatest enhancement of BOLD signal. On the other hand, a region that becomes disinhibited may increase its functional coupling to downstream areas and hence may show increased functional connectivity even when it does not show a strong enhancement in BOLD signal (Gusnard et al., 2001). This may explain why the dlPFC shows the most extensive increases in functional connectivity (Gopinath et al., 2016) but only moderate increases in BOLD signal during ketamine infusion (De Simoni et al., 2013; Maltbie et al., 2016).

Future studies should use phMRI to address several additional questions ketamine's pharmacology. The dose-response relationship for ketamine remains poorly understood. This is true both for the efficacy of ketamine as an antidepressant and for the acute effects of ketamine on brain activity. De Simoni et al. (2013) reported that BOLD activation increased with increasing dose, however no peak dose has been established and no investigation of dose dependency with functional connectivity has been conducted. Further, no phMRI studies have investigated the effects of repeated ketamine treatments despite the potential relevance of chronic administration to the use of ketamine for the treatment of depression (aan het Rot et al., 2010; Papp et al., 2017).

The independent contributions of the individual pharmacological components of ketamine remain largely unknown. Ketamine is a chiral compound consisting of a pair of (R,S) enantiomers and there is some evidence suggesting that R-ketamine may have greater antidepressant efficacy (Zhang et al., 2014) while also producing fewer psychotomimetic effects (Yang et al., 2015). Further, there is one report that found a specific metabolite of ketamine to be sufficient for producing antidepressant effects (Zanos et al., 2016). phMRI with these independent components of ketamine may lead to important new insights into mechanism of action and therapeutic utility. Such experiments may also help to determine whether the psychotomimetic effects of ketamine can be truly segregated from the antidepressant effects.

### 1.7.2 phMRI and translational models

Nonhuman primate models offer translational advantages in behavioral and pharmacological research (Phillips et al., 2014). The introduction of techniques for performing phMRI experiments in awake nonhuman primates provides even greater translational relevance. As detailed in this review, phMRI coupled with sub-anesthetic ketamine infusion has been used to create a promising translational pharmacological model of schizophrenia in nonhuman primates (Gopinath et al., 2016; Maltbie et al., 2016). Indeed, awake nonhuman primate phMRI can provide important insights into the therapeutic mechanisms of ketamine.

There are limitations to traditional animal models of major depression (Berton et al., 2012), with treatment-resistant depression proving to be particularly challenging (Willner and Belzung, 2015). While nonhuman primate models have been underutilized in studies of depression (Shively and Willard, 2012), the use of phMRI in conscious

animals could be particularly important for investigating the mechanisms underlying the rapid antidepressant effects of ketamine. The only study to investigate the sustained effects of ketamine in nonhuman primates (Lv et al., 2016) reported significant changes to functional connectivity 24 hours post-infusion. However, very different analysis methods were used than Abdallah et al. (2016) and the use of anesthesia represents a potential confound (Hodkinson et al., 2012; Hudetz, 2012). Replicating this study in awake animals should be informative.

Further investigation of sub-anesthetic ketamine as a treatment for drug addiction in humans, as proposed above, could benefit significantly from the use of nonhuman primate models. Nonhuman primate self-administration represents the gold standard for modeling the abuse-related effects of drugs in animals, and phMRI studies provide strong evidence that ketamine induces highly translational effects on BOLD signal and functional connectivity in nonhuman primates. Thus, nonhuman primates may provide a valid animal model for investigating the efficacy of ketamine for reducing drug self-administration, as well as the predictive value of dlPFC functional connectivity as a biomarker for abuse-related behavior.

Ketamine has already shown tremendous therapeutic value in the treatment of major depression, and the results from functional imaging experiments provide important neurocircuitry-level evidence for additional therapeutic uses for ketamine. The finding that ketamine enhances connectivity to the dlPFC (Gopinath et al., 2016), and potentially causes neuroplastic changes that strengthen executive control, has major implications for the potential use of ketamine in treating other psychiatric disorders. Impaired executive control has been associated with multiple disorders and is a particularly common finding

in drug addiction (Goldstein and Volkow, 2011; Jentsch and Taylor, 1999; Volkow et al., 2011). Indeed, acute administration of cocaine has been shown to significantly reduce functional connectivity between dlPFC and nucleus accumbens in awake nonhuman primates, and the connectivity between these regions is negatively correlated with cocaine intake during self-administration (Murnane et al., 2015). There is already some evidence to indicate that sub-anesthetic ketamine infusion may be an effective treatment for cocaine abuse (Dakwar et al., 2016; Dakwar et al., 2014). Given the lack of FDA approved medications for the treatment of psychostimulant abuse, further investigation is certainly warranted.

## **1.8 Conclusions**

Pharmacological imaging has proven extremely useful for studying the effects of ketamine in the brain. Acute administration of sub-anesthetic ketamine produces a robust, global increase in BOLD signal that is correlated with the psychotomimetic effects of ketamine. Functional connectivity also undergoes robust, global increases during acute ketamine administration that correlate with the psychotomimetic effects of ketamine. These effects are very well conserved across primate species and could be used to create a translational pharmacological model of schizophrenia in nonhuman primates. Ketamine shows exciting potential as a therapeutic and the results from phMRI experiments suggest it may strengthen executive control circuits, making it a particularly good candidate for investigation in the treatment of drug abuse. Future phMRI studies may be able to elucidate many of the questions that remain unanswered about the mechanisms mediating the effects of ketamine.



## **1.9 Dissertation overview**

Given the extensive interest in ketamine and importance of understanding the neural mechanisms underlying its effects, this dissertation starts out in Chapters 2 and 3 by examining the effects of ketamine using phMRI in awake rhesus monkeys. This methodology is possible because of the development of a scanning apparatus and animal training procedures that allow for the collection of quality phMRI data without the need for anesthesia and with minimal stress for the animals (Murnane and Howell, 2010). These techniques were recently used to collect phMRI data characterizing the effects of acute administration of cocaine in awake rhesus monkeys (Murnane et al., 2015).

Building on these successful studies, this dissertation begins in Chapter 2 by investigating the effects of sub-anesthetic ketamine infusion (i.v.) on BOLD activation in awake rhesus monkeys. As described in the introduction above, the effects of ketamine infusion on BOLD activation in human subjects are well characterized in the literature (De Simoni et al., 2013; Deakin et al., 2008). Chapter 2 demonstrates ketamine-induced BOLD activation in awake rhesus monkeys similar to that in humans, lending validity to the translational model. Chapter 2 further shows that pretreatment with the antipsychotic drug risperidone attenuates the BOLD activation induced by ketamine, again corroborating published data in human subjects (Doyle et al., 2013).

Expanding on these phMRI results, Chapter 3 uses different analysis methods on the same data as Chapter 2 to examine the effects of ketamine on FC to six cortico-limbic seed regions. Similar studies in human subjects show a pattern of ketamine-induced hyperconnectivity (Dandash et al., 2015; Driesen et al., 2013a) as well as an attenuation of the effects of ketamine on FC after pretreatment with risperidone (Joules et al., 2015). In

Chapter 3, ketamine is shown to induce hyper-connectivity in rhesus monkey cortico-limbic circuits with every seed region displaying increased FC to other cortico-limbic brain areas. These ketamine-induced changes to FC are also shown to be attenuated by pretreatment with risperidone in the rhesus, lending further validity to the translational model. Chapter 3 further presents the key finding of extensive ketamine-induced increases in FC to the dlPFC, including increases in dlPFC-NAcc FC. Murnane et al. (2015) showed dlPFC-NAcc FC to be negatively correlated with cocaine intake during self-administration and to be reduced during acute administration of cocaine. Together, these findings of opposing effects of ketamine and cocaine on this important circuitry – thought to be related to executive control over reward-based decision making – provided the core rationale for the experiments in Chapters 4 and 5 investigating the interaction of ketamine treatment with the effects of cocaine.

Loss of executive control over reward-based decision making is commonly described as a characteristic of substance use disorders (Koob and Volkow, 2010) and may be caused by deficits in glutamatergic projections between prefrontal cortex and NAcc (Kalivas, 2009). These observations have led to glutamatergic medications being proposed for the treatment of substance use disorders (Kalivas and Volkow, 2011). Chapter 4 examines the interaction of sub-anesthetic ketamine with the effects of cocaine on FC using phMRI in awake rhesus monkeys. Pretreatment with ketamine, 48h prior to scanning, is shown to attenuate the effects of cocaine on FC at the whole-brain level and dlPFC-NAcc FC specifically, when evaluated in subjects with no recent drug history.

Chronic exposure to cocaine has been shown to alter brain function (Henry et al., 2010; Porrino et al., 2007), motivating the further investigation into the effects of chronic

cocaine self-administration on FC in Chapter 4. Chronic cocaine self-administration is demonstrated to reduce FC in a pattern mirroring the effects of acute administration of cocaine. Subsequently, the interaction of sub-anesthetic ketamine with the acute effects of cocaine on FC is examined following the period of chronic self-administration. However, no interaction of ketamine with cocaine is observed following chronic self-administration.

In a pair of pilot-studies in cocaine-dependent human subjects, ketamine pretreatment has been shown to decrease cocaine craving (Dakwar et al., 2014) and reduce cocaine choice behavior (Dakwar et al., 2016). Chapter 5 investigates the effects of sub-anesthetic ketamine infusion on reinstatement and reacquisition of cocaine self-administration in rhesus monkeys. Ketamine pretreatment, administered 48h prior, is shown to attenuate response rates during reinstatement testing. However, ketamine does not alter reacquisition of cocaine self-administration, even following repeated ketamine treatments. Overall, the results of Chapter 5 suggest that ketamine pretreatment decreases cocaine-seeking, but does not alter the reinforcing effects of cocaine.

The dissertation concludes in Chapter 6 with a discussion of limitations and future directions for the use of phMRI in awake rhesus monkeys, particularly for the continued study of substance use disorders. Finally, given that the evidence presented in Chapters 4 and 5 supports the potential efficacy of ketamine in the treatment of cocaine use disorder, the present use of ketamine as a therapeutic and whether ketamine or analogous compounds may be effective in the treatment of substance use disorders are discussed.

**Table 1-1** Translational comparison of sub-anesthetic ketamine doses shown to produce psychotomimetic effects, antidepressant effects, and BOLD activation. Typical ketamine doses used for anesthesia are also shown.

	<b>Common active sub-anesthetic ketamine doses (plasma concentration)</b>	<b>Anesthetic ketamine dose (plasma concentration)</b>
<b>Human</b>	~0.5 mg/kg I.V. over 40 minutes (50-250 ng/mL) <sup>a,b</sup>	~1-2 mg/kg I.V. (>1,080 ng/mL) <sup>d</sup>
<b>Rhesus Monkey</b>	~1 mg/kg I.M. (100-200 ng/mL) <sup>c</sup>	~10 mg/kg I.M.
<b>Rat</b>	~10 mg/kg I.P. (100-300 ng/mL) <sup>c</sup>	~100 mg/kg I.P. (>2,000 ng/mL) <sup>e</sup>

a De Simoni et al. (2013); b Krystal et al. (1994); c Shaffer et al. (2014); d Domino et al. (1984); e Veilleux-Lemieux et al. (2013)

**Table 1-2** Dosing procedures for ketamine pHMRI studies.

<i>Study</i>	<i>Sub-anesthetic ketamine dose (plasma concentration, if available)</i>	<i>Duration of infusion</i>	<i>Duration of scan</i>	<i>N Subjects (Condition)</i>	<i>Analysis Methods</i>
<i>(De Simoni et al., 2013)</i>	Low: 0.08 mg/kg + 0.23 mg/kg/hr I.V. (target of 50 ng/mL) High: 0.12 mg/kg bolus + 0.31 mg/kg/hr I.V. (73 ng/mL)	75 min	15 min	10 Human (Healthy Control)	BOLD activation
<i>Doyle et al. (2013)</i>	0.12 mg/kg bolus + 0.31 mg/kg/hr I.V. (63 ng/mL)	75 min	15 min	16 Human (Healthy Control)	BOLD activation
<i>Deakin et al. (2008)</i>	0.26 mg/kg bolus + 0.25 mg/kg/hr I.V.	8 min	16 min	33 Human (Healthy Control)	BOLD activation
<i>Downey et al. (2016)</i>	0.5 mg/kg constant infusion I.V.	60 min	45 min	19 Human (Major Depressive Disorder)	BOLD Activation
<i>Driesen et al. (2013a); (Driesen et al., 2013b)</i>	0.23 mg/kg bolus + 0.58 mg/kg/hr I.V. (162 ng/mL)	45 min	2 hr	Human (Healthy Control)	(a) GBC (b) Seed-based functional connectivity
<i>(Abdallah et al., 2016)</i>	0.5 mg/kg constant infusion I.V.	40 min	4 min (before, and 24 hrs after, infusion)	Human (N=18 Major Depressive Disorder) (N=25 Healthy Control)	GBC and Seed-based functional connectivity
<i>(Anticevic et al., 2015)</i>	0.23 mg/kg bolus + 0.58 mg/kg/hr I.V. (121 ng/mL)	1 hr	4.15 min	96 Human (Healthy Control)	GBC
<i>(Joules et al., 2015)</i>	0.12 mg/kg bolus + 0.31 mg/kg/hr (63 ng/mL)	75 min	15 min (5 min pre-infusion)	16 Human (Healthy Control)	Graph network analysis
<i>(Dandash et al., 2015)</i>	Bolus + automated I.V. infusion targeting 100 ng/mL (69 ng/mL)	15 min	10 min	19 Human (Healthy Control)	Seed-based functional connectivity
<i>(Grimm et al., 2015)</i>	Humans: 0.5 mg/kg I.V. (365 ng/mL) Rats: 25 mg/kg S.C.	Single bolus	Humans: 10 min	Humans: N=24	Seed-based functional connectivity

	(1700 ng/mL)		Rats: 8.5 min	(Healthy Control) Rats: N=9	
<i>Gopinath et al. (2016)</i>	0.345 mg/kg bolus + 0.256 mg/kg/hr I.V. (104 ng/mL)	53 min	55 min	4 Nonhuman primate	Seed-based functional connectivity
<i>Maltbie et al. (2016)</i>	0.345 mg/kg bolus + 0.256 mg/kg/hr I.V. (104 ng/mL)	53 min	55 min	4 Nonhuman primate	BOLD activation
<i>(Chin et al., 2011)</i>	30 mg/kg I.P.	Single bolus	40 min	5 Rat	BOLD activation

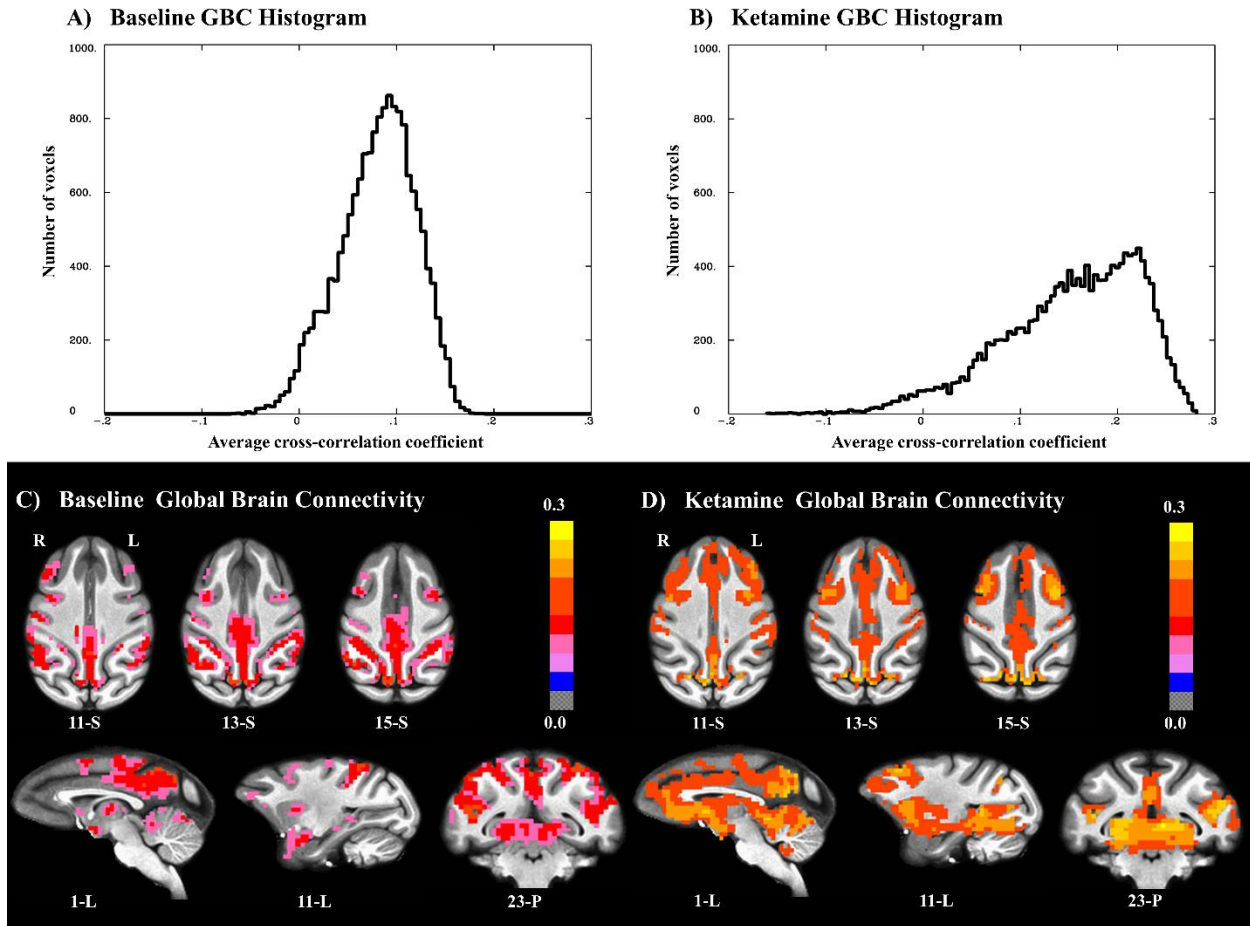


**Figure 1-1** Sub-anesthetic ketamine increases global brain connectivity (GBC) in the awake rhesus brain (N=4). GBC for each voxel is expressed as the effective average cross-correlation (constructed by averaging z-transformed cross-correlations with all other voxel time courses and expressing the result in the form of effective cross-correlation): **(a)** Histogram showing the distribution of GBC in all gray matter voxels during baseline; **(b)** Histogram showing the distribution of GBC in all gray matter voxels during ketamine infusion. The noticeable rightward shift in B compared to A indicates increased connectivity between brain regions during ketamine infusion; **(c)** Voxel-wise GBC maps during baseline. Voxels with GBC > 0.1 are highlighted; **(d)** Voxel-wise GBC maps during ketamine infusion. Voxels with GBC > 0.15 are highlighted. Ketamine-induced increases in GBC are noticeable throughout the brain and appear particularly intense in frontal and subcortical regions.

**Chapter 2: Ketamine-induced effects on brain activation in conscious nonhuman primates**



## **2.1 Context, Author's Contribution, and Acknowledgement of Reproduction**

The following chapter examines the effects of sub-anesthetic ketamine infusion on brain activation in conscious nonhuman primates. The dissertation author contributed by training the nonhuman primate subjects along with Marisa Olsen, collaboratively designing the experiments, analyzing the data, and writing the first of two companion manuscripts (now published) with equal contribution from Dr. Kaundinya Gopinath, under the guidance of Dr. Leonard Howell. The chapter is reproduced with minor edits from:

Maltbie E, Gopinath K, Urushino N, Kempf D, Howell L (2016) Ketamine-induced brain activation in awake female nonhuman primates: a translational functional imaging model. *Psychopharmacology (Berl)*. **233**: 961-972.

## **2.2 Abstract**

**Rationale:** There is significant interest in the NMDA-receptor antagonist ketamine due to its efficacy in treating depressive disorders and its induction of psychotic-like symptoms that make it a useful tool for modeling psychosis.

**Objective:** The present study extends the successful development of an apparatus and methodology to conduct pharmacological MRI studies in awake rhesus monkeys in order to evaluate the CNS effects of ketamine.

**Methods:** Functional MRI scans were conducted in four awake adult female rhesus monkeys during sub-anesthetic i.v. infusions of ketamine (0.345 mg/kg bolus followed by 0.256 mg/kg/hr constant infusion) with and without risperidone pretreatment (0.06mg/kg). Statistical parametric maps of ketamine-induced BOLD activation were

obtained with appropriate GLM models incorporating motion and hemodynamics of ketamine infusion.

**Results:** Ketamine infusion induced and sustained robust BOLD activation in a number of cortical and subcortical regions, including the thalamus, cingulate gyrus, and supplementary motor area. Pretreatment with the antipsychotic drug risperidone markedly blunted ketamine-induced activation in many brain areas.

**Conclusions:** The results are remarkably similar to human imaging studies showing ketamine-induced BOLD activation in many of the same brain areas, and pretreatment with risperidone or another antipsychotic blunting the ketamine response to a similar extent. The strong concordance of the functional imaging data in humans with these results from nonhuman primates highlights the translational value of the model and provides an excellent avenue for future research examining the CNS effects of ketamine. This model may also be a useful tool for evaluating the efficacy of novel antipsychotic drugs.

### **2.3 Introduction**

Ketamine is a non-competitive N-methyl-D-aspartate glutamate receptor (NMDAR) antagonist that has become the focus of a great deal of recent research in disparate fields of psychiatry because of a number of remarkable properties. While commonly used medically as a general anesthetic (Rowland, 2005), sub-anesthetic ketamine infusion produces schizophrenia-like symptoms in healthy humans (Krystal et al., 1994), generates a rapid antidepressant response in patients with treatment resistant depression (Berman et al., 2000), and shows efficacy in treating neuropathic pain (Schwartzman et

al., 2009). This extraordinary profile of effects makes ketamine a key research target for improving the scientific understanding of schizophrenia and depression.

Interest in glutamatergic agents as potential treatments for schizophrenia is based primarily on the effects of NMDAR antagonists, and ketamine in particular, which acutely mimic the positive, negative, and cognitive symptoms of schizophrenia in healthy humans (Krystal et al., 2013; Olney and Farber, 1995). All antipsychotic medications in current clinical use act primarily on the dopamine system (most are D2 antagonists) and are only efficacious for positive symptoms with little efficacy for alleviating the negative or cognitive symptoms (Miyamoto et al., 2005). Recently, research has shifted increasingly towards glutamatergic compounds (Stone, 2011), however, thus far large clinical trials have been unsuccessful (Weiser et al., 2012). PET imaging has shown that acute administration of ketamine increases dopamine release in the striatum, and the extent of dopamine elevation in the ventral striatum correlates strongly with onset of positive symptoms (Vollenweider et al., 2000). Thus, acute ketamine challenge as a model for schizophrenia is consistent with evidence for the involvement of both the dopaminergic and glutamatergic systems (Frohlich and Van Horn, 2014).

Pharmacological MRI (phMRI) has been used to identify the pattern of activation induced by sub-anesthetic doses of ketamine in human volunteers by measuring changes in blood oxygenation level dependent (BOLD) signal (De Simoni et al., 2013; Deakin et al., 2008; Doyle et al., 2013). These changes in BOLD signal correlate with the subjective effects of ketamine (Deakin et al., 2008) and this technique also has shown very good test-retest reliability (De Simoni et al., 2013). Thus, phMRI provides a reliable, *in vivo* imaging methodology for studying the whole-brain pharmacological effects of ketamine. Of

particular relevance to schizophrenia, pretreatment with the antipsychotic risperidone has been shown to attenuate the subjective effects (Schmechtig et al., 2013), BOLD activation (Doyle et al., 2013), and functional changes (Joules et al., 2015) induced by ketamine. This is particularly interesting because while risperidone acts as an antagonist with high affinity for dopamine D2, 5-HT<sub>2a</sub>, and a number of other receptors (Meltzer and McGurk, 1999), like other clinical antipsychotic compounds it does not interact directly with NMDARs. Risperidone may provide a good benchmark for comparison of the effectiveness of novel antipsychotics to attenuate or reverse the CNS effects of ketamine, and evidence suggests that phMRI provides a unique tool for making this comparison.

Nonhuman primate (NHP) models offer distinct advantages for studying cognitive dysfunction and psychopathology (Phillips et al., 2014). Both schizophrenia (Lewis and Lieberman, 2000) and depression (Mayberg, 2003) are characterized in part by altered processing in prefrontal cortex (PFC) and limbic circuits and NHPs represent an excellent animal model because their behavioral repertoires are sophisticated and their PFC is closely aligned with humans (Preuss, 1995). The present study extends the successful development of an apparatus and methodology to conduct phMRI studies in conscious rhesus monkeys (Murnane et al., 2015; Murnane and Howell, 2010) in order to evaluate the CNS effects of antipsychotics. The first aim of this study was to validate NHPs as a model for studying the CNS effects of ketamine by using phMRI in awake rhesus monkeys to examine BOLD activation/deactivation profile of ketamine against time. To evaluate the translational utility of this model the whole brain profile is presented along with in depth analysis of particular regions that are known to be involved in the psychopathology

of both schizophrenia and depression. A second aim of the study was to evaluate the interaction of ketamine with the clinical antipsychotic drug risperidone. The results obtained provide a sound metric for evaluating novel antipsychotics.

## **2.4 Materials and Methods**

### 2.4.1 Subjects:

The subjects were four adult female rhesus monkeys (*Macaca mulatta*) weighing 5.4-7.7 kg. All subjects were initially naïve to any experimental drugs and all underwent the same experiments and served as their own controls to increase statistical power and reduce the number of subjects necessary to complete the scientific objectives of the study. Clinical veterinarians at the Yerkes Center use ketamine for chemical restraint during animal surveys so all subjects had previous exposure to the drug. The endocrine status of the female subjects was not monitored. Animal use procedures were in strict accordance with the National Institutes of Health's "Guide for the Care and Use of Laboratory Animals" and were approved by the Institutional Animal Care and Use Committee of Emory University.

### *Surgery*

Subjects were surgically implanted with chronic indwelling venous catheters as described previously (Howell and Fantegrossi, 2009). Briefly, under isoflurane anesthesia, a silicone catheter was implanted in the femoral vein and was passed to the level of the vena cava. The distal end was attached to a titanium port located subcutaneously in the mid-scapular region.

### *Animal habituation protocol*

In order to minimize motion and stress, all subjects were extensively and gradually habituated to all procedures necessary for these experiments over a period of several months. Subjects were first acclimated to transportation within the frame of the custom apparatus and being brought to the laboratory for 30-minute sessions three times per week. Gradually an increasing number of the pieces of the apparatus were added from session to session until the subject was finally placed in the entire setup for several sessions. Sessions were then reduced to one per week and the duration of immobilization within a session was gradually increased from 30 minutes to 2 hours. Audio recordings of several MR pulse sequences were played during these sessions to acclimate the subjects to the noises produced by the MR scanner. Finally, several full mock scanning sessions were undertaken where the subjects were immobilized in the apparatus and placed within the bore of the Yerkes Imaging Center MRI scanner to expose the subject to the scanner environment prior to the collection of experimental data.

#### 2.4.2 MRI data acquisition:

The apparatus and animal habituation protocol have been described in detail previously (Murnane and Howell, 2010). Scans were conducted in a Siemens (Siemens Healthcare, Erlangen, Germany) Trio 3 Tesla magnet. The monkeys lay prone in a custom-built restraint cradle optimized for acquiring phMRI data from fully-conscious rhesus monkeys (Murnane and Howell, 2010) and attached to a NHP head coil (RAPID MR International, LLC). Heart rate, oxygen saturation and expired gases were continuously monitored to ensure the safety of the animals inside the scanner. In each scanning session, BOLD sensitive phMRI images were collected utilizing a whole-brain gradient echo single-shot echo planar imaging (EPI) sequence. The scan parameters for this sequence were

Repetition Time (TR) = 3000ms; Echo Time (TE) = 32ms; Flip Angle (FA) = 90°; Field of View (FOV) = 96cm, 1.5mm X 1.5mm in-plane resolution with 42 coronal slices covering the whole-brain; slice thickness = 1.5mm; 1100 measurements). Field inhomogeneities were mapped using a standard Siemens dual gradient echo based field mapping sequence for later correction of any EPI image distortions. A T1-weighted (T1w) a 3-dimensional (3D) magnetization prepared rapid gradient echo (MPRAGE) sequence (TR = 2300 ms; TE = 2.7ms; Inversion Time (TI)=800 ms; FA = 8°; FOV = 96cm; 1.5mm X 1.5mm X 1.5mm resolution) was also acquired to assist in co-registration of the EPI time-series to the high-resolution T1w anatomic acquired in a different session. For each monkey, a set of 7 high resolution T1w anatomic scans were acquired in a separate scanning session with a 3D MPRAGE sequence with scan parameters: TR = TR = 2300 ms; TE = 3.4ms; TI = 800ms; FA = 8°; FOV = 128cm; 0.5mm X 0.5mm X 0.5mm resolution. The 7 high-resolution anatomic images were averaged together to yield a final 3D T1w anatomic image with high SNR and resolution for anatomic reference.

#### 2.4.3 Drug infusion protocols:

Each subject underwent two 55-min pharmacological MRI scans in separate scanning sessions:

- 1) One minute baseline followed by a 1 minute bolus i.v. infusion of 0.345 mg/kg of ketamine followed by 53 minute continuous infusion of 0.256 mg/kg/hr ketamine;
- 2) Same as (1) but with risperidone (0.06 mg/kg, i.v.) administered 1 hour prior to the MRI session;

Note the infusion and dosing parameters were determined empirically from pharmacokinetic evaluations in order to achieve steady-state plasma levels of

ketamine at approximately 100 ng/mL. Further, in order to ensure that expected drug levels were achieved during scanning, blood samples were acquired immediately following each scan. Drug levels were determined from heparinized plasma by Tandem Labs using gas chromatography and mass spectrometry.

The effects of ketamine under dosing conditions identical to those employed during MRI scans were evaluated while subjects were seated in a standard primate chair in the behavioral laboratory. Subjects were fully conscious and responsive to auditory and tactile stimulation.

#### 2.4.4 Pharmacological MRI data analysis:

##### *Preprocessing and spatial normalization*

MRI data analysis was conducted with AFNI (Cox, 1996) and FSL (Smith et al., 2004) software packages. The phMRI time-series images were first corrected for distortions introduced by magnetic field inhomogeneities (estimated by the gradient echo field map). Voxel time-series in the phMRI dataset were temporally shifted to account for differences in slice acquisition times. The 3D scan volumes were then registered to a base volume to account for motion.

The skull-stripped averaged high-resolution T1w anatomic structural image of subject RNE13 was chosen as the template brain for the four-subject dataset. RNE13's brain was chosen due to its image quality and symmetry being the best among the four subjects scanned. Each subject's averaged high-resolution high SNR T1w anatomic was registered to this template T1w dataset. For each subject, the low-resolution T1w anatomic acquired



during the drug–infusion scan session was aligned to the template brain via the averaged high-resolution high SNR T1w anatomic acquired in a separate scanning session through image registration tools available in FSL. The motion-corrected EPI drug-infusion phMRI time-series was aligned to the low-resolution T1w anatomic acquired in the same session with a rigid registration algorithm and then aligned to the template brain through the warp calculated during the low-resolution T1w anatomic to template brain registration described above. The resultant EPI time-series were spatially smoothed with a full-width at half-maximum (FWHM) = 3mm isotropic Gaussian filter. The brain activation to each drug paradigm was assessed using this preprocessed phMRI time-series as described below.

#### *Pharmacological MRI data quality control*

The phMRI image time-series data were examined for large motions defined as more than 2mm displacement. Due to large motion exhibited by the NHPs during the end of a number of drug infusion scans, all the phMRI time-series were curtailed to 40 minutes. More than 2mm motion in more than 10% of the phMRI volumes within the first 40 minutes of a dataset was considered unusable. None of the scans acquired for these experiments exceeded this threshold and thus no scanning sessions were discarded or repeated.

#### *Activation mapping*

For each subject, brain activation to ketamine was estimated by adapting a ketamine phMRI model described in the literature (De Simoni et al., 2013) to observed region of interest (ROI) averaged ketamine infusion phMRI time-series in *a priori* ROIs (see below) across subjects. These drug infusion ROI-averaged phMRI responses were

sustained (see Figure 4) throughout the duration of the drug infusion (after an initial ramp-up period of 2-3 minutes) in a number of ROIs (as opposed to the transient response shown in (De Simoni et al., 2013)). To maintain a degree of translatability with human ketamine infusion studies and as well as to maintain consistency with observed sustained *a priori* ROI-averaged drug infusion responses, we employed the signal model in De Simoni et al. 2013 as a gamma-variate kernel (with parameters adjusted to achieve a time to peak of 2 minutes) with which we convolved the drug infusion time-course to obtain a reference phMRI signal time series,  $S$  (normalized to a peak value = 1) for our general linear model.

$$S(t) = \left( \frac{t}{t_{\max}} \right)^{b \cdot t_{\max}} e^{-b \cdot (t_{\max} - t)} \otimes D(t) \quad \text{Eq. (1),}$$

where  $S(t)$  is the modeled phMRI BOLD signal,  $D(t)$  is the drug infusion protocol,  $b$  is a shape parameter with value  $b = 0.01$  and  $t_{\max}$  is the time-to-peak amplitude. We set  $t_{\max} = 120 \text{ sec}$  (as opposed to 240 sec in humans estimated by De Simoni et al.) due to the smaller brain size of NHPs compared with humans, as well as to maintain consistency with the observed signal in *a priori* brain ROIs. The reference vector  $S(t)$  (normalized to a peak value = 1), better represented the observed phMRI signal observed in this study.

The voxel phMRI time-series was modeled as

$$y_i = \hat{\beta} \times S_i + \sum_k \hat{a}_k M_i^k + \varepsilon_i \quad \text{Eq. (2),}$$

where  $y_i$  is the voxel intensity at  $i^{\text{th}}$  time-point,  $S_i$  is the  $i^{\text{th}}$  time-point of the reference signal time-course,  $M_i^k$  is the value of the  $k^{\text{th}}$  motion parameter ( $k = 1$  to 6 corresponding to 6 degrees of rigid body motion) for the  $i^{\text{th}}$  volume.  $\beta$  is the amplitude of phMRI signal

(Eq. (1)) and  $a^k$  denotes the proportion of voxel phMRI time-series that is related to the  $M^{kth}$  motion parameter.  $\beta$  and  $a^k$  are obtained from Eq. (2) through least squares linear regression. Volumes exhibiting more than 2mm motion were discarded from analysis.

*Accounting for variations in durations of drug response in different brain regions*

The drug infusion model employed assumes that the brain activation assessed by the phMRI BOLD response is persistent throughout the drug infusion periods. In order to account for brain regions which (unlike the *a priori* ROIs) may lose responsiveness to drug infusion after varying time durations, the general linear regression model (GLM) described in Eq. (2) was fitted for 22 different periods of drug infusion: 6 min to 40 min (in steps of 2 min) as well as odd multiples of 5 from 5 min to 35 min. This procedure captures the complete drug response profile of all voxels in the brain. It is an adaptation of a well-established unconstrained BOLD response estimation technique in long block fMRI paradigms (Cato et al., 2004; McGregor et al., 2015; Moffett et al., 2015) to the constrained phMRI BOLD response estimation employed in this study. The only difference being instead of simultaneously estimating the amplitude of the BOLD response at 22 different time points after the start of infusion in one GLM, 22 separate GLMs were run and the amplitude of the BOLD response and its associated t-statistic were computed for each of the 22 infusion periods. This amplitude t-statistic is a standardized quantity that accounts for both the intensity of estimated amplitude as well as the error in the estimate. It was expected that voxels exhibiting sustained phMRI response throughout the 40 minute duration of the drug infusion modeled would exhibit strong and significant GLM-estimate amplitude t-statistic in GLM analyses corresponding to all 22 infusion periods, and voxels with transient phMRI signal

responses will exhibit loss of significance in the GLMs corresponding to the infusion periods where the voxel signal departs from the modeled sustained response. The summary statistics combining all the GLM-estimate amplitude t-statistics described below will express the strength of activation across the 40 minute drug infusion duration.

#### *Group-level drug treatment-induced whole brain activation maps*

The dose response profile for each voxel using the above procedure is a 22-point time course comprised of amplitudes (expressed in standardized t-scores) of pHMRI BOLD response at each of 22 different modeled periods of drug infusion. For each voxel, the area under the curve (AUC) of the dose response curve (Cato et al., 2004; McGregor et al., 2015; Moffett et al., 2015), expressed as the mean of the 22-point GLM-estimate amplitude t-statistic time-course was employed to assess brain activation to each drug treatment paradigm (ketamine and ketamine after risperidone pretreatment). Group-level activation maps for ketamine and ketamine after risperidone pretreatment were obtained through 1-sample t-test on the individual subject whole-brain voxel-wise AUC maps.

#### *Between-treatment differences in whole brain activation*

The group-level differences in brain activation between different drug treatment conditions were obtained through a paired 2-sample t-test between the individual subject AUC maps of the two conditions. The drug treatment related brain activation and between-treatment t-test maps were clustered and the significance of activations accounting for multiple comparisons were derived by means of Monte Carlo simulation of the process of image generation, spatial correlation of voxels, intensity thresholding, masking and cluster identification (Forman et al., 1995) through the *3dClustSim* program

implemented in AFNI software. Specifically, all the p-values reported in the *Results* section pertaining to whole-brain activation maps are reported at a multiple-comparisons corrected significance of  $p < 0.05$ . To achieve this significance, the activation and contrast maps were masked with a whole-brain EPI mask, and activation intensity thresholded at individual voxel-level test-statistic threshold of  $p < 0.05$ , and clustered with a minimum volume threshold of 94 voxels arrived at by performing the Monte-Carlo simulation mentioned above through the *3dClustSim* program.

#### *Non-parametric analysis*

Finally, due to the small sample size ( $N= 4$ ), voxelwise Wilcoxon signed rank test was also performed to assess between-treatment differences in brain activation, as a non-parametric equivalent of the paired t-test. Multiple comparison corrected significance was obtained through the method described above (Forman et al., 1995).

#### *Analysis of activation in specific a priori brain ROIs*

In order to examine the temporal evolution of the drug response in selected *a priori* brain ROIs pre-defined ROIs were manually delineated by a single highly experienced rater (Dr. Urushino) in direct reference to the Paxinos rhesus monkey brain atlas (Paxinos et al., 2000). ROIs were drawn on the high resolution anatomical images to include every voxel fully contained within the following brain areas: anterior, mid, and posterior cingulate cortex (ACC, MCC, and PCC), dorsolateral prefrontal cortex (dlPFC), medial prefrontal cortex (mPFC), orbital frontal cortex (OFC), supplementary motor area (SMA), superior frontal cortex, superior temporal gyrus (STG), caudate, putamen, thalamus, and amygdala. These areas have been shown to activate during ketamine infusion (De Simoni et al., 2013; Deakin et al., 2008) or be involved in cortico-limbic processing (Haber, 2003;

Johansen-Berg et al., 2008). All ROIs were drawn bilaterally, however amygdala, caudate, and STG were later separated into left and right hemispheres because significant clusters of ketamine activation or attenuation of ketamine activation by risperidone were seen in only one hemisphere. For each ROI, significant ketamine-induced brain activation and differences between drug treatment conditions were assessed by masking the group-level activation and t-contrast maps by each ROI. These masked statistical parametric maps were thresholded at individual voxel-level  $p < 0.05$  and clustered with a minimum volume threshold corresponding to the extent needed to be significant at a multiple comparisons (incorporating both voxels in each ROI and the number of ROIs) corrected significance level of  $p < 0.05$  obtained through Monte Carlo simulations (Forman et al., 1995) implemented with the *3dClustSim* program. Multiple comparisons correction for the number of ROIs was conducted with the bonferroni method. Since the number of ROIs were  $N = 16$  this amounted to setting the cluster-volume threshold for clusters within each ROI at the level needed to obtain a cluster-level  $p < 0.003$ .

#### *phMRI BOLD drug response time-course in specific a priori brain ROIs*

ROI-average BOLD dose response curves were obtained for each subject for each ROI by averaging the voxel time-series (after regressing out signal proportion to motion parameters (Bullmore et al., 1999)). The individual subject BOLD dose response curves for each ROI were averaged together to form group-averaged BOLD drug response time-course for that ROI.

#### 2.4.5 Clinical Ratings of Behavior:

The effects of risperidone (0.06 mg/kg) on clinical ratings of behavior (Casey et al., 2001) were evaluated while subjects were seated in a standard primate chair in the behavioral

laboratory. Behaviors were scored before and 15, 30, 45, 60, 75, 90, 105, 120 min after risperidone (0.06 mg/kg) administration. Behaviors rated included: eye blinking (number/30 s), tongue protrusions (number/30 s), oral facial dyskinesias (involuntary repetitive movements of the mouth and face, number/30 s), chewing (number/30 s), sedation (0-3), stereotypy (constant repetition of certain meaningless gestures or movements, 0-3), dystonia of the head and neck (impairment of muscle tone, 0-3), trunk (0-3), upper limbs (0-3), and lower limbs (0-3); bradykinesia (0-3), tremor (involuntary trembling movement, 0-3), salivation (0-3), locomotor activity (-3-0, 0-3), and reactivity (-3-0,0-3). The absolute value of the score corresponds to 0 = normal behavior or symptoms not present; 1 = mild (behavior occasionally present); 2 = moderate (behavior regularly present but interrupted); and 3 = significant (behavior continuously present). Eye blinking, tongue protrusions, oral facial dyskinesias, and chewing scores are the average number per 30 s of three consecutive 30-s rating periods. Reactivity responses to external stimuli and locomotor activity were scored with a scale range of -3 to +3. Reactivity responses were assessed as the reaction to the observer standing approximately 3 feet from the animal and moving one hand toward the animal over a 15-inch distance as if to touch the animal. This hand movement should evoke a consistent threat display toward the observer (0 = subject is alert, exhibits normal vigilance and responsiveness to the stimulus; -1 = slight decrease in responsiveness; -2 = moderate decrease in responsiveness to the stimulus; -3 = no response to stimulus at all, +1 = slight increase in responsiveness to the stimulus, +2 = moderate increase in reaction to the stimulus, +3 = marked exaggerated response to the stimulus). Locomotor responses were assessed as follows: 0 = subject is alert, exhibits normal amount of activity, -1 = slight decrease in activity, -2 = moderate decrease in

activity, -3 = significant decrease in activity, +1 – slight increase in activity, +2 = moderate increase in activity, +3 = significant increase in activity.

## **2.5 Results**

### 2.5.1 Blood plasma drug levels

Blood samples taken immediately after scanning were analyzed for plasma levels of ketamine and risperidone (**Table 2-1**). Measurements indicate a mean plasma ketamine concentration of  $104 \pm 8$  ng/mL following the ketamine infusion phMRI scan (Scan 1 in Table 1) and  $96 \pm 24$  ng/mL following the ketamine infusion phMRI scan conducted *after* risperidone pretreatment (Scan 2 in Table 1). The mean plasma risperidone concentration following Scan 2 was  $1.7 \pm 0.4$  ng/mL. All plasma drug levels were within the expected range and ketamine dosage was sufficient to produce a significant drug effect in every scan.

### 2.5.2 Ketamine-induced BOLD activation

Ketamine infusion induced significant ( $p < 0.05$ ) activation in an extensive number of brain areas as shown in **Figure 2-1** and summarized in **Table 2-2**. Areas of significant activation include the superior frontal gyrus, supplementary motor area (SMA), anterior cingulate cortex (ACC), insula, superior temporal gyrus (STG), precuneus, primary somatosensory cortex (S1), thalamus and basal ganglia, and cerebellum. The strongest activation to ketamine was observed in the cingulate gyrus, SMA, and thalamus. There were no areas where significant deactivation was observed.



### 2.5.3 Reduction in Ketamine-induced Activation by Risperidone pretreatment

Pretreatment with risperidone (0.06 mg/kg) an hour prior to infusion of ketamine reduced both the magnitude and extent of ketamine-induced brain activation. However, significant ( $p < 0.05$ ) residual brain activation to ketamine infusion remained in a number of areas (shown in **Figure 2-2** and summarized in **Table 2-2**). This decrease in activation is clearly seen by comparing **Figure 2-2** with **Figure 2-1** (which use the same activation color scale, and slices to map ketamine activation) and is highlighted further by **Figure 2-3** which shows areas where risperidone pretreatment caused a significant ( $p < 0.05$ ) change in ketamine-induced brain activation. Risperidone pretreatment significantly reduced (shown in blue in **Figure 2-3**) ketamine-induced brain activation in the SMA, cingulate gyrus, superior frontal gyrus and left hemisphere thalamus, caudate and putamen. No brain areas exhibited a significantly greater response to ketamine following risperidone pretreatment.

### 2.5.4 Ketamine-induced effects within a priori ROIs

Specific effects of ketamine infusion within *a priori* ROIs that contained clusters of significant ketamine-induced activation following bonferroni correction for multiple comparisons are shown in **Table 2-3**. These *a priori* ROIs were selected either because they showed a strong response to ketamine in the literature or because of the importance of the region within the cortico-limbic circuit. As seen in the table, within these specific ROIs the strongest ketamine-induced activation occurred in the ACC, MCC, thalamus, caudate, putamen, and precuneus. Risperidone pretreatment reduced the response to ketamine in both magnitude and extent in almost every ROI with the largest effects seen in the ACC, anterior STG, thalamus, caudate, and putamen. All ROIs are bilateral except

for amygdala, caudate, and STG where left and right hemispheres are considered separately because significant clusters of ketamine activation or attenuation of ketamine activation by risperidone were seen in only one hemisphere.

#### 2.5.5 ROI-averaged Group-mean Time Courses

**Figure 2-4** shows the ROI-average group-mean drug time-course plots for the anterior cingulate cortex (ACC), thalamus, orbitofrontal cortex (OFC), and the left caudate nucleus. The percentage change in BOLD signal during ketamine infusion is plotted over time. Each of the selected areas exhibit robust activation to ketamine infusion. The drug time-course curves indicate that ketamine-induced activation in these areas becomes evident within five minutes of the initial bolus and remains constant through the duration of the infusion. Pretreatment with risperidone blunts the ketamine response over the full time-course in each of these regions. The low between-subject variation (indicated by the relatively small error bars) suggests that both ketamine-induced activation and the blunting of the ketamine response by risperidone are highly consistent across subjects over the full course of the infusion.

#### 2.5.6 Clinical Ratings of Behavior

Behavioral ethograms were evaluated in all 4 subjects at baseline and following acute risperidone challenge. Risperidone (0.06 mg/kg, i.v.) induced marked effects on sedation, motor activity and reactivity as shown in the ethograms reported in **Table 2-4**.

## **2.6 Discussion**

The results of this pHMRI study in fully-conscious NHPs show robust BOLD activation induced by a sub-anesthetic ketamine dosing regimen. These data are in excellent

agreement with human phMRI imaging studies (De Simoni et al., 2013; Deakin et al., 2008; Doyle et al., 2013) which consistently show a pattern of brain activation following ketamine administration that is strikingly similar to the NHP data presented here. De Simoni et al. (2013) reported the most robust ketamine response in midline regions including the ACC, PCC, paracingulate gyrus, SMA, precuneus, cerebellum, thalamus, and brainstem. The ketamine response in the NHPs exhibited a nearly identical profile with each of those regions becoming significantly activated and the cingulate, SMA, and thalamus showing the greatest response. The excellent concordance between the human and NHP data suggests that phMRI in conscious NHPs provides a reliable and translational animal model for investigating the CNS effects of subanesthetic ketamine.

Interestingly, the subgenual cingulate was one brain region in which the NHP data did not replicate the human results. This region is of particular interest because it appears to be located at a critical juncture of the cortico-limbic pathway (Mayberg, 2003) and could play an important role in mediating the antidepressant effects of ketamine (Mayberg et al., 2005). No significant response to ketamine was detected in this region despite previous studies showing a significant ketamine-induced deactivation in humans. However, De Simoni et al. (2013) found that the reduction of BOLD signal with ketamine in the subgenual cingulate had a relatively low effect size and was much less reliable than BOLD increases observed in other regions such as the ACC, PCC, and thalamus. Indeed, with only four subjects, the present study may have been underpowered for detecting a deactivation in the subgenual cingulate. Thus, the lack of an observed deactivation in the subgenual cingulate does not necessarily represent a meaningful difference between the human ketamine response profile and that of NHPs.

Further evidence for the utility of this NHP ketamine model for evaluating antipsychotic drugs is provided by the results of pretreatment with the standard clinical antipsychotic risperidone. While risperidone pretreatment significantly attenuated the ketamine response, strong residual ketamine-induced activation was still observed. This result is in excellent agreement with the human data and closely mirrors the findings from Doyle et al. (2013). Overall the similarity observed between human and NHP data in the results of risperidone pretreatment on the ketamine response lends further validity to the use of the NHP model and also provides both a proof of concept and a sound benchmark for using this model to test novel antipsychotics.

A number of sex differences have been associated with both schizophrenia (Abel et al., 2010) and depression (Young and Korszun, 2010), so it should be noted that all four subjects in this study were female. This may be considered an advantage of the present study as all of the human ketamine phMRI data in previous studies were collected only in men. Given that males have been shown to be more vulnerable to the cognitive effects of ketamine than females (Morgan et al., 2006), it is critical to evaluate drug effects in both sexes.

### *Limitations*

One limitation of the present study is that the menstrual cycles of the female subjects were not monitored. While it is possible that the endocrine status of the subjects affected our results, most of the evidence in the literature suggests that any effects should be minimal at most. A review of the effects of ovariectomy on NMDARs found no effects in brain regions with the exception of the hippocampus (Cyr et al., 2001). Further, a recent study

found no effect of ovariectomy on the disruption of pre-pulse inhibition by ketamine in rats (van den Buuse et al., 2015).

Another limitation which is general to all awake NHP MRI studies is potential for motion artifacts to influence the results. In this study, the NHPs were trained extensively to tolerate the MRI scanner environment. In terms of data analysis, we regressed out phMRI signal proportional to movement parameters and furthered censored volumes of the phMRI signal time course during which the NHPs exhibited more than 2 mm motion. However residual motion artifacts may in part contribute to the increased variability seen in ROI-averaged ketamine infusion-induced phMRI response time-courses seen in Figure 4 when compared to those from the ketamine infusion scans conducted after pre-treatment with risperidone. Interestingly, the results from blood samples showed that between-subject variance in plasma ketamine levels was *greater in risperidone* pretreatment condition than ketamine-alone scans. These seemingly contradictory results can be explained in part by the observation that while all subjects remained awake and alert during the risperidone pretreatment scans, they exhibited significantly less motion compared to the ketamine-alone scans presumably due to the sedative effects of risperidone seen at clinical doses of the kind administered in this study. The reduction in amount of movement may explain the reduced variability in risperidone pretreatment ROI-averaged time courses seen in **Figure 2-4**. However, it must be noted that even given the increased variability in the ketamine-alone condition significant widespread activation in expected brain regions was observed, and statistically significant attenuation in phMRI response to ketamine was observed after pre-treatment with risperidone as expected.

No experiments were done to test the BOLD response to risperidone alone. While this may be an interesting future direction, to our knowledge no phMRI testing has examined the effects of risperidone (or other antipsychotic) alone, only the interaction with a task (Bolstad et al., 2015) or a psychotomimetic such as ketamine (Doyle et al., 2013).

Paliperidone, the 9-OH metabolite of risperidone, produces similar antipsychotic effects to the parent compound and was likely present in significant concentrations during this study, however only measurements of the risperidone concentration were taken. Previous literature (Muly et al., 2012) has indicated the half-life of risperidone in rhesus monkeys to be approximately three hours and the blood samples in this study were taken 2-hours post injection. Hence, we expected risperidone to be the predominant compound. Further, Muly et al. (2012) found that serum levels of risperidone and paliperidone were highly correlated in rhesus monkeys following i.v. risperidone.

As discussed previously, unlike previous experiments in humans, the NHP data shows no deactivation was observed in the subgenual cingulate in response to ketamine. This may represent a true species difference and could be a limitation to the translational validity of the model. However, data for this study was collected in only 4 subjects. While the effects shown are robust and appear to be highly consistent with previous studies in humans in the remainder of the brain, the small sample size limits the conclusions that can be drawn from these results.

### *Future directions*

Pharmacological MRI in NHPs shows great promise as a translational model for the CNS effects of ketamine. Future studies should employ this model to examine drug interactions with the ketamine response as a method to further the understanding of the

effects of this remarkable compound on the CNS. As a model for schizophrenia, phMRI in NHPs may be particularly effective for evaluating novel antipsychotics. The antipsychotic drugs currently in clinical use tend to feature moderate to severe side effects (Kim et al., 2007) and have shown little efficacy for treating the negative and cognitive symptoms of schizophrenia (Strous et al., 2003). Novel compounds that show similar efficacy to current antipsychotics could potentially be superior therapeutics if they simply exhibit a reduced side effect profile or provide effective treatment for the negative symptoms of schizophrenia.

Important questions regarding the efficacy of ketamine for treating depression remain unanswered. Randomized controlled trials have shown that a single I.V. infusion of ketamine can reliably generate a rapid antidepressant response in patients with treatment resistant depression (Aan Het Rot et al., 2012), yet the mechanisms underlying the antidepressant effects of ketamine remain incompletely understood. Increased excitatory glutamatergic signaling may be necessary for the antidepressant effects of ketamine (Maeng et al., 2008) as well as synaptic strengthening in prefrontal (Li et al., 2010) and limbic (Autry et al., 2011) regions. Indeed, the increased neural plasticity induced by ketamine in cortico-limbic circuits may be a critical factor underlying its efficacy for treating both depression (Thompson et al., 2015) and neuropathic pain (Doan et al., 2015). As a highly translational model, phMRI in awake NHPs provides a valuable tool for studying the broad CNS effects induced by ketamine.

**Table 2-1** Blood plasma levels for ketamine and risperidone in each of the 4 subjects. Acquisition of blood samples occurred immediately after scanning. Drug levels were determined from heparinized plasma by Tandem Labs using gas chromatography and mass spectrometry.

Subject	Scan 1: Ketamine	Scan 2: Ketamine after Risperidone Pretreatment	
	Plasma ketamine (ng/mL)	Plasma ketamine (ng/mL)	Plasma risperidone (ng/mL)
RIc13	114	129	1.51
RRb13	95	89	1.93
RZo13	103	72	1.23
RNe13	106	94	2.09



**Table 2-2** Summary of brain areas activated in whole-brain, group-level analysis during ketamine infusion, and ketamine infusion after risperidone pretreatment. Multiple comparison corrected cluster-level  $p < 0.05$

<b>Drug Treatment</b>	<b>Brain Areas Activated at corrected <math>p &lt; 0.05</math></b>
<i>Ketamine</i>	Bilateral: superior frontal gyrus, middle frontal gyrus, supplementary motor area (SMA), anterior cingulate cortex (ACC), cingulate gyrus, insula, superior temporal gyrus (STG), middle temporal cortex, hippocampus, parahippocampal cortex, precuneus, posterior parietal cortex, paracentral lobule (PCL), primary somatosensory cortex (S1), primary motor cortex (M1), thalamus, caudate, putamen, cerebellum and brainstem
<i>Risperidone + Ketamine</i>	Bilateral: superior frontal gyrus, SMA, M1, parahippocampal cortex, hippocampus, brainstem, cerebellum  Left hemisphere: cingulate gyrus, insula, STG, middle temporal cortex

**Table 2-3** Group-level brain activation in *a priori* areas of interest (ROIs) during ketamine infusion, ketamine infusion following pretreatment with risperidone, and the difference between the two conditions. The table reports median t-stat and number of voxels for clusters of significant (multiple comparisons-corrected  $p < 0.05$ ) activation within each ROI. Only ROIs with significant clusters are shown, NS = no significant cluster.

ROI	<b>Ketamine</b>	<b>Risperidone+Ketamine</b>	<b>Risperidone Subtraction</b>
	median t-stat (voxels)	median t-stat (voxels)	median t-stat (voxels)
Anterior cingulate cortex	5.14 (148)	NS	4.79 (132)
Mid-cingulate cortex	5.78 (95)	NS	4.11 (40)
Left anterior superior temporal gyrus	4.28 (75)	NS	4.37 (53)
Right anterior superior temporal gyrus	5.01 (78)	4.47 (75)	NS
Supplementary motor area	4.47 (49)	4.65 (44)	5.24 (30)
Thalamus	5.27 (151)	4.43 (92)	NS
Left caudate	3.71 (91)	NS	4.46 (81)
Right caudate	4.21 (108)	NS	NS
	4.13 (15)	NS	NS

## Left amygdala

Precuneus	4.46 (231)	5.32 (45)	4.29 (52)
Putamen	4.07 (219)	4.63 (93)	4.29 (106)

**Table 2-4** Behavioral ethogram indicating clinical ratings of behavior at baseline and following acute risperidone challenge (0.06 mg/kg, i.v.). Mean and standard deviation of behavioral ratings across subjects are presented for baseline and at 15-minute intervals post-injection.

Ethogram	Time post-injection (Mean $\pm$ standard deviation)								
	Baseline	15 min	30 min	45 min	60 min	75 min	90 min	105 min	120 min
Eye blinking (#/30s)	7.92 $\pm$ 2.06	2.08 $\pm$ 0.96	0.92 $\pm$ 1.07	1.75 $\pm$ 0.32	3.67 $\pm$ 3.28	2.52 $\pm$ 2.32	1.67 $\pm$ 0.27	2.5 $\pm$ 1.69	2.41 $\pm$ 0.99
Tongue protrusions (#/30s)									
Oral facial dyskinesias (#/30s)									
Chewing (#/30s)	0.08 $\pm$ 0.17	0							
Sedation (0-3)		2.75 $\pm$ 0.50	2.5 $\pm$ 1	2.75 $\pm$ 0.5	2.5 $\pm$ 0.5	2.5 $\pm$ 0.58	2.75 $\pm$ 0.5	2.5 $\pm$ 0.58	2.75 $\pm$ 0.5
Stereotypy (0-3)									
Dystonia head and neck (0-3)									
Dystonia trunk (0-3)				0.25 $\pm$ 0.5					

Dystonia upper limbs (0-3)		0.50 ± 1 0.50	0.5 ± 1 0.5	0.5 ± 1 0.5	0.25 ± 0.43 0.25 ± 0.5				
Dystonia lower limbs (0-3)			0.25 ± 0.5 0.5	0.25 ± 0.5 0.5					
Bradykinesia (0-3)		0.25 ± 0.50 0.50	0.25 ± 0.5 0.5						
Tremor (0-3)		0.25 ± 0.50 0.50	0.25 ± 0.5 0.5						
Salivation (0-3)				0.25 ± 0.5 0.5					
Locomotor activity (-3 to 3)		-2.0 ± 2.0 2.0	-2.25 ± 1.5 1.5	-2 ± 2 2	-2.25 ± 1.3 1.3	-2.75 ± 0.5 0.5	-2.5 ± 1 1	-2.75 ± 0.5 0.5	-2.5 ± 1 1
Reactivity (-3 to 3)		-2.5 ± 1.0 1.0	-2.25 ± 0.96 0.96	-2.25 ± 1.5 1.5	-1.75 ± 1.09 1.09	-1.5 ± 1.3 1.3	-0.75 ± 0.5 0.5	-0.75 ± 0.5 0.5	-0.75 ± 0.5 0.5

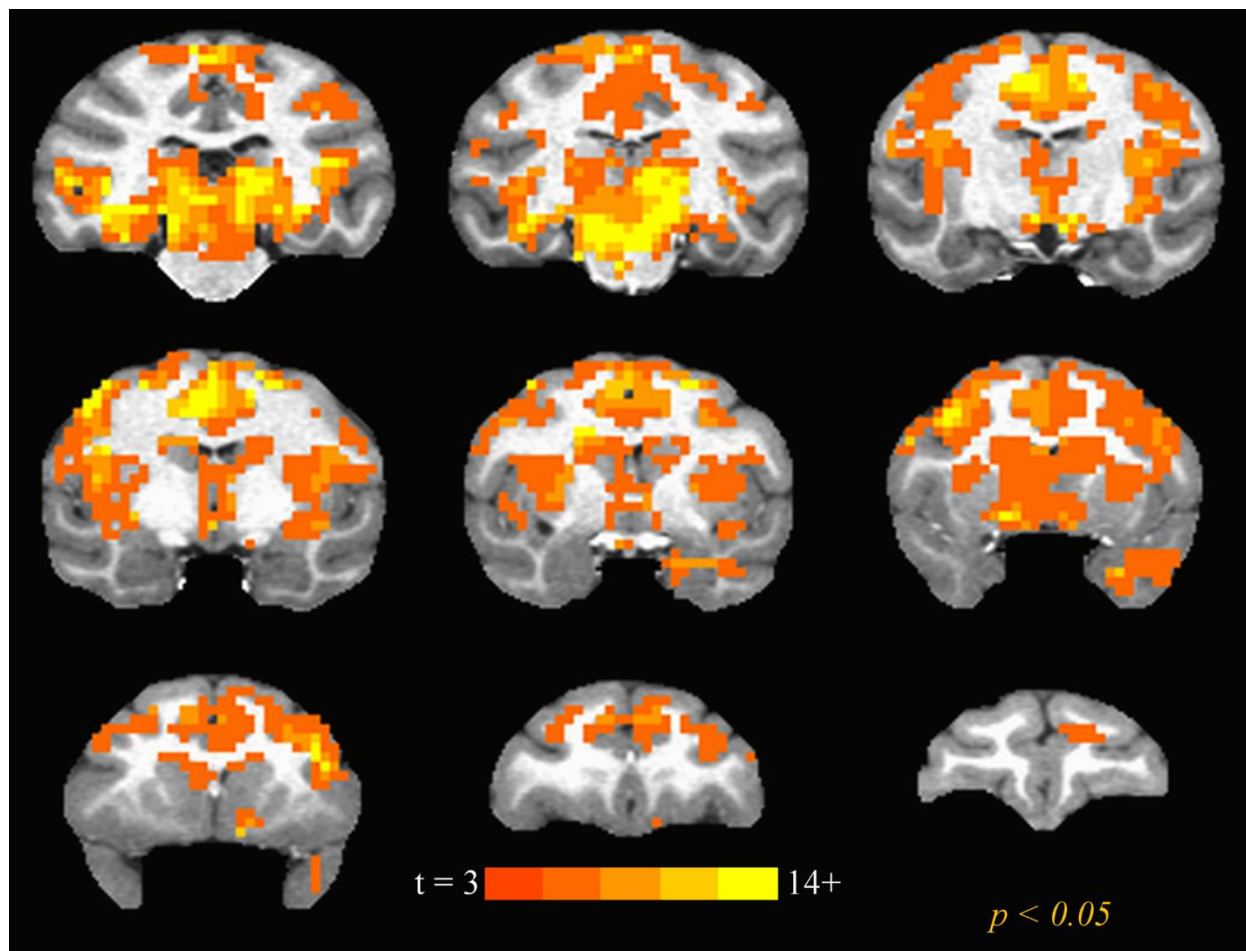


**Figure 2-1** Group-level brain activation to ketamine: Map of 1-sample group t-test on individual subject dose-response AUC (see text) shows areas of significant brain activation during ketamine infusion. Ketamine induces extensive activation throughout the brain. Cluster-level multiple comparison corrected  $p < 0.05$ . Slices progress from posterior (top-left) to anterior (bottom-right).

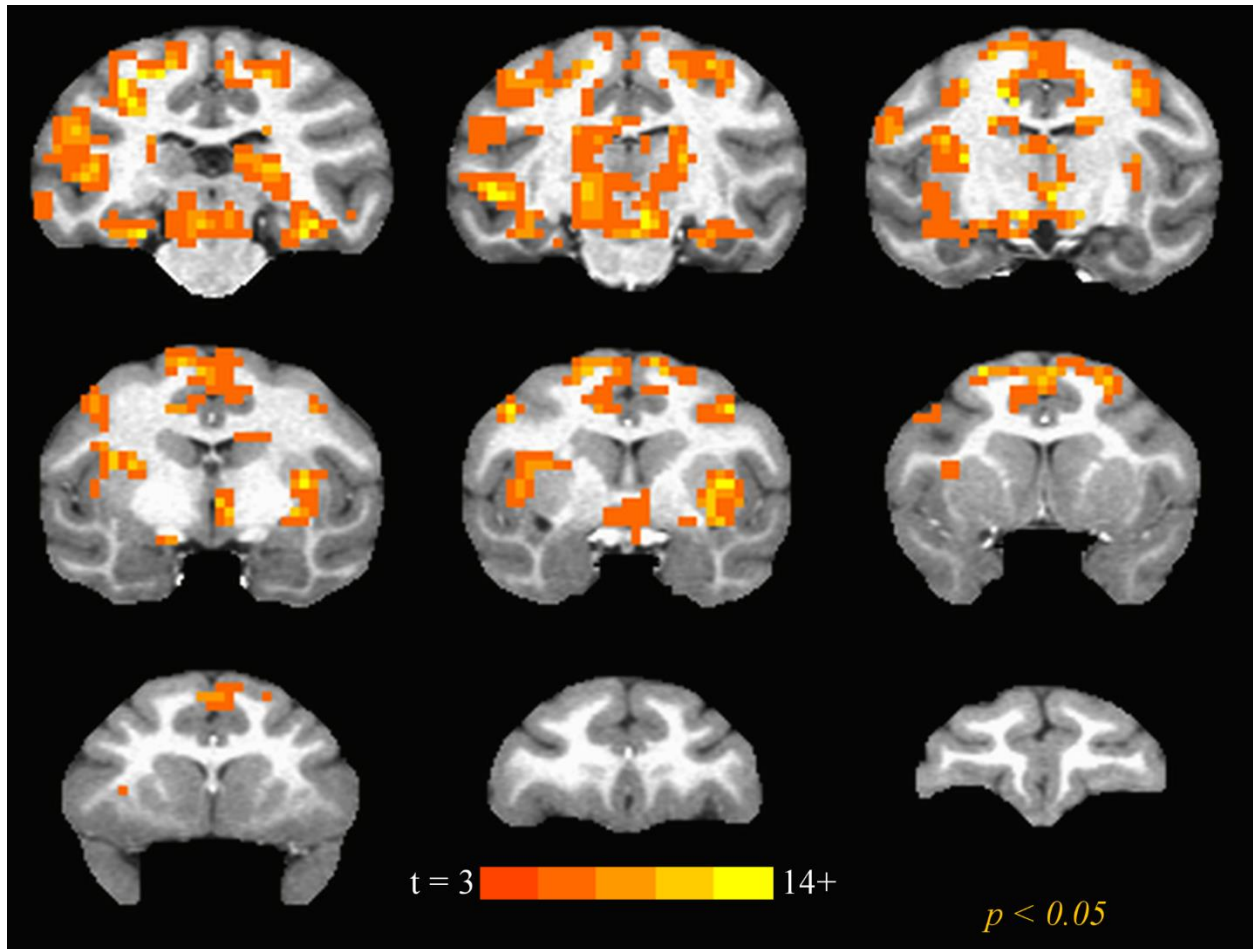


**Figure 2-2** Group-level brain activation to ketamine after risperidone pretreatment: Map of 1-sample group t-test on individual subject dose-response AUC (see text) shows areas of significant brain activation during ketamine infusion. Ketamine induced brain activation is still evident, but is considerably less extensive following risperidone pretreatment. Cluster-level multiple comparison corrected  $p < 0.05$ . Slices progress from posterior (top-left) to anterior (bottom-right).

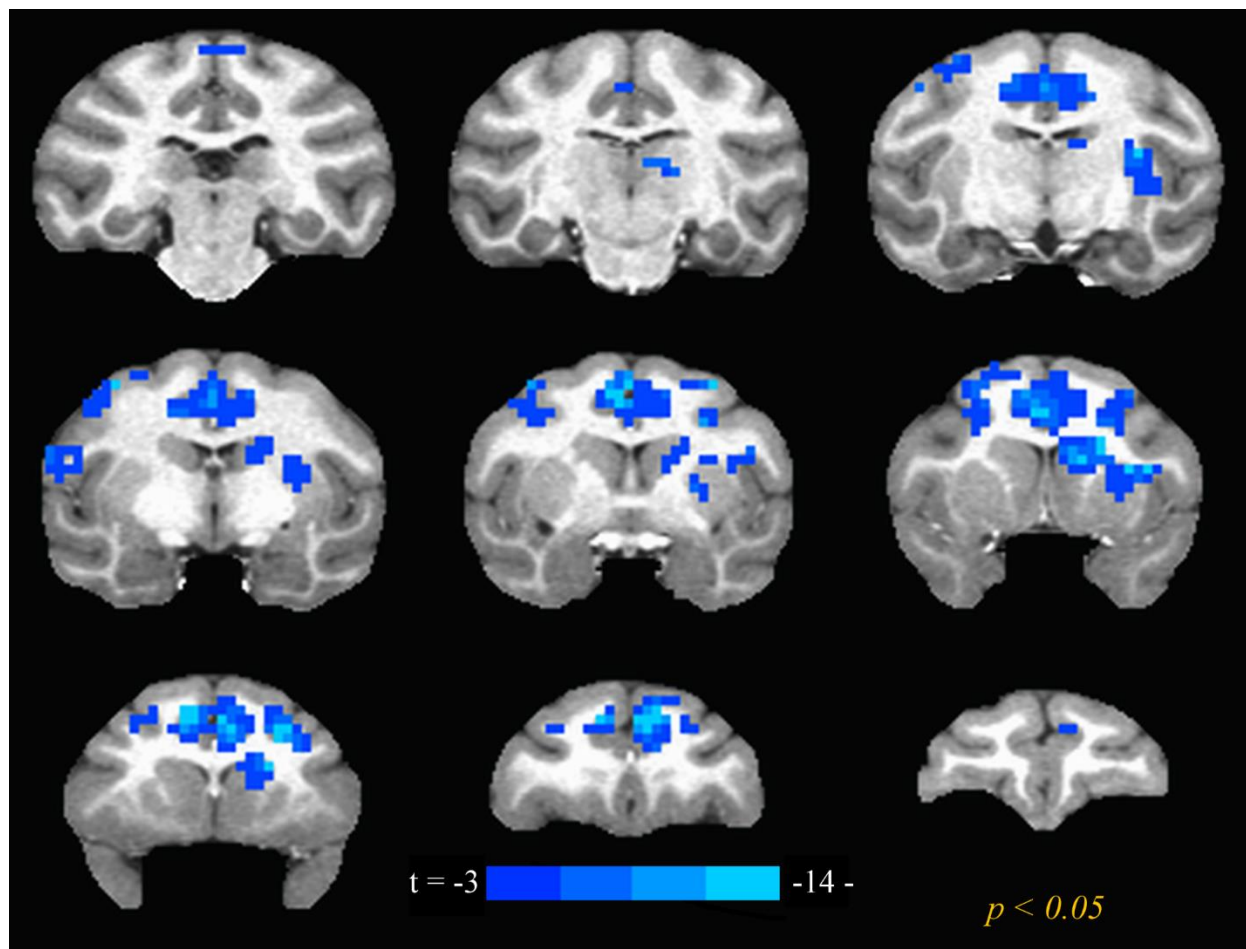


**Figure 2-3** Group-level difference in brain activation to ketamine after pretreatment with the anti-psychotic risperidone. Map of between-condition paired t-test shows areas where risperidone pretreatment significantly reduced brain activation to ketamine. Cluster-level multiple comparison corrected  $p < 0.05$ . Slices progress from posterior (top-left) to anterior (bottom-right).



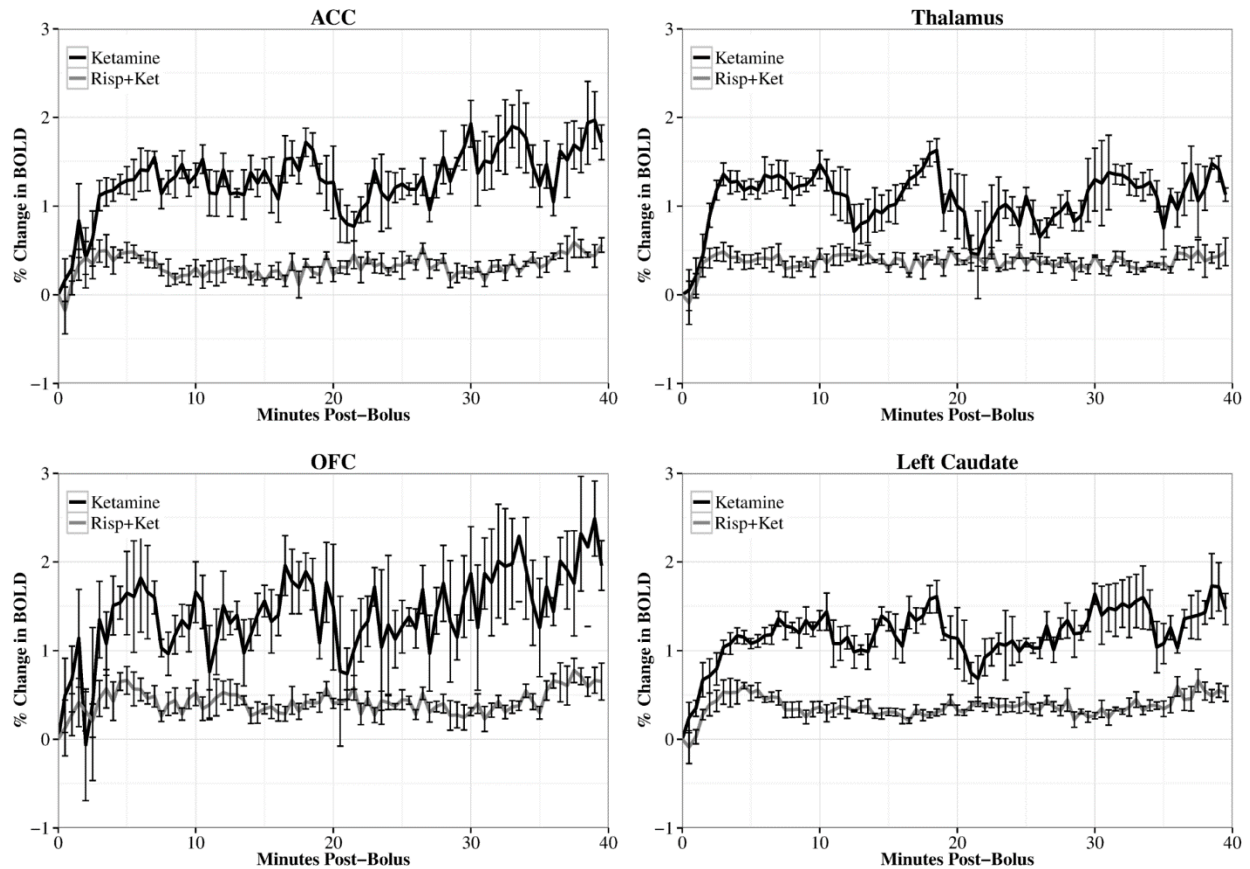


**Figure 2-4** ROI-average group-mean drug time-course curves during ketamine infusion are plotted for anterior cingulate cortex (ACC), thalamus, orbitofrontal cortex (OFC), and the left caudate nucleus. The percentage change in BOLD signal during ketamine infusion is plotted over time. Error bars indicate standard error of the mean. Risp+Ket = Ketamine activation after risperidone pretreatment.

**Chapter 3: Ketamine-induced changes in connectivity of functional brain networks in awake female nonhuman primates: a translational functional imaging model.**

### 3.1 Context, Author's Contribution, and Acknowledgement of Reproduction

The following chapter examines the effects of sub-anesthetic ketamine infusion on functional connectivity in awake nonhuman primates. The dissertation author contributed by training the nonhuman primate subjects along with Marisa Olsen, collaboratively designing the experiments, analyzing the data, and writing the published manuscript (along with its companion) with equal contribution from Dr. Kaundinya Gopinath, under the guidance of Dr. Leonard Howell. The chapter is reproduced with minor edits from:

Gopinath K, Maltbie E, Urushino N, Kempf D, Howell L (2016). Ketamine-induced changes in connectivity of functional brain networks in awake female nonhuman primates: a translational functional imaging model. *Psychopharmacology (Berl)* **233**: 3673-3684.

### 3.2 Abstract

**Rationale:** There is significant interest in the NMDA-receptor antagonist ketamine due to its efficacy in treating depressive disorders and its induction of psychotic-like symptoms that make it a useful tool for modeling psychosis. Pharmacological MRI in awake nonhuman primates provides a highly translational model for studying the brain network dynamics involved in producing these drug effects.

**Objective:** The present study evaluated ketamine-induced changes in functional connectivity (FC) in awake rhesus monkeys. The effects of ketamine after pretreatment with the antipsychotic drug risperidone were also examined.

**Methods:** Functional MRI scans were conducted in four awake adult female rhesus monkeys during sub-anesthetic i.v. infusions of ketamine (0.345 mg/kg bolus followed by 0.256 mg/kg/hr constant infusion) with and without risperidone pretreatment (0.06mg/kg). A 10-minute window of stable BOLD signal was used to compare FC between baseline and drug conditions. FC was assessed in specific regions of interest using seed-based cross-correlation analysis.

**Results:** Ketamine infusion induced extensive changes in FC. In particular, FC to the dorsolateral prefrontal cortex (dlPFC) was increased in several cortical and subcortical regions. Pretreatment with risperidone largely attenuated ketamine-induced changes in FC.

**Conclusions:** The results are highly consistent with similar human imaging studies showing ketamine-induced changes in FC, as well as a significant attenuation of these changes when ketamine infusion is preceded by pretreatment with risperidone. The extensive increases shown in FC to the dlPFC are consistent with the idea that disinhibition of the dlPFC may be a key driver of the antidepressant and psychotomimetic effects of ketamine.

### **3.3 Introduction**

Ketamine has an extraordinary profile of pharmacological effects which make it a key research target for advancing the understanding and treatment of several psychiatric disorders, including schizophrenia and mood disorders. Sub-anesthetic infusions of ketamine have been shown to produce schizophrenia-like symptoms in healthy human volunteers (Frohlich and Van Horn, 2014; Krystal et al., 1994) while also generating a rapid antidepressant response in patients with treatment-resistant depression (Berman

et al., 2000; Krystal et al., 2013) at identical doses. Thus, ketamine challenge is currently being used experimentally both as way to model schizophrenia and as a treatment for depression and other mood disorders. However, the mechanisms by which ketamine produces these effects remain incompletely understood. As a non-competitive N-methyl-D-aspartate glutamate receptor antagonist, ketamine produces widespread effects throughout the brain (De Simoni et al., 2013; Deakin et al., 2008). The global scope of the ketamine-response poses a challenge to the identification of the specific brain circuitry responsible for producing the psychotomimetic and antidepressant effects of ketamine.

One way to probe specific brain circuitry underlying the psychotomimetic and antidepressant effects of ketamine is to employ pharmacological MRI (phMRI) to measure changes in brain functional connectivity (FC) networks induced by ketamine administration. While ketamine has been shown to increase FC globally (Driesen et al., 2013a; Joules et al., 2015), changes in FC between specific regions have been found to correlate with the subjective effects of ketamine (Dandash et al., 2015; Driesen et al., 2013a). Indeed, this regional specificity may be particularly important because both schizophrenia (Meyer-Lindenberg, 2010; Woodward et al., 2011) and mood disorders (Anand et al., 2009; Greicius et al., 2007; Wessa et al., 2014) have been associated with alterations in resting-state FC networks albeit in distinct regional patterns (Chai et al., 2011; Goya-Maldonado et al., 2016). Thus, measuring changes to FC with phMRI provides an excellent tool for examining the effects of ketamine on specific brain circuitry and how it relates to psychiatric disorders. Recently, this technique has become even more powerful following the successful development of an apparatus and methodology

(Murnane and Howell, 2010) to conduct phMRI studies in conscious rhesus monkeys (Maltbie et al., 2016; Murnane et al., 2015; Murnane and Howell, 2010).

Nonhuman primate (NHP) models offer distinct advantages for studying cognitive dysfunction and psychopathology (Phillips et al., 2014). Both schizophrenia (Lewis and Lieberman, 2000) and mood disorders (Mayberg, 2003) are characterized in part by altered processing in prefrontal cortex (PFC) and limbic circuits, and NHPs represent an excellent animal model because their behavioral repertoires are sophisticated and their PFC is closely aligned with humans (Preuss, 1995). We recently reported that the blood oxygenation level-dependent (BOLD) activation to ketamine infusion produced a response pattern in conscious NHPs (Maltbie et al., 2016) that was highly concordant with effects observed in human studies (De Simoni et al., 2013; Deakin et al., 2008). Further, we also reported (Maltbie et al., 2016) that pretreatment with the antipsychotic drug risperidone attenuated the ketamine response to a similar magnitude and extent as observed in humans (Doyle et al., 2013). This indicates that NHPs may provide a highly translational animal model for studying the effects of ketamine as well as the pharmacological interaction between ketamine and other compounds.

The present study evaluated further the validity of the NHP model by investigating the effects of ketamine on resting-state FC in conscious rhesus monkeys. The effects of ketamine on FC in brain networks known to be affected by schizophrenia and mood disorders were examined and compared to findings from the literature in human subjects. The effect of pretreatment with risperidone on FC changes induced by ketamine was also examined. The findings present important precursors for future research investigating

the mechanisms by which ketamine produces psychotomimetic and antidepressant effects as well as a potential model for evaluating novel antipsychotics.

### **3.4 Materials and Methods**

#### *3.4.1 Subjects:*

A complete description of the animals, surgery, and habituation protocol employed in this study has been described in detail in chapter 2 (2.4.1). Briefly four adult female rhesus monkeys (*Macaca mulatta*) were included in the study. They were all initially naïve to any experimental drugs and underwent the same experiments. Animal use procedures were in strict accordance with the National Institutes of Health's "Guide for the Care and Use of Laboratory Animals" and were approved by the Institutional Animal Care and Use Committee of Emory University. In order to habituate the animals to the MRI environment all subjects were extensively and gradually habituated to all procedures necessary for these experiments over a period of several months.

#### *MRI data acquisition*

A complete description of the MRI imaging methods employed in the companion paper (Maltbie et al., 2016). Briefly the monkeys lay prone in a custom-built restraint cradle (Murnane and Howell, 2010) attached to a NHP head coil. In each scanning session, BOLD MRI images were collected utilizing a whole-brain gradient echo single-shot echo planar imaging (EPI) sequence (TR/TE/FA = 3000ms/32ms/90°; 1.5x1.5x1.5 mm; resolution; 1100 measurements). A low-resolution T1-weighted (T1w) anatomic scan was acquired with a 3D MPRAGE sequence (TR/TE/TI/FA = 2300ms/2.7ms/800ms/8°; 1.5x1.5x1.5mm resolution) to assist in spatial normalization. Further for each monkey, a

set of seven high (0.5x0.5x0.5mm ) resolution T1w 3D MPRAGE anatomic scans were acquired in a separate scanning session and averaged together to yield a final high quality anatomic image for anatomic reference and spatial normalization.

### 3.4.2 Drug infusion protocols

The drug infusion protocol is described in detail in the companion paper (Maltbie et al., 2016). Briefly, each subject underwent two 55-min pharmacological MRI scans in separate scanning sessions. In both sessions (one with and one without pretreatment with risperidone (0.06 mg/kg, i.v.) administered 1 hour prior to the MRI session) there was a 1 minute baseline followed by a 1 minute bolus i.v. infusion of 0.345 mg/kg of ketamine followed by 53-minute continuous infusion of 0.256 mg/kg/hr ketamine. This ketamine dosing regimen was chosen to target a plasma concentration of 100 ng/mL, which has been used in a previous FC study (Dandash et al., 2015). The literature (Muly et al., 2012) suggested a dose of 0.1 mg/kg of risperidone would correspond closely to a clinical maintenance dose, however, this dose induced sleep in two of the animals. Administration of a dose one half-log unit lower (0.03 mg/kg) was found to be well tolerated in all four animals, as was an intermediate dose of 0.06 mg/kg. The intermediate dose of 0.06 mg/kg of risperidone produced the expected behavioral response, as detailed in (Maltbie et al., 2016), and was selected for use in the imaging experiments.

The results from the phMRI study (Maltbie et al., 2016) showed that the ketamine-induced phMRI signal increase across the brain peaked around 4-5 minutes after the onset of drug infusion ( $t_{on}$ ) and remained relatively steady until around 18-20 minutes after the onset of drug infusion. Also, all the monkeys exhibited the least motion during this time window. Hence a steady state block of phMRI time-series from 7-16 sec after  $t_{on}$



was selected to assess functional connectivity networks in the brain during ketamine infusion with/without pre-treatment with risperidone.

### *Baseline Resting State fMRI*

Apart from the phMRI scans mentioned above, two 10-minute resting state fMRI (rsfMRI) scans were acquired in a separate session. The second rsfMRI scan was employed to assess FC during resting baseline for all the monkeys, to ensure that monkeys were relaxed and maximally acclimatized to the scanning environment.

### *fMRI Data Quality Control*

The fMRI image time-series data were examined for large motions defined as more than 0.5 mm frame-to-frame displacement. If a given monkey exhibited motion above this threshold in more than 10% of the fMRI volumes within the 10 minutes of a drug treatment dataset employed to assess functional connectivity, the scan was repeated in another session, and the motion corrupted dataset was discarded. None of the scans acquired for these experiments exceeded this threshold and thus no scanning sessions were discarded or repeated.

### 3.4.3 fMRI Data Analysis:

#### *Preprocessing and spatial normalization*

MRI data analysis was conducted with AFNI (Cox, 1996) and FSL (Smith et al., 2004) software packages as well as in-house Matlab™ (Natick, MA) scripts. The fMRI time-series images were first corrected for distortions introduced by magnetic field inhomogeneities, temporally shifted to account for differences in slice acquisition times and registered to a base volume to account for motion. Each subject's averaged high-

resolution high SNR T1w anatomic was registered to the INIA19 NHP template atlas (Rohlfing et al., 2012) using an affine image registration algorithm. For each subject, the motion-corrected EPI drug-infusion fMRI time-series was aligned to the low-resolution T1w anatomic (*lores-anat*) acquired in the same session with a rigid registration algorithm and then aligned to INIA19 template brain through the warp calculated in the alignment of the *lores-anat* to the high resolution T1w anatomic in INIA19 co-ordinate space. The resultant EPI time-series were further denoised by replacing spikes in signal intensity resulting from motion and other spurious noise sources which exceeded 3.5 times median absolute deviation from time-series baseline with the 5 timepoint median of the EPI time-series centered at each spike. Finally, the denoised EPI time-series were spatially smoothed with a full-width at half-maximum (FWHM) = 3mm isotropic Gaussian filter. As a quality control step, time-series volumes that exhibited more than 0.5 mm frame-to-frame displacement were censored from functional connectivity analysis.

### *Functional Connectivity Analysis*

Seed based cross-correlation analysis (CCA) was employed to assess the strength of functional connectivity networks during each of the drug treatment conditions and baseline. A priori seed regions of interest (ROIs) of areas implicated in schizophrenia (Frangou, 2014; Meyer-Lindenberg, 2010; Minzenberg et al., 2009) and mood disorders (Anand et al., 2009; Mayberg, 2003; Phillips and Swartz, 2014) were demarcated on the INIA19 NHP atlas based on associated NeuroMaps labels (Rohlfing et al., 2012). Left (as well as right) hemisphere ROIs of the entire dorsolateral prefrontal cortex (dlPFC), orbital frontal cortex (OFC), subgenual cingulate (SgC), nucleus accumbens (NAcc), and

amygdala (Amyg) and posterior cingulate cortex (PCC) were demarcated by appropriately aggregating and segregating NeuroMaps labeled areas pertaining to each of the ROIs (see **Figure 3-1**). Since averaging all voxels within large ROIs can lead to enhanced sensitivity to motion artifacts (Power et al., 2012) and global signal (Saad et al., 2012), each ROI was subdivided into 3x3x3mm non-overlapping sub-ROIs and all EPI voxel time-series within each sub-ROI were averaged to construct sub-ROI reference vectors. The z-transformed cross-correlation coefficient (CC) maps of all constituent sub-ROIs of a given ROI (e.g. dlPFC) were averaged to construct subject-level functional connectivity (FC) maps for that ROI. Due to the small sample-size ( $N = 4$ ) nonparametric statistical analysis was employed to assess brain FC. Group-level FC maps for each ROI, for each session were constructed with appropriate Wilcoxon 1-sample signed rank test (nonparametric equivalent of 1-sample t-test) on the individual subject FC maps for the corresponding ROI. Group level differences in FC between ketamine, baseline and ketamine after pretreatment with risperidone (*RispKet*) for each ROI were assessed with the Wilcoxon signed rank test (nonparametric equivalent of paired t-test) on the individual subject FC maps for the corresponding ROI. The Wilcoxon signed rank 1-sample and between condition z-maps were clustered and the significance of activations accounting for multiple comparisons are derived by means of Monte Carlo simulation of the process of image generation, spatial correlation of voxels, intensity thresholding, masking and cluster identification (Forman et al., 1995) through the 3dClustSim program implemented in AFNI software. All the significant reported in the *Results* section are corrected for multiple comparisons at  $p < 0.05$  unless otherwise indicated.

## 3.5 Results

### 3.5.1 Blood plasma drug levels

Blood samples taken immediately after scanning were analyzed for plasma levels of ketamine and risperidone. Blood plasma results have been published in the companion paper (Maltbie et al., 2016). Plasma ketamine ranged from 72 ng/mL to 129 ng/mL in all scans and averaged 104 ng/mL in scans with ketamine alone and 96 ng/mL in scans where ketamine followed risperidone pretreatment. This ketamine dosage was sufficient to produce a significant drug effect in every scan.

### 3.5.2 Ketamine-induced changes in FC to dlPFC

Ketamine induced (**Figure 3-2**) widespread changes in dlPFC FC with a number of different brain regions. When *compared with the baseline* session, ketamine induced (**Figure 3-3, Table 3-1**) significantly ( $p < 0.05$ ) *increased* dlPFC FC with areas involved in affective processing and mood regulation: e.g., ventral anterior cingulate (vACC), SgC, amygdala, NAcc, anterior insula, anterior superior temporal gyrus (STG), caudate, putamen and dlPFC. In addition, dlPFC FC to sensorimotor and attention areas: e.g. premotor cortex (PMC), primary motor (M1) and somatosensory (S1) cortices, supplementary motor area (SMA), cingulate gyrus and posterior STG also *increased* significantly from baseline during ketamine infusion.

Pretreatment with risperidone (0.06 mg/kg) an hour prior to infusion of ketamine (*RispKet*), significantly attenuated (**Figure 3-3; Table 3-1**) the effects of ketamine. During the *RispKet* session dlPFC FC was significantly *decreased*, when *compared with ketamine*, to limbic and affective processing areas: SgC, NAcc, caudate, putamen,

amygdala, anterior insula, anterior STG and vIPFC. At the same time dlPFC FC to superior parietal lobule (SPL) was *increased* when *compared with ketamine*. However, RispKet still resulted in *increased* dlPFC FC *compared to baseline* (Table 2) with some of the same affective processing and sensorimotor areas as ketamine, albeit with reduced extent.

### 3.5.3 Ketamine-induced changes in FC to SgC

During ketamine infusion, the SgC exhibited (**Figure 3-4**) significant ( $p < 0.05$ ) FC with limbic and affective processing areas, as well as dlPFC, SMA, premotor cortex, STG and supramarginal gyrus (SMG). Ketamine induced *higher* SgC FC *compared to baseline* in a number of these areas; however, ketamine  $>$  baseline effects were significant ( $p < 0.05$ ) (**Table 3-1**) only in dlPFC, and some sensorimotor areas: premotor cortex, STG, insula and cerebellum.

The RispKet session exhibited (**Figure 3-5; Table 3-1**) significantly *decreased* SgC FC when *compared with ketamine* to limbic and affective processing areas: vACC, OFC, SgC, amygdala, NAcc, caudate, putamen, and anterior insula, in addition to dlPFC and sensorimotor areas. Interestingly, the RispKet session exhibited (**Figure 3-5; Table 3-1**) *decreased* SgC FC with limbic and affective processing areas also *compared to baseline*.

### 3.5.4 Ketamine-induced changes in FC to Amygdala

During ketamine infusion, the amygdala exhibited (**Figure 3-6**) significant ( $p < 0.05$ ) FC to limbic and affective processing areas. Ketamine induced significantly *enhanced* amygdala FC (**Table 3-1**) with SgC, ventral striatum, anterior ventral putamen, caudate and contralateral amygdala when *compared to baseline*. Amygdala FC with posterior default mode network (DMN) areas (PCC and lateral parietal cortex) was attenuated

compared to baseline during ketamine infusion (**Figure 3-6**), but the effect was not significant. During the RispKet session, the amygdala displayed (**Figure 3-7; Table 3-1**) significantly *decreased* FC compared with ketamine to areas involved in limbic and affective processing: NAcc, caudate, putamen, thalamus, amygdala, anterior insula, and STG, apart from dlPFC and sensorimotor and associative/DMN areas: premotor cortex, insula, STG, secondary somatosensory cortex, SFC, parietal SMG and SPL. Further, during the RispKet session the amygdala showed (**Figure 3-7; Table 3-1**) significantly *reduced* FC with these same regions when compared to baseline.

### 3.5.5 Ketamine-induced changes in FC to Nucleus Accumbens

During ketamine infusion, the NAcc exhibited (**Figure 3-8**) significant ( $p < 0.05$ ) FC to striatal and temporal limbic and affective processing areas as well as dlPFC, attention, sensorimotor and DMN areas. Ketamine induced NAcc FC was (**Figure 3-9; Table 3-1**) significantly *increased compared with baseline* to limbic and affective processing areas: caudate, putamen, amygdala, anterior insula and anterior STG, in addition to PCC, cingulate and SFC. During the RispKet session the NAcc displayed significantly *decreased* (**Figure 3-9; Table 1**) FC compared to ketamine with all of these above areas and as well as dlPFC, SMA, and ACC.

### 3.5.6 Ketamine-induced changes in FC to other ROIs

**Table 3-1** lists the between-session differences in FC to the two other ROIs described in the methods. RispKet session FC of OFC (like those of dlPFC, NAcc, SgC, amygdala) was significantly *attenuated compared to ketamine* in limbic and affective processing areas. Also, RispKet session FC of OFC (like the FCs of SgC and amygdala) with limbic and affective processing areas was significantly *reduced compared to baseline*.

Finally, during ketamine infusion the PCC (which is a hub of the DMN) exhibited *increased* FC with striatal limbic and affective processing areas: NAcc, anterior caudate and putamen; as well as with SMA and cingulate *compared to baseline*. Pretreatment with risperidone *decreased* ketamine induced PCC FC to limbic areas. Further, the RispKet session showed significantly higher PCC FC with anterior DMN regions and retrosplenial cortex compared to baseline while inducing decreased FC to affective processing regions.

### 3.5.7 Ketamine-induced inter-hemispheric asymmetry in FC networks

**Table 3-2** lists the regions in the brain, for each seed ROI, that exhibited significant differences in FC between the seed's left and right hemisphere homologs, under each scan condition. At baseline, very few regions exhibited preferential FC to any given hemisphere. Ketamine induced a breakdown in hemispheric symmetry in FC in all the seed ROIs examined except NAcc (**Table 3-2; Figure 3-10**). Ketamine induced increased FC of left dlPFC (compared with its right hemisphere homolog) with areas in sensorimotor, salience and limbic networks. Pre-treatment with risperidone (RispKet) increased left dlPFC FC with bilateral nucleus reuniens and increased right dlPFC FC to right amygdala, compared to their contralateral homologs.

Ketamine induced increased FC of right amygdala (compared with left amygdala) to limbic and salience monitoring network regions (**Table 3-2; Figure 3-10**). RispKet exhibited increased right amygdala FC with posterior default mode network as well as cingulate and hippocampus. Both ketamine and RispKet sessions exhibited increased left OFC FC, left PCC FC and right SgC FC with a number of brain areas compared to the respective seeds' contralateral homologs.

### 3.6 Discussion

The results described above reveal a number of interesting changes in brain FC network characteristics induced by ketamine, and the modulation of ketamine-induced changes in FC network by pretreatment with risperidone. Sub-anesthetic ketamine infusion at similar doses is employed in human subjects both as a model for schizophrenia (Frohlich and Van Horn, 2014; Krystal et al., 1994) and as a treatment for depression (Berman et al., 2000; Krystal et al., 2013). While previous studies have shown ketamine-induced changes to FC, each has employed either a global analysis (Anticevic et al., 2015; Driesen et al., 2013a; Joules et al., 2015) or examined FC changes to seeds in a single region (Dandash et al., 2015; Driesen et al., 2013b; Grimm et al., 2015). The present study provides a more extensive analysis of the effects of ketamine on cortico-limbic connectivity than has been previously published.

The strongest brain FC network changes induced by ketamine were in connection with the dlPFC, a region strongly implicated in schizophrenia (Arnsten et al., 2012; Meyer-Lindenberg, 2010; Meyer-Lindenberg et al., 2005; Minzenberg et al., 2009), bipolar disorder (Anticevic et al., 2013; Frangou et al., 2008), and major depression (Concerto et al., 2015; Dutta et al., 2014). Ketamine induced significant increases in dlPFC FC with frontal, striatal and temporal areas of limbic and affective processing networks in addition to sensorimotor and attention networks. Increases in FC between dlPFC and hippocampus have been reported in both humans and rats (Grimm et al., 2015), and the widespread increase in FC from baseline observed in this study could be related to the disinhibition of dlPFC after ketamine administration that has been reported by many systems neuroscience studies (Arnsten et al., 2012; Wang and Arnsten, 2015).



Pretreatments with the anti-psychotic drug risperidone attenuated ketamine-induced increases in FC to dlPFC from a number of regions, especially limbic and affective processing areas. This indicates that one mechanism of risperidone action is to counteract the effects of dlPFC disinhibition.

Ketamine infusion also increased the FC of SgC, amygdala, and OFC to limbic and affective processing networks. Disruptions in FC within these cortico-limbic networks has been shown repeatedly in mood disorders (Anand et al., 2009; Mayberg, 2003; Phillips and Swartz, 2014) and the ketamine-induced increases in connectivity in these networks may be related to its efficacy as an antidepressant. Risperidone pretreatment substantially attenuated ketamine-induced FC within affective processing network. In fact, ketamine-RispKet effects of FC in limbic and affective processing networks were much stronger in extent than ketamine-baseline effects because the RispKet session exhibited *reduced* FC within affective processing networks compared to baseline. This indicates that risperidone is acting to decrease the functional connections in limbic networks, which may be related to some of the side effects associated with risperidone treatment (Miyamoto et al., 2005).

Ventral striatum (NAcc) plays an important role in motivation and mood regulation. The results of this study showed that ketamine induced increased FC of ventral striatum with amygdala and temporal affective processing regions as well as the default mode network. These effects were counteracted by pretreatment with risperidone, and in fact, reductions in FC between striatum and parietal regions of the DMN have been associated with alleviation in symptoms following antipsychotic treatment (Sarpal et al., 2015).

Finally, PCC (which is a major hub in the DMN) exhibited increased FC with NAcc and striatal affective processing regions after ketamine infusion. The DMN shows abnormal FC in both mood disorders (Greicius et al., 2007; Ongur et al., 2010) and schizophrenia (Rotarska-Jagiela et al., 2010; Woodward et al., 2011). Pretreatment with risperidone attenuated these effects while increasing PCC FC to anterior DMN regions. This result was reinforced by the RispKet-baseline comparison which revealed *increased* PCC FC to DMN regions and reduced PCC FC with affective processing regions during RispKet.

Rhesus macaque resting state FC networks are known to show little difference between contralateral and ipsilateral FC (Adachi et al., 2012; Hutchison et al., 2012). The FC networks examined in the baseline session in this study were consistent with prior studies exhibiting little hemispheric asymmetry. However, ketamine infusion resulted in significant departures from hemispheric symmetry in most of the FC networks examined in this study. These results are consistent with breakdown in interhemispheric symmetry of FC networks in human models of schizophrenia and other mood disorders (Guo et al., 2013; Zhang et al., 2015). Pre-treatment with risperidone (RispKet) reduced the hemispheric asymmetry in FC networks induced by ketamine for the dlPFC and amygdala seeds.

Overall, these results indicate that ketamine induces hyperconnectivity in NHP functional brain networks associated with emotional regulation, cognitive control, and motivation. These findings are highly consistent with similar studies of the effects of ketamine on FC in concordant human brain networks (Anticevic et al., 2015; Dandash et al., 2015; Driesen et al., 2013a). Further, pretreatment with risperidone significantly attenuated the effects of ketamine, which is also consistent with findings in human subjects (Joules et al., 2015).

### 3.6.1 Insights into the results of the ketamine drug infusion phMRI study

In the recently published companion paper (Maltbie et al., 2016) we reported sustained robust BOLD phMRI response to ketamine infusion in a number of cortical and subcortical regions including anterior and mid-cingulate cortex, anterior STG, SMA and thalamus, which were consistent with results of human studies on BOLD response to ketamine-infusion induced (De Simoni et al., 2013; Doyle et al., 2013). Ketamine induced BOLD phMRI response to dlPFC was significant but not as strong as the areas mentioned above. Thus, the fact that the strongest changes in FC with respect to baseline during sustained ketamine infusion occurs in brain networks connected to dlPFC indicates that FC is sensitive to brain mechanisms distinct from mere blood flow response to ketamine infusion. This result is consistent with studies in human subjects (Khalili-Mahani et al., 2015) which report spatial heterogeneity between CBF and FC network changes after ketamine infusion. Indeed, since FC network alterations induced by ketamine administration are consistent with those caused by schizophrenia (Anticevic et al., 2015; Driesen et al., 2013a) measures of functional connectivity in brain networks may in fact elucidate more pertinent information regarding disease mechanisms than pure phMRI BOLD activation maps regarding the effects of ketamine on brain function.

### 3.6.2 Limitations

Ketamine challenge is not an exact model of schizophrenia (Cohen et al., 2015). One recent paper suggests that this may be due to changes over the time course of disease pathology, and the ketamine model may be consistent with early-but not chronic-schizophrenia (Anticevic et al., 2015). No experiments were done to test the effects of risperidone alone on FC of brain networks. While this may be an interesting future

direction, to our knowledge no studies have examined the effects of risperidone challenge (or other acute second-generation antipsychotic) alone on FC, though several studies have investigated the effects of chronic antipsychotic treatment (Hadley et al., 2014; Kraguljac et al., 2016). Finally, the small sample size ( $N = 4$ ) is another limitation of this study, rendering it not amenable to more sophisticated statistical analyses which may lend more accurate and quantitative estimates of the effects of ketamine on brain function networks.

While antipsychotics, such as risperidone, are administered chronically in the treatment of schizophrenia, only acute administration was considered in this study. The therapeutic response occurs gradually, with symptoms decreasing over a period of days and weeks (Agid et al., 2003). However, the effects of risperidone are mediated primarily via D2 and 5-HT<sub>2</sub> receptor antagonism with high occupancy levels being achieved within hours of acute administration (Nyberg et al., 1993) and there is evidence suggesting that D2 receptor occupancy on the second day of treatment is predictive of the eventual clinical response (Catafau et al., 2006). Thus, the acute effects of risperidone should provide important insights into the validity of our translational model.

The endocrine status of the female subjects featured in this study was not monitored. To the knowledge of the author, no sex differences have been previously reported for the psychotomimetic effects of ketamine in humans. While it is possible that the endocrine status of the subjects affected the results, the evidence in the literature suggests that any effects should be minimal. A review (Cyr et al., 2001) found no effects of ovariectomy on NMDARs in brain regions other than the hippocampus. Further, a recent study in rats showed no effect of ovariectomy on the disruption of pre-pulse inhibition by ketamine (van den Buuse et al. 2015).

### **3.7 Conclusion**

In conclusion, this study adds to previous evidence that phMRI in NHPs can provide a highly translational model for studying the effects of ketamine, which may provide new insights into multiple brain disorders and could also be used for evaluating novel antipsychotics. Indeed, measures of FC may provide more information regarding the effects of ketamine on brain circuitry than general ketamine-induced BOLD response changes. The finding that the dlPFC exhibits such broad and robust increases in functional connectivity implies that altered processing in this region may be a critical driver of the behavioral effects of ketamine.

**Table 3-1** Areas showing significant (voxel-level  $p < 0.07$ ; multiple comparison corrected cluster-level  $\alpha < 0.05$ ) differences based on Wilcoxon signed rank-test z-scores in seed-FC between different drug-infusion conditions as well as between these drug-infusion conditions and baseline; for all seed ROIs selected for cross-correlation analysis.

<b>Dorsolateral Prefrontal Cortex</b>	
Ketamine > Baseline	Ventral anterior cingulate (vACC), orbitofrontal cortex (OFC), subgenual cingulate (SgC), dorsal anterior cingulate (dACC), ventrolateral prefrontal cortex (vlPFC), dlPFC, superior frontal cortex (SFC), nucleus accumbens (NAcc), caudate, putamen, anterior insula, amygdala, inferior frontal gyrus (IFG), insula, anterior superior temporal gyrus (STG), STG, posterior STG, anterior inferior temporal gyrus (ITG), anterior middle temporal gyrus (MTG), supplementary motor area (SMA), cingulate, premotor cortex (PMC), primary motor cortex (M1), primary somatosensory cortex (S1), cerebellum
Ketamine > RispKet	SgC, NAcc, caudate, putamen, globus pallidus, thalamus, amygdala, anterior insula, anterior STG, vlPFC, SFC, STG, MTG, cerebellum
RispKet > Ketamine	Superior aspects of SMG, superior parietal lobule (SPL)

RispKet > Baseline	SgC, dACC, NAcc, ventral caudate and putamen, SFC, dlPFC, SMA, cingulate, PCC, posterior parahippocampal cortex (PHC), precuneus
Baseline > RispKet	Thalamus, MTG
<b>Orbitofrontal Cortex</b>	
Ketamine > Baseline	SFC, dlPFC, ventral tegmental area (VTA), retrosplenial cortex , posterior PHC, cerebellum
Ketamine > RispKet	SgC, ACC, OFC, caudate, NAcc, amygdala, anterior STG, STG, insula, MTG, cerebellum
RispKet > Ketamine	Lateral parietal cortex, precuneus
RispKet > Baseline	SFC, dlPFC, dACC, retrosplenial cortex and cerebellum
Baseline > RispKet	Ventral ACC, ventromedial PFC, OFC, anterior caudate and putamen, NAcc, amygdala

<b>Subgenual Cingulate</b>	
Ketamine > Baseline	SFC, dlPFC, STG, insula, premotor cortex, SMA, cingulate, IFG, cerebellum
Ketamine > RispKet	vACC, OFC, SgC, dACC, vlPFC, dlPFC, SFC, NAcc, caudate, putamen, anterior insula, amygdala, anterior STG, IFG, insula, SMA, cingulate, STG, MTG, SMG
Baseline > RispKet	caudate, putamen, NAcc, anterior insula, amygdala, vlPFC, OFC, SgC, anterior STG, anterior insula, IFG, insula, MTG, STG
<b>Nucleus Accumbens (VS)</b>	
Ketamine > Baseline	caudate, putamen, thalamus, amygdala, anterior insula, anterior STG, PCC, SMA, SFC, lateral SMG, posterior STG, MTG
Ketamine > RispKet	NAcc, caudate, putamen, amygdala, thalamus, dlPFC, SFC, anterior insula, anterior STG, vlPFC, SMA, PCC, STG, SMG, MTG
<b>Amygdala</b>	
Ketamine > Baseline	SgC, NAcc, anterior caudate and putamen, amygdala



Ketamine > RispKet	NAcc, caudate, putamen, thalamus, amygdala, anterior insula, anterior STG, IFG, insula, STG
Baseline > RispKet	SgC, vACC, vlPFC, OFC, NAcc, caudate, putamen, thalamus, amygdala, anterior insula, anterior STG, dlPFC, SFC, IFG, insula, STG, secondary somatosensory cortex, SPL
<b>Posterior Cingulate</b>	
Ketamine > Baseline	NAcc, anterior caudate and putamen , SMA, cingulate, posterior PHC, cerebellum,
Ketamine > RispKet	NAcc, anterior caudate and putamen, anterior STG
RispKet > Ketamine	Medial PFC, ACC
RispKet > Baseline	SFC, dlPFC, cingulate, SMA, dACC, PCC, retrosplenial cortex, posterior PHC, cerebellum
Baseline > RispKet	NAcc, caudate, putamen, globus pallidus, thalamus, amygdala

**Table 3-2** Areas showing significant (voxel-level  $p < 0.07$ ; multiple comparison corrected cluster-level  $\alpha < 0.05$ ) differences based on Wilcoxon signed rank-test z-scores in FC between left and right hemisphere seeds, during different scan conditions.

<b>Dorsolateral Prefrontal Cortex</b>	
<b><i>Ketamine</i></b>	
Left seed-FC > Right seed-FC	Left: SFC, FEF, PMC, M1, S1, insula, SMG, amygdala  Bilateral: caudate, NAcc, putamen, amygdala, IFG, OFC, ACC, SgC, STG
<b><i>RispKet</i></b>	
Left seed-FC > Right seed-FC;	Bilateral thalamus: nucleus reuniens
Right seed-FC > Left seed-FC	Left amygdala
<b><i>Baseline</i></b>	
Left seed-FC > Right seed-FC	Right amygdala
Right seed-FC > Left seed-FC	Right caudate

<b>Amygdala</b>	
<b><i>Ketamine</i></b>	
Right seed-FC > Left seed-FC	Right: IFG, thalamus, anterior temporal lobe  Bilateral: SMA, cingulate gyrus, precuneus, PMC, STG, MTG, anterior insula, putamen, caudate, NAcc, SgC, OFC
<b><i>RispKet</i></b>	
Right seed-FC > Left seed-FC	Bilateral: PCC, cingulate, hippocampus, posterior PHC  Left: SPL, SMG
<b>Orbitofrontal Cortex</b>	
<b><i>Ketamine</i></b>	
Left seed-FC > Right seed-FC	Bilateral: ACC, SgC, SFC, dlPFC, cingulate, PCC, SMG, posterior MTG, STG, anterior insula, caudate, putamen, amygdala, thalamus
<b><i>RispKet</i></b>	

Left seed-FC > Right seed-FC	Bilateral: ACC, SgC, SFC, dlPFC, IFG, cingulate, PCC, insula, putamen, PHC; Right lateral parietal cortex
<b>Baseline</b>	
Left seed-FC > Right seed-FC	Bilateral: putamen, insula Left STG; Right: SPL, SMG
<b>Subgenual Cingulate</b>	
<b>Ketamine</b>	
Right seed-FC > Left seed-FC	Bilateral: OFC, ACC, SFC, dlPFC, insula, STG, MTG, thalamus, caudate, amygdala, hippocampus
<b>RispKet</b>	
Right seed-FC > Left seed-FC	Bilateral: dlPFC, SgC, cingulate, SMA, PCC, insula, STG, MTG, thalamus, PHC; Right: caudate, putamen
<b>Baseline</b>	
Right seed-FC > Left seed-FC	Right ventral striatum

<b><i>Posterior Cingulate Cortex</i></b>	
<b><i>Ketamine</i></b>	
Left seed-FC > Right seed-FC	Bilateral: cingulate gyrus, thalamus, PHC  Left: putamen, globus pallidus, insula, STG  Right: dlPFC, SFC
<b><i>RispKet</i></b>	
Left seed-FC > Right seed-FC	Bilateral: cingulate gyrus, thalamus, dlPFC, SFC, STG, SMG  Right: insula, IFG
<b><i>Baseline</i></b>	
Left seed-FC > Right seed-FC	Left: putamen, globus pallidus

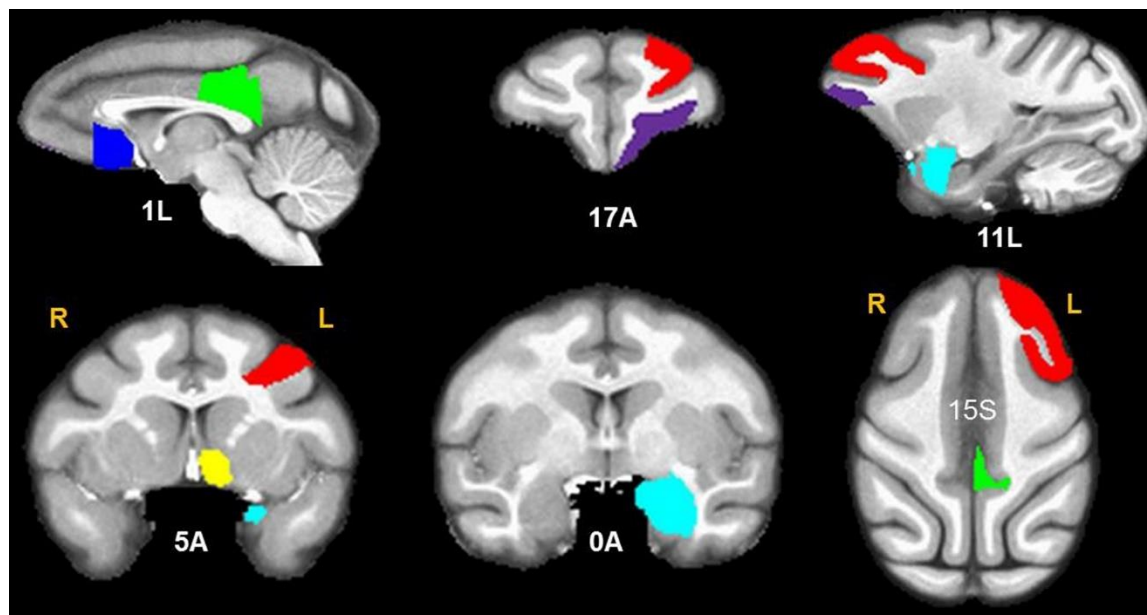


**Figure 3-1** A priori seed ROI masks drawn based on INIA19 NHP atlas: Red = dorsolateral prefrontal cortex; violet = orbitofrontal cortex; blue = subgenual cingulate cortex; yellow = nucleus accumbens; green = posterior cingulate cortex. Slice locations indicate INIA19 NHP atlas coordinates. Only left hemisphere seed ROIs are highlighted for clarity.

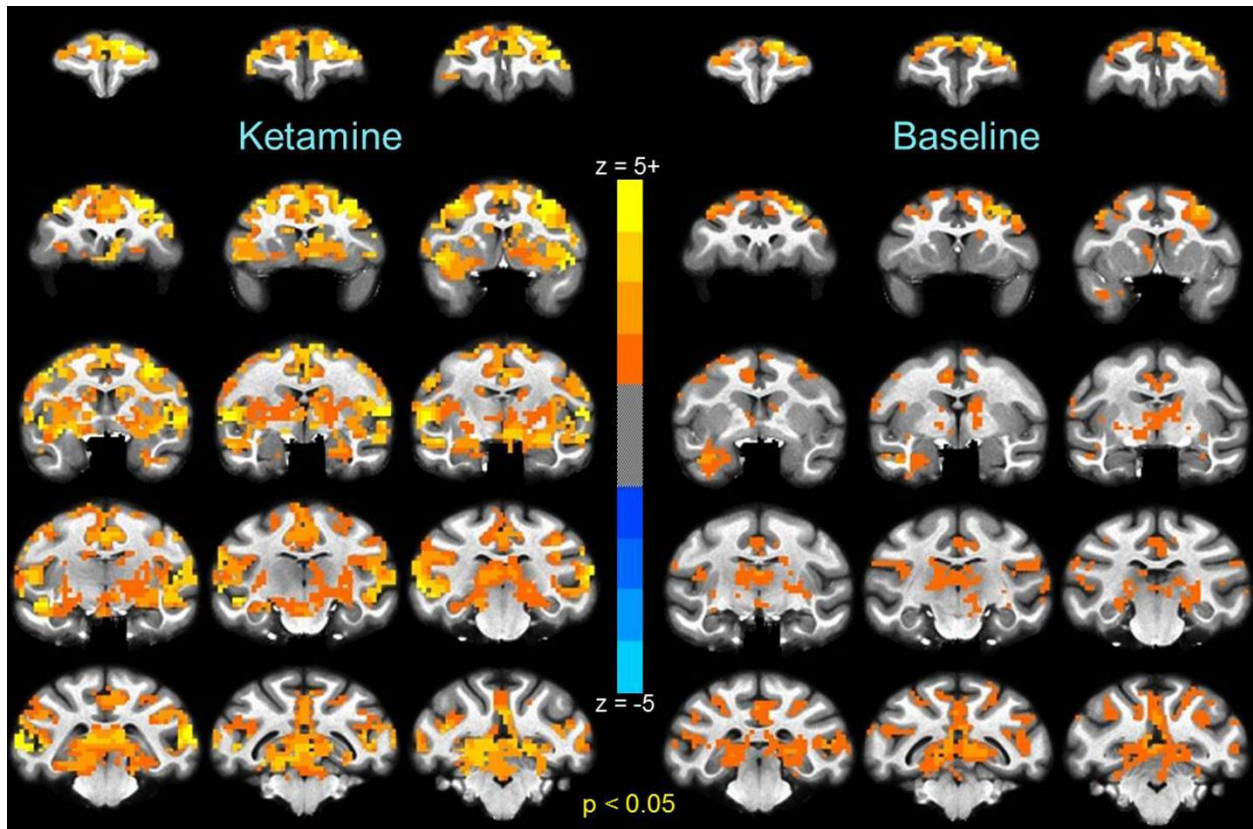


**Figure 3-2** Map of group median z-transformed CC expressing **functional connectivity of left dorsolateral prefrontal cortex** (left) induced by sustained ketamine infusion and (right) at baseline. All the voxels shown are significant at cluster-level  $p < 0.05$  based on the Wilcoxon 1-sample signed rank test (see *Methods*). Coronal slices in the montages proceed from A19 to P23 in INIA19 NHP space in steps of 3mm.

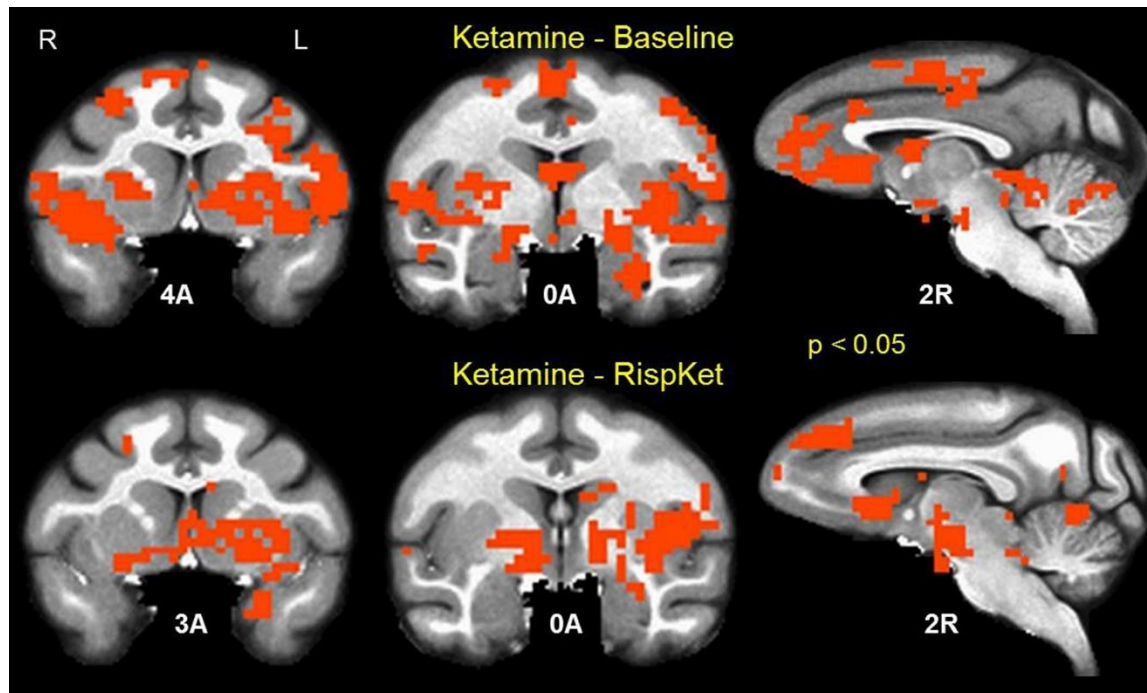


**Figure 3-3** Group Wilcoxon signed rank test results showing regions with significant (cluster-level  $p < 0.05$ ) differences in left dlPFC FC; (top) ketamine induced FC > RispKet session FC (red); and (bottom) ketamine induced FC > baseline FC (red). Slice locations indicate INIA19 NHP atlas coordinates.



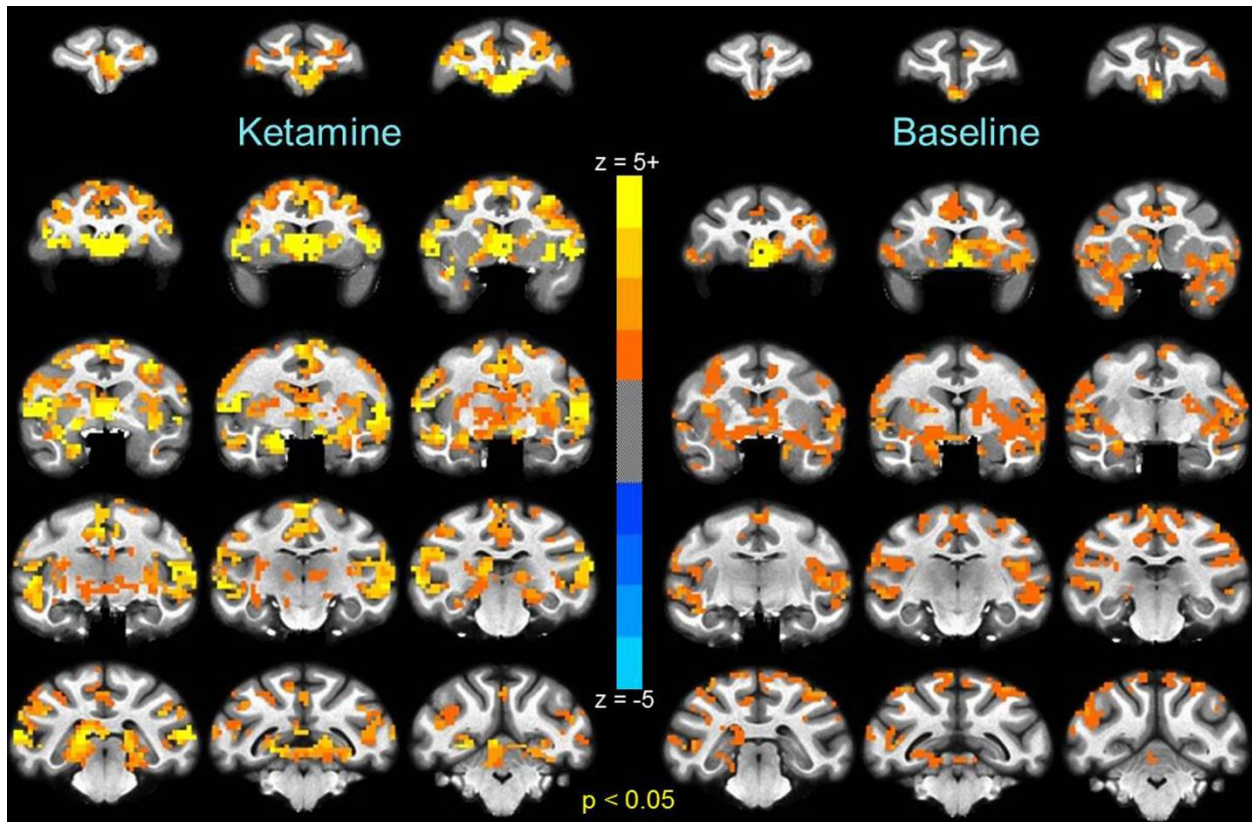


**Figure 3-4** Map of group median z-transformed CC expressing **functional connectivity of left subgenual cingulate** (left) induced by sustained ketamine infusion and (right) at baseline. All the voxels shown are significant at cluster-level  $p < 0.05$  based on the Wilcoxon 1-sample signed rank test (see *Methods*). Coronal slices in the montages proceed from A19 to P23 in INIA19 NHP space in steps of 3mm.

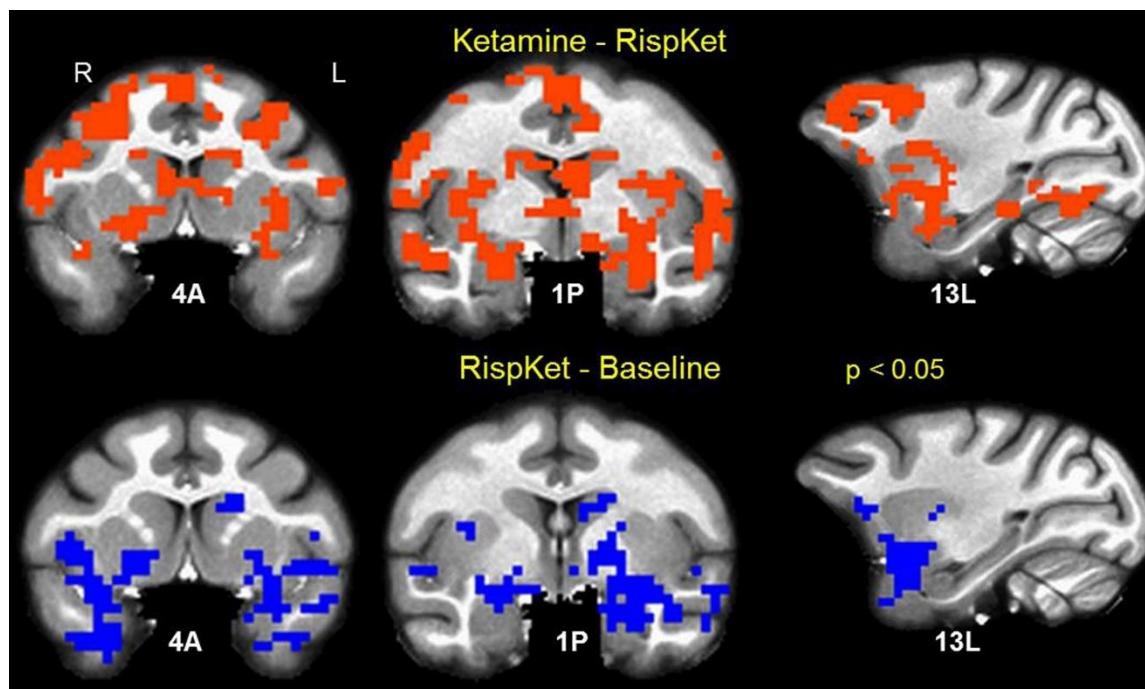


**Figure 3-5** Group Wilcoxon signed rank test results showing regions with significant (cluster-level  $p < 0.05$ ) differences in left SgC FC; (top) ketamine induced FC > RispKet session FC (red); and (bottom) RispKet session FC < baseline FC (blue). Slice locations indicate INIA19 NHP atlas coordinates.

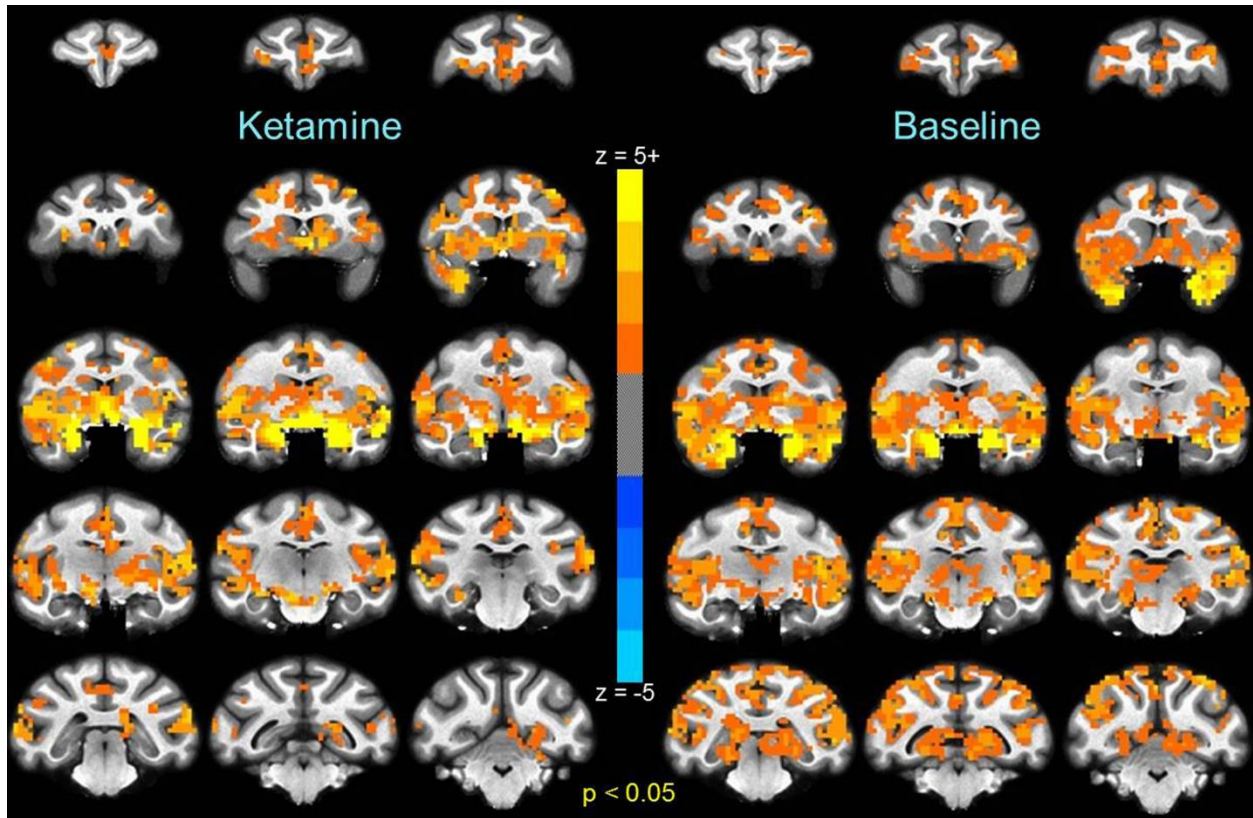


**Figure 3-6** Map of group median z-transformed CC expressing **functional connectivity of left amygdala** (left) induced by sustained ketamine infusion and (right) at baseline. All the voxels shown are significant at cluster-level  $p < 0.05$  based on the Wilcoxon 1-sample signed rank test (see *Methods*). Coronal slices in the montages proceed from A19 to P23 in INIA19 NHP space in steps of 3mm.

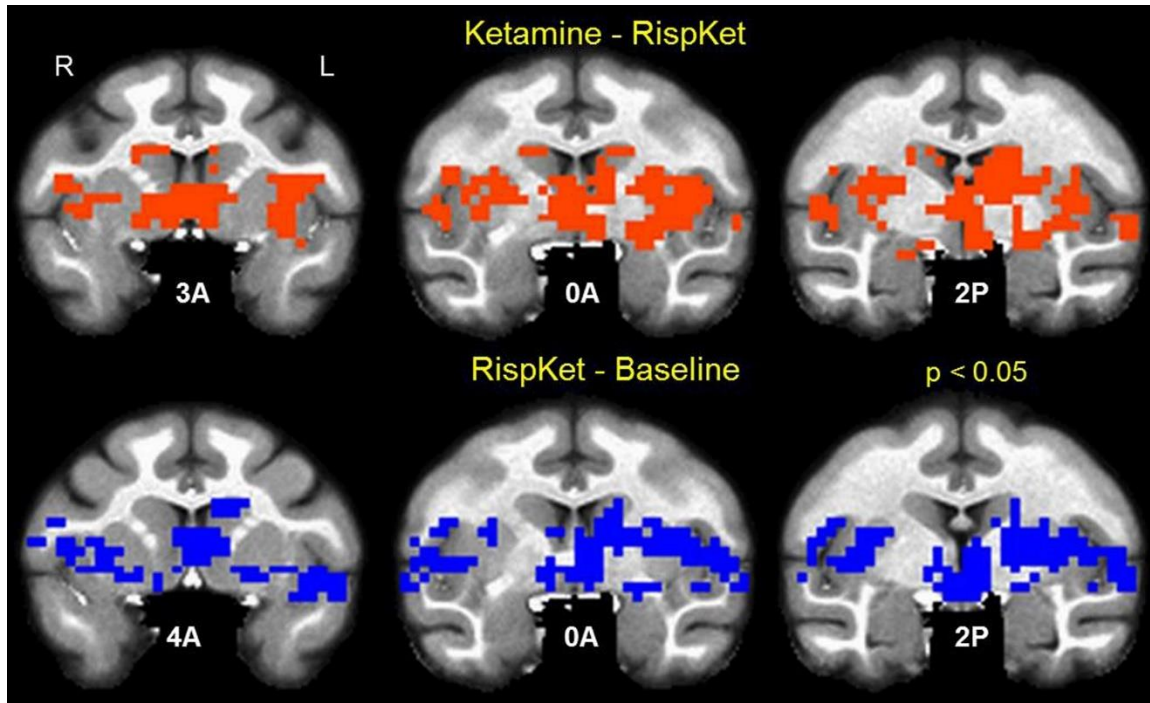


**Figure 3-7** Group Wilcoxon signed rank test results showing regions with significant (cluster-level  $p < 0.05$ ) differences in left amygdala FC; (top) ketamine induced FC > RispKet session FC (red); and (bottom) RispKet session FC < baseline FC (blue). Slice locations indicate INIA19 NHP atlas coordinates.

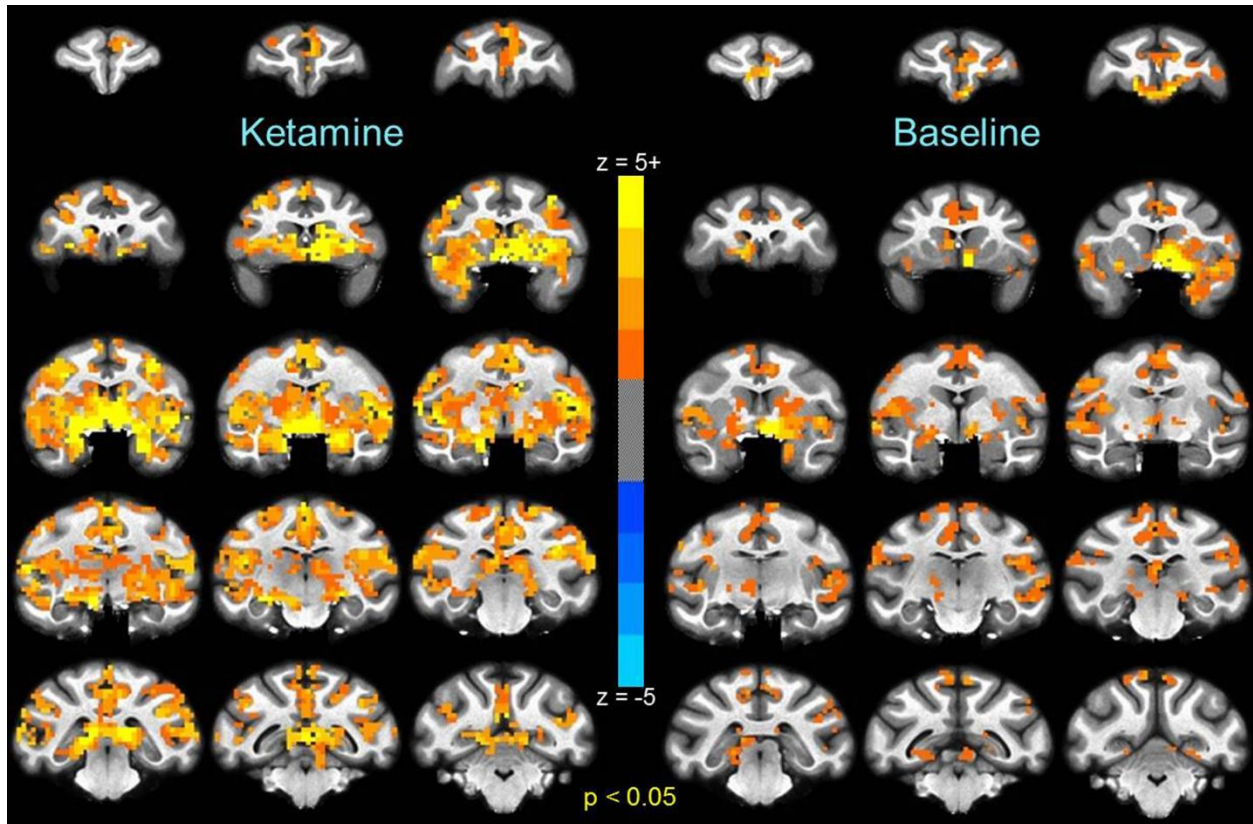


**Figure 3-8** Map of group median z-transformed CC expressing **functional connectivity of left nucleus accumbens (ventral striatum)** (left) induced by sustained ketamine infusion and (right) at baseline. All the voxels shown are significant at cluster-level  $p < 0.05$  based on the Wilcoxon 1-sample signed rank test (see *Methods*). Coronal slices in the montages proceed from A19 to P23 in INIA19 NHP space in steps of 3mm.

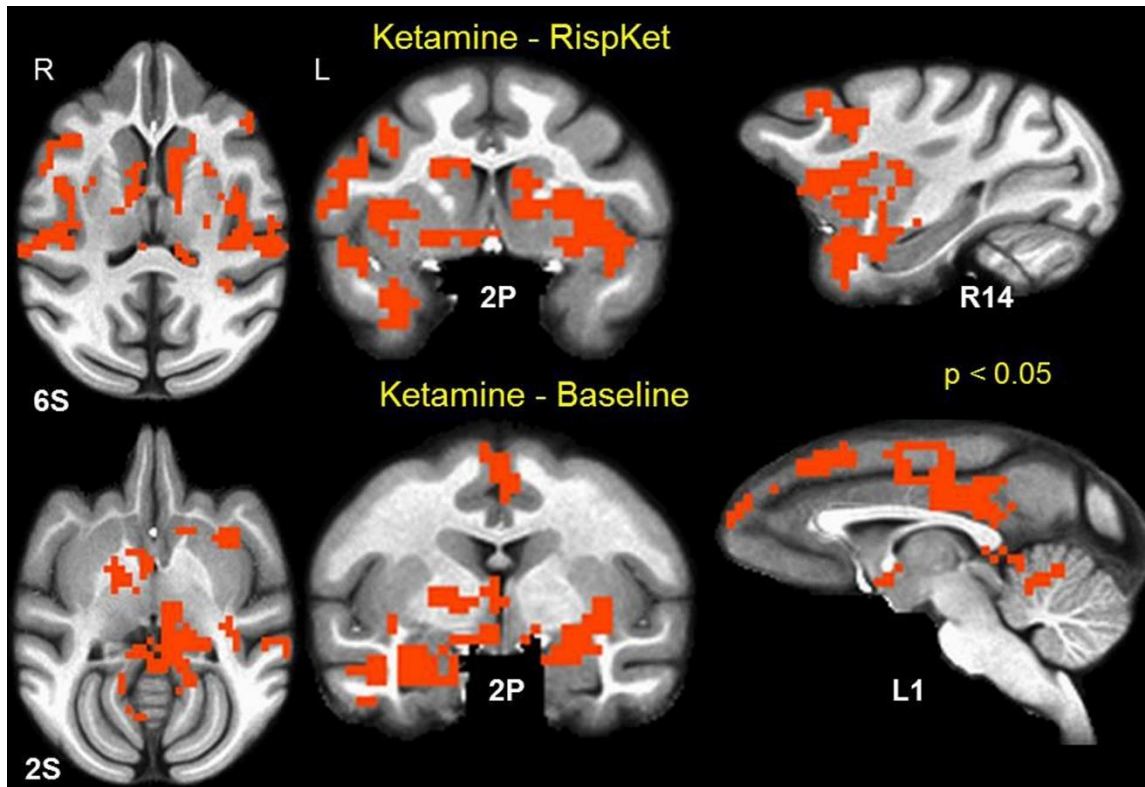


**Figure 3-9** Group Wilcoxon signed rank test results showing regions with significant (cluster-level  $p < 0.05$ ) differences in left NAcc FC; (top) ketamine induced FC > RispKet session FC (red); and (bottom) ketamine induced FC > baseline FC (red). Slice locations indicate INIA19 NHP atlas coordinates.

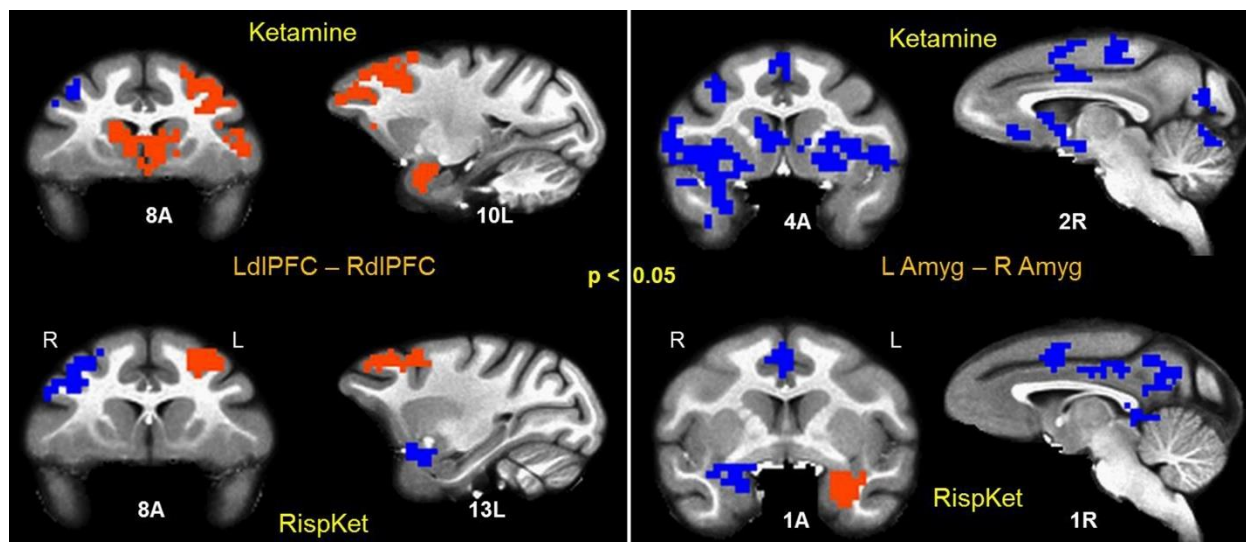


**Figure 3-10** Group Wilcoxon signed rank test results showing regions with significant (cluster-level  $p < 0.05$ ) differences between FC to left and right hemisphere dlPFC (left) and amygdala (right) seed ROIs during ketamine and RispKet session. Left dlPFC/amygdala FC > right dlPFC/amygdala FC (red); right dlPFC/amygdala FC > Left dlPFC/amygdala FC (blue). Slice locations indicate INIA19 NHP atlas coordinates.

**Chapter 4: The interaction of ketamine pretreatment with the disruptive effects of cocaine on functional connectivity in awake rhesus monkeys**



#### **4.1 Context, Author's Contribution, and Acknowledgement of Reproduction**

The following chapter examines the interaction of sub-anesthetic ketamine with the acute effects of cocaine on FC using pharmacological MRI (phMRI) in awake rhesus monkeys. Surgeries were performed by Juliet Brown, animal training and scanning procedures were performed by the author with the help of Marisa Olsen, and MRI data acquisition protocols were designed by the author with the help of Dr. Kaundinya Gopinath, who also contributed valuable data analysis advice. The following unpublished manuscript was written in its entirety, and all experiments were designed, performed, and analyzed by the dissertation author under the guidance of Dr. Leonard Howell.

#### **4.2 Abstract**

**Rationale:** Substance use disorders are characterized by a loss of executive control over reward-based decision making. Deficits in glutamatergic projections between the dorsolateral prefrontal cortex (dlPFC) and nucleus accumbens (NAcc) have been implicated in this process. Acute administration of cocaine decreases functional connectivity (FC) between the dlPFC and NAcc. Ketamine evokes the direct opposite effect on dlPFC-NAcc FC, however the interaction of ketamine and cocaine on FC has not previously been evaluated. Further, while chronic exposure to cocaine has been shown to alter brain function, the effects of drug history on FC remain unknown.

**Objective:** The present study examines the interaction of sub-anesthetic ketamine, given as a pretreatment, with the acute effects of cocaine on FC using pharmacological MRI (phMRI) in awake rhesus monkeys. Further, to evaluate the effects of drug history on FC and the interaction of ketamine with cocaine, scanning is initially performed in drug

naïve/abstinent subjects and subsequently repeated following chronic cocaine self-administration.

**Methods:** One saline and two cocaine (0.3 mg/kg; i.v.) phMRI scans were conducted in three awake adult female rhesus monkeys with no recent drug history. Cocaine scans occurred with and without sub-anesthetic i.v. infusions of ketamine (0.345 mg/kg bolus followed by 0.256 mg/kg/h constant infusion over 1h) 48h prior. These scans were repeated following a two-month period of daily cocaine self-administration. Global brain connectivity (GBC) and dlPFC-NAcc FC were assessed for each scanning session.

**Results:** Pretreatment with ketamine attenuated the effects of cocaine on GBC at the whole-brain level as well as dlPFC-NAcc FC. The reduction in dlPFC-NAcc FC induced by acute cocaine infusion was correlated with response rates during cocaine self-administration. Following chronic cocaine self-administration, whole brain GBC and dlPFC-NAcc FC were reduced. No interaction effect of ketamine pretreatment with acute cocaine infusion was observed following chronic self-administration.

**Conclusions:** These findings have broad implications for the treatment of stimulant use disorder, providing evidence for the potential efficacy of ketamine as a treatment and the important relationship between the connectivity of functional brain networks and substance use disorders.

### **4.3 Introduction**

The global burden of psychostimulant abuse and dependence is substantial, with estimates of prevalence numbering in the tens of millions (Degenhardt et al., 2014). Stimulant use disorder is characterized by an inability to control use despite negative

consequences (Hasin et al., 2013). There is thought to be a loss of executive control over reward-based decision making that leads to compulsive drug use (Everitt and Robbins, 2005). Regions of the prefrontal cortex responsible for executive functions have consistently shown dysfunction associated with substance use disorders in human imaging studies (Goldstein and Volkow, 2011; Koob and Volkow, 2010). The pathways linking prefrontal regions to the reward processing regions of the striatum are well characterized (Haber and Knutson, 2010), and the dysfunction of this fronto-striatal circuitry has also been implicated in substance use disorders (Jentsch and Taylor, 1999; Kalivas, 2009; Kalivas et al., 2005).

Further evidence in the literature specifically implicates aberrant processing by glutamatergic neurons connecting the prefrontal cortex (PFC) to the nucleus accumbens (NAcc) in substance use disorders (Kalivas, 2009), and this pathway has been hypothesized as a potential target for novel treatments (Kalivas and Volkow, 2011). A recent neuroimaging study using functional magnetic resonance imaging (fMRI) in awake rhesus monkeys (Murnane et al., 2015), demonstrated that an acute i.v. dose of cocaine robustly decreased functional connectivity (FC) between the dorsolateral PFC (dlPFC) and the NAcc, indicating a direct effect of the drug on processing within this neural circuitry. Furthermore, the same study found that baseline FC between those same regions (dlPFC-NAcc) was negatively correlated with cocaine intake during self-administration, providing evidence for the behavioral relevance of FC within this circuitry. These findings implicate dlPFC-NAcc FC as a possible biomarker for vulnerability to substance use disorders and clearly warrant further investigation.

One of the few interventions that has been shown to directly affect dlPFC-NAcc FC is sub-anesthetic infusion of the NMDA receptor antagonist, ketamine. As detailed in Chapter 3, ketamine significantly increases FC to the dlPFC from many brain regions, including the NAcc, in rhesus monkeys. While these effects were measured during acute ketamine administration, there is ample evidence (detailed in Chapter 1) for sub-anesthetic ketamine causing neuroplasticity that leads to prolonged behavioral changes. Indeed, sub-anesthetic ketamine treatment has recently been shown to reduce cocaine craving while increasing motivation to quit (Dakwar et al., 2014) and to decrease cocaine choice (versus money) and self-reported cocaine intake (Dakwar et al., 2016) in cocaine dependent human subjects.

Drug history plays an important role in substance use disorders and a distinct advantage of nonhuman primate models is allowing for the use of longitudinal designs that can be utilized to assess within-subject changes caused by chronic drug exposure. Chronic exposure to cocaine has been shown to cause neuroplasticity (Kalivas, 2009) that has been demonstrated to alter both brain structure (DePoy and Gourley, 2015) and function (Porrino et al., 2007). Indeed, the acute effects of cocaine on brain show changes associated with drug history, generating greater metabolic activation following chronic cocaine self-administration (Henry et al., 2010). However, the effects of chronic cocaine exposure on FC remain unknown and could influence baseline FC, the effects of acute cocaine administration, or treatment effects.

The present study used fMRI in awake rhesus monkeys to investigate the interaction of exposure to sub-anesthetic ketamine infusion and cocaine on FC. The acute effects of cocaine on FC, at both the whole-brain level and between the dlPFC and NAcc specifically,

were examined with and without ketamine pretreatment two days prior. The experiments were conducted initially in naïve/abstinent subjects and then repeated following a period of cocaine self-administration to evaluate the effects of chronic cocaine exposure on FC and evaluate whether drug history influences the treatment effects of ketamine.

## **4.4 Methods**

### ***4.4.1 Subjects***

The subjects were three adult female rhesus monkeys (*Macaca mulatta*). Two of the subjects (RRy7 and RMm7) had no previous history of exposure to cocaine or sub-anesthetic ketamine. The third subject (RJz6) had been trained to undergo daily i.v. cocaine self-administration for a previous study, but had no exposure to cocaine during the three years prior to the start of the present study and no prior history of exposure to sub-anesthetic ketamine infusion. All protocols and animal care and handling strictly followed the National Institutes of Health Guide for the Care and Use of Laboratory Animals (8th edition, revised 2011) and the recommendations of the American Association for Accreditation of Laboratory Animal Care, and were approved by the Institutional Animal Care and Use Committee of Emory University.

### ***4.4.2 Surgery and habituation to MRI***

A complete description of the surgery and habituation protocol employed in this study has been described in Chapter 2 (2.4.1) and in greater detail previously (Murnane and Howell, 2010). Briefly, each subject was surgically implanted with chronic indwelling venous catheter attached to a subcutaneous vascular access port prior to being habituated to MRI for the present study. Following surgery, all subjects were gradually habituated to

the scanning apparatus, environment, and all procedures necessary for these experiments over a period of greater than one year.

#### 4.4.3 MRI data acquisition

The MRI imaging methods employed were described previously in Chapter 2. Briefly, the monkeys lay prone in a custom-built restraint cradle (Murnane and Howell, 2010) attached to a head coil designed specifically for rhesus monkeys. In each scanning session, BOLD MRI images were collected utilizing a whole-brain gradient echo single-shot echo planar imaging (EPI) sequence (TR/TE/FA = 2400ms/27ms/90°; 1.5x1.5x1.5 mm; resolution; 1200 measurements). Field inhomogeneities were mapped using a standard Siemens dual gradient echo based field mapping sequence for later correction of any EPI image distortions. A low-resolution T1-weighted (T1w) anatomic scan was acquired using a 3D MPRAGE sequence (TR/TE/TI/FA = 2300ms/2.7ms/800ms/8°; 1.5x1.5x1.5mm resolution) to assist in spatial normalization. Further, for each subject a high resolution (0.5x0.5x0.5mm) T1w 3D MPRAGE anatomic scan was acquired in a separate scanning session to provide a high quality anatomic image for anatomic reference and spatial normalization.

#### 4.4.4 Drug infusion protocol

EPI scans were 48-minutes in duration and consisted of an 8-minute baseline period prior to an i.v. infusion of 0.3 mg/kg of cocaine (or saline control) and followed by 40-minutes of continued scanning. Cocaine scans were performed alone first, then following a sub-anesthetic ketamine pretreatment 48h prior to the cocaine scans. The dose of cocaine has been shown to produce significant effects on FC previously (Murnane et al., 2015) and the 40-minute time-course was chosen because this duration is sufficient to

capture the onset, peak, and offset of the neuropharmacological effects of cocaine in rhesus monkeys (Banks et al., 2009). Cocaine hydrochloride was supplied by the National Institute on Drug Abuse (Bethesda, MD, USA) and dissolved in physiological saline.

#### 4.4.5 fMRI Data Quality Control

The fMRI image time-series data were examined for large motions defined as more than 0.5 mm frame-to-frame displacement. Exclusion criteria were defined as motion above this threshold in more than 10% of the fMRI volumes. None of the scans acquired for these experiments exceeded this threshold and thus no scanning sessions were discarded or repeated.

#### 4.4.6 Ketamine treatment

Ketamine treatments were performed two days (~48h) prior to MRI scanning and occurred with each subject seated in a standard primate chair (primate products) while in an open laboratory environment under the supervision of the experimenter. The dosing regimen was identical to what was used for experiments in Chapters 2-3 and consisted of a one-minute i.v. bolus of 0.345 mg/kg followed by a one-hour constant i.v. infusion of 0.256 mg/kg/h.

#### 4.4.7 fMRI preprocessing and spatial normalization

The fMRI data analysis was described previously in Chapter 3. In brief, all analysis was conducted with AFNI (Cox, 1996) and FSL (Smith et al., 2004) software packages as well as in-house Matlab™ (Natick, MA) scripts. The fMRI time-series images were corrected for field inhomogeneities, temporally shifted, and registered to a base volume. The fMRI time-series were then aligned to the INIA19 rhesus monkey template atlas (Rohlfing et

al., 2012) using the procedure described in Chapter 3. After registration to the atlas, excessive noise was removed from the EPI time-series using the AFNI 3dDespike tool. Finally, the denoised EPI time-series were spatially smoothed with a full-width at half-maximum (FWHM) = 3mm isotropic Gaussian filter.

#### 4.4.8 FC Analysis

The 48-minute fMRI time-series were segmented into 8-minute blocks, consisting of one baseline block and five post-infusion blocks. Functional connectivity (FC) was then calculated independently for each block resulting in an FC time-course for each individual scan. To control for variability across subjects, individual subject data were normalized to the average within-subject baseline prior to self-administration. Normalized subject-level data were averaged together at each separate block to generate group-level FC time-course data.

Global brain connectivity (GBC) was used to examine drug effects on FC at the whole-brain level (Cole et al., 2010). GBC was calculated for each voxel by averaging z-transformed cross-correlations with all other voxel time-courses and expressing the result in the form of effective cross-correlation.

Seed-based cross-correlation analysis (CCA) was employed to assess the strength of FC between the dlPFC seed region and NAcc target region (bilateral). The left hemisphere dlPFC was chosen to be consistent with Chapter 3 and (Murnane et al., 2015). As in Chapter 3, the regions were demarcated on the INIA19 NHP atlas based on associated NeuroMaps labels (Rohlfing et al., 2012). To reduce sensitivity to motion artifacts (Power et al., 2012) and global signal (Saad et al., 2012), the left dlPFC was subdivided into 3x3x3mm non-overlapping sub-regions. The EPI voxel time-series within each sub-



region was averaged to construct sub-region reference vectors. Within each voxel of the NAcc, the z-transformed cross-correlation coefficients of all constituent sub-regions of the left dlPFC were averaged to construct subject-level dlPFC-NAcc FC.

#### 4.4.9 Data analysis

One-way analysis of variance (ANOVA) was used to test for statistical significance. In the event of an overall effect of drug treatment condition, post-hoc Tukey tests were used to establish statistical significance for differences between each drug treatment condition. The standard significance threshold of  $p < 0.05$  was used.

#### 4.4.10 Cocaine Self-administration

To investigate the relationship between cocaine exposure, FC, and behavior, following the first set of scans the subjects were exposed to 40 daily sessions of self-administration (SA). Subjects were trained to self-administer cocaine on a fixed ratio (FR) 20 response schedule of i.v. drug administration in an operant test chamber (Wilcox et al., 2005) using a computer controlled operant panel equipped with stimulus lights and a response lever (MedPC, MedAssociates, St Albans, VT, USA). Drug infusions of 0.03 mg/kg were delivered by an automated pump and paired with the brief illumination of a red light and followed by a 30-second timeout. Each session lasted until 20 infusions were earned or one hour had elapsed, whichever occurred first. Response rates for each subject served as a measure of the reinforcing effects of cocaine.

#### 4.4.11 Experimental timeline

The experimental timeline is detailed in **Table 4-1**. The initial scans consisted of a saline scan, then a cocaine scan with no pretreatment, then a cocaine scan following ketamine

pretreatment (KetCoc scan) in each subject. Following the initial scans, each subject self-administered cocaine daily for 8-10 weeks. The scanning procedures were then repeated with a three-day abstinence period (no SA) preceding a saline scan, then three days of SA and three days of abstinence followed by a cocaine scan, and finally three days of SA and a ketamine treatment on the second of three abstinence days prior to the final KetCoc scan.

## 4.5 Results

### 4.5.1 Acute cocaine administration robustly decreased FC

The acute effects of cocaine on FC prior to the start of self-administration protocols are illustrated in **Figure 4-1**. Acute administration of 0.3 mg/kg of cocaine significantly reduced GBC in gray matter voxels at the whole-brain level. The distribution of voxel-wise differences in GBC between cocaine and saline control are shown in **Figure 4-1a**. Compared to saline control, cocaine administration induced a significant ( $p < 0.05$ ) reduction of -1.31 standard deviations in the mean GBC across 16,048 gray matter voxels. Qualitatively, the cocaine-induced reduction in GBC was evident in nearly every region of the brain, with the notable exception of the nucleus accumbens (NAcc) which exhibited (non-significant) increased GBC compared to saline, as shown overlaid on a coronal section in **Figure 4-1b**.

The delineation of dlPFC and NAcc by NeuroMaps labels (Rohlfing et al., 2012) that was used for regional analysis of the effects of cocaine on FC is shown in **Figure 4-1c**. Cocaine administration induced decreased FC between the dlPFC and NAcc as plotted over time in **Figure 4-1d**. The cocaine-induced reduction in dlPFC-NAcc FC follows a 'U'-shaped

curve characterized by a nadir of  $33 \pm 5\%$  of the average baseline connectivity between 8 and 16 minutes, and a recovery to baseline levels after 32-minutes.

#### 4.5.2 Ketamine pretreatment attenuated cocaine-induced changes in FC

The effects of cocaine administration 48h after sub-anesthetic ketamine infusion (labeled KetCoc) are shown in **Figure 4-2**. Following ketamine pretreatment, there was no effect of cocaine on GBC at the whole-brain level (**Figure 4-2a**). The mean difference in GBC among all gray matter voxels was only -0.02 standard deviations (non-significant) when acute cocaine followed ketamine pretreatment. **Figure 4-2b** displays qualitative differences in GBC between KetCoc and saline control in a coronal section that shows the anterior striatum. KetCoc induced (non-significant) increases to GBC in the NAcc, but overall the contrast map (**Figure 4-2b**) resembles random noise with no consistent global effect compared to the saline control.

Ketamine pretreatment also attenuated the effects of acute cocaine on FC between the dlPFC and NAcc. The time-course of dlPFC-NAcc FC over time for the KetCoc scan (**Figure 4-2c**) reveals a cocaine-induced reduction leading to a 'U'-shaped curve with a nadir of  $49 \pm 21\%$  of the average baseline connectivity between 8 and 16 minutes, qualitatively similar to the time-course for acute cocaine alone. However, following ketamine pretreatment, the effects of cocaine were attenuated at every timepoint, leading to a significant ( $p < 0.05$ ) attenuation of the drug effect when averaged over 32-minutes (**Figure 4-2d**). Indeed, over 32-minutes with no pretreatment, cocaine significantly ( $p < 0.05$ ) reduced dlPFC-NAcc FC to  $46 \pm 5\%$  of the average baseline level. However, following ketamine pretreatment, there was not a significant effect of cocaine, with

dIPFC-NAcc FC falling to  $84 \pm 13\%$  of the average baseline compared to  $96 \pm 13\%$  for saline control (**Figure 4-2d**).

#### 4.5.3 The effects of cocaine on FC predicted response rates during self-administration

Following the initial fMRI experiments, each subject was trained to self-administer cocaine and given daily access to up to 0.6 mg/kg for a two-month period. Details of self-administration for each subject are provided in **Table 4-2**. As noted in the methods, one of the three subjects (RJz6) had a prior history of self-administration and the familiarity with the behavior likely influenced the high response rate in that individual. One of the other subjects (RRy7) exhibited lower sensitivity to cocaine, and a unit dose 0.03 mg/kg did not maintain responding in that animal. Even after being switched to a unit dose of 0.1 mg/kg RRY7 had a considerably lower response rate than the other two subjects. Response rates increased over time for all subjects, as evidenced by the average response rate over the final 10 sessions being higher than the overall average response rate in each subject.

As shown in **Figure 4-3**, the peak reduction (difference from within-session baseline to 12-minute timepoint) in dIPFC-NAcc FC induced by cocaine (prior to self-administration), was significantly correlated ( $R^2 = 0.9992$ ) with the average response rate over the final ten sessions. The final ten-session response rate was used to reduce the effect of training that may be present in the earlier sessions, and may provide a more direct representation of the reinforcing effects of the drug than the overall rate.

#### 4.5.4 Chronic cocaine self-administration robustly decreased FC

The effects of chronic cocaine self-administration on FC were evaluated and the results are shown in **Figure 4-4** (see **Table 4-1** for experimental timeline). Saline scans obtained after self-administration (Post-SA saline) were contrasted with saline control scans performed prior to the initiation of self-administration protocols (Pre-SA). The two-month period of cocaine self-administration led to a robust decrease in GBC at the whole-brain level (**Figure 4-4a**) that was similar to what was observed during the acute effects of Pre-SA cocaine (**Figure 4-1a**). During the Post-SA saline scan, the mean GBC across all gray matter voxels was shifted -1.64 standard deviations compared to the Pre-SA saline control scan. The Post-SA saline scans exhibited decreased GBC in nearly all brain regions apart from the NAcc (**Figure 4-4b**), where there were (non-significant) increases in GBC compared to Pre-SA saline control. These effects of chronic cocaine self-administration on GBC followed the same pattern observed for the acute effects of cocaine prior to the initiation of self-administration protocols (**Figure 4-1a-b**).

Following the two-month period of self-administration, there was also a reduction in FC between the dlPFC and NAcc. **Figure 4-4c** displays the average dlPFC-NAcc FC over the full 48-minute Post-SA saline scan compared to the full 48-minute Pre-SA saline scan. There was a significant ( $p < 0.05$ ) reduction in dlPFC-NAcc FC following cocaine self-administration. During the Post-SA saline scan, the average dlPFC-NAcc FC was  $49 \pm 8\%$  of the Pre-SA baseline. For comparison, during the Pre-SA saline scan, the average dlPFC-NAcc FC was  $105 \pm 13\%$  of the Pre-SA baseline.

#### 4.5.5 Acute effects of cocaine on FC following chronic self-administration

Following the two-month self-administration period and subsequent saline scans (see **Table 4-1** for experimental timeline), further scans occurred during which cocaine was

acutely administered (Post-SA cocaine). The results of the Post-SA cocaine scan are displayed in **Figure 4-5**. In contrast to the robust effect of acute cocaine on GBC prior to self-administration (shown in **Figure 4-1a**), Post-SA cocaine did not induce a significant effect on GBC (**Figure 4-5a**). During the Post-SA cocaine scan, the mean GBC in all gray matter voxels differed by -0.40 standard deviations (non-significant) compared to the Pre-SA saline control. There was also an interesting qualitative contrast in the effects of acute cocaine during the Post-SA and Pre-SA cocaine scans. Unlike the pattern observed for Pre-SA cocaine (**Figure 4-1b**), the NAcc did not show elevated GBC relative to other brain regions during the Post-SA cocaine scan (**Figure 4-5b**).

The effects of acute cocaine on dlPFC-NAcc FC were qualitatively similar during the Post-SA cocaine scan compared to the Pre-SA cocaine scan, following a 'U'-shaped curve as illustrated in **Figure 4-5c**. However, during the Post-SA cocaine scan, dlPFC-NAcc FC exhibited a nadir of  $45 \pm 17\%$  of the average (Pre-SA) baseline connectivity during the first 8 minutes after cocaine administration, before recovering to  $62 \pm 25\%$  of the average Pre-SA baseline during the 8 to 16-minute block and remaining just above 60% before recovering to over 80% of (Pre-SA) baseline levels after 32-minutes.

#### 4.5.6 Effects of ketamine pretreatment on FC after self-administration

**Figure 4-6** shows the Post-SA effects of acute cocaine on FC following ketamine pretreatment 48h prior (labeled as Post-SA KetCoc). At the whole-brain level, the Post-SA KetCoc scan closely resembled Post-SA cocaine. The mean GBC in all gray matter voxels was -0.44 standard deviations different (non-significant) from the Pre-SA saline control during Post-SA KetCoc (distribution shown in **Figure 4-6a**). The qualitative pattern of Post-SA KetCoc effects on GBC is displayed in **Figure 4-6b** and closely

resembles the pattern observed for Post-SA cocaine shown in **Figure 4-5b**. Unlike the Pre-SA cocaine and KetCoc scans, there was no evidence of elevated GBC in the NAcc relative to other brain regions during Post-SA KetCoc.

The time-course of dlPFC-NAcc FC during the Post-SA KetCoc scan (shown in **Figure 4-6c**) initially mirrors that of Post-SA cocaine, decreasing to a nadir of  $52 \pm 7\%$  of the average (Pre-SA) baseline connectivity over the 8 to 16-minute time block. After the 16-minute mark of the Post-SA KetCoc scan, the dlPFC-NAcc FC displays a high degree of variability resulting from a combination of both large within-subject fluctuations and high variability between the individual subjects. When averaged over the 32-minutes following cocaine infusion, there was not a significant difference in dlPFC-NAcc FC between Post-SA cocaine ( $58 \pm 5\%$  of Pre-SA baseline) and Post-SA KetCoc ( $68 \pm 11\%$ ) as shown in **Figure 4-6d**.

#### 4.5.7 Individual subject results for dlPFC-NAcc FC

The average dlPFC-NAcc FC measured for individual subjects under each of the drug conditions is displayed in **Figure 4-7**. Two of the subjects that underwent these experiments had no prior history of drug self-administration. The third (RJz6) did have a history of cocaine self-administration, but had not had access to any psychostimulant drugs for a three-year period prior to the initiation of the study. Thus, while the present study was not powered to examine differences caused by differing drug histories, it may be notable that (as shown in **Figure 4-7a**) RJz6 exhibited the largest acute effect of cocaine (Pre-SA) on dlPFC-NAcc FC and also exhibited the smallest attenuation of the cocaine effect following ketamine pretreatment (Pre-SA).

Following the two-month period of self-administration, RJz6 further exhibited the lowest dlPFC-NAcc FC during the Post-SA saline scan, as illustrated in **Figure 4-7b**. In contrast to the Pre-SA results showing that ketamine pretreatment increased dlPFC-NAcc FC during acute cocaine in all 3 subjects, the Post-SA results showed a substantial effect of ketamine pretreatment for RMm7, but very little effect for the other two subjects (**Figure 4-7b**). Compared to Pre-SA cocaine, there was a larger effect of Post-SA cocaine in RRY7, but a smaller effect of cocaine in the other two subjects.

#### **4.6 Discussion**

Global and region-specific changes to FC were characterized following acute i.v. administration of cocaine in conjunction with fMRI in awake rhesus monkeys. A series of repeated scans was performed to examine the effects of pretreatment with sub-anesthetic ketamine and a two-month period of cocaine self-administration on the changes to functional connectivity induced by acute cocaine. The results demonstrate that acute administration of cocaine induces a pronounced reduction in voxel-wise GBC at the whole-brain level as well as in FC between the dlPFC and NAcc regions specifically. Both the reduction in whole-brain GBC and the reduction in dlPFC-NAcc FC were attenuated following ketamine pretreatment 48h prior. During an ensuing period of cocaine self-administration, response rates were correlated with the size of the reduction in dlPFC-NAcc FC induced by cocaine during the prior scans. Following the two-month period of self-administration, both whole-brain GBC and dlPFC-NAcc FC showed robust decreases during a saline control scan. The Post-SA response to cocaine was attenuated for both whole-brain GBC and dlPFC-NAcc FC compared to Pre-SA cocaine. In addition, ketamine



pretreatment did not alter the Post-SA response to acute administration of cocaine at either the whole-brain level or between the dlPFC and NAcc.

Acute administration of cocaine has previously been found to induce reductions in measures of whole brain FC and dlPFC-NAcc FC in awake female rhesus monkeys (Murnane et al., 2015). The study was performed in a sample of three subjects, all with an extensive history of psychostimulant self-administration but following a multi-year period with no access to psychostimulants. The results showed a significant correlation between baseline dlPFC-NAcc FC and cocaine intake during ensuing self-administration. Those findings were strongly corroborated by the results of the present study, which showed nearly identical effects of acute cocaine on whole-brain connectivity and dlPFC-NAcc FC. The design of the present study was intended to maintain a consistent level of cocaine intake across subjects during self-administration. Hence, the correlation of baseline dlPFC-NAcc FC to cocaine intake could not be tested. However, a similar correlation was found between the reduction in dlPFC-NAcc FC induced by acute administration of cocaine and response rates during cocaine self-administration. While cocaine intake was limited in the present design, response rate was allowed to vary and provides a quantitative measure of the reinforcing effects of cocaine (Howell and Fantegrossi, 2009). Notably, the single subject (RJz6) with a previous history of self-administration displayed the highest reduction in dlPFC-NAcc FC during the pre-SA cocaine sessions and also had the highest response rate during self-administration. The prior drug history for this subject may have been related to these findings and may have been important for driving the observed correlation.

The present study is the first to investigate the effects of pretreatment with sub-anesthetic ketamine on cocaine-induced changes in FC. The findings of a significant attenuation of the reductions to whole-brain GBC and dlPFC-NAcc FC induced by acute administration of cocaine, provide evidence for the potential efficacy of ketamine infusion as a pharmacotherapy for psychostimulant use disorders and warrant additional investigation. Moreover, these findings further support the use of FC as a biomarker. The present study was motivated in large part by prior findings that acute sub-anesthetic ketamine infusion induced robust increases in whole-brain GBC (Chapter 1) and functional connectivity from many regions, including the NAcc, to the dlPFC (Chapter 3), in direct opposition to the acute effects of cocaine (Murnane et al., 2015). Future investigation of interventions known to affect FC for the potential treatment of drug abuse is warranted. One such intervention is transcranial magnetic stimulation (Fox et al., 2012), which is already being investigated in conjunction with FC measurements for the treatment of cocaine use disorder (Hanlon et al., 2015a; Hanlon et al., 2015b; Hanlon et al., 2016). Specifically targeting interventions that increase dlPFC-NAcc FC may prove particularly efficacious given the associations of this connection with self-administration behavior described above.

The present finding of decreased GBC at the whole-brain level, but not within the NAcc, following a period of self-administration, agrees with the results of brain imaging studies performed in humans. In a cross-sectional study comparing active cocaine users to matched healthy control subjects, Gu et al. (2010) found cocaine users to have decreased resting-state FC to five of six mesocorticolimbic seeds tested. These included the amygdala, hippocampus, mediodorsal thalamus, rostral anterior cingulate cortex, and

ventral tegmental area. The lone exception was the NAcc, which showed no difference between cocaine users and healthy controls. Indeed, the network connectivity related to the NAcc may be a particularly important biomarker for cocaine abuse, as two human brain imaging studies in abstinent cocaine users found high resting-state FC to NAcc to be associated with relapse (Camchong et al., 2014; Contreras-Rodriguez et al., 2015). Future longitudinal imaging studies should be conducted in translational animal models, such as awake rhesus monkeys, to further characterize the effects of cocaine use on FC.

The blunting of the acute effects of cocaine on FC following a two-month period of self-administration was unexpected, however there are a few possible explanations that may explain this result. Prolonged cocaine use is known to induce various neurobiological changes (DePoy and Gourley, 2015; Porrino et al., 2007), including decreased availability of striatal dopamine receptors (Nader et al., 2002; Volkow et al., 1990) as well as diminished extracellular accumulation of striatal dopamine induced by acute cocaine (Kirkland Henry et al., 2009). The latter effect has even been observed in rhesus monkeys following a limited access period of cocaine self-administration very similar to that employed in the present study (Kirkland Henry et al., 2009). Further, cocaine dependence is a chronic, relapsing disorder (McLellan et al., 2000) and the present study was designed to model a pattern of abstinence and repeated use. Thus, the acute cocaine scans following self-administration were preceded by a two-week block that included a one-week abstinence period followed by three consecutive days of self-administration, followed three more days of abstinence prior to the scan. This procedural schedule (**Table 1**) may have more closely modeled withdrawal than active use. The brain metabolic response to acute cocaine has been shown to be blunted in rhesus monkeys following a 4-

month period of withdrawal from cocaine self-administration as compared to the drug-naïve state (Henry et al., 2010).

#### 4.6.1 Limitations

The primary limitation of the present study was the small sample size consisting of just three subjects. The experiments utilized repeated measurements within each subject to maximize statistical power, however there was not sufficient power to broaden the number of regions of interest or to investigate differences between subjects. Indeed, the subject-level results suggest there may be individual differences in the efficacy of ketamine treatment, but no conclusions could be drawn from the current data. Individual differences in vulnerability to drug dependence have been hypothesized previously (George and Koob, 2010) and future investigation of the efficacy of ketamine as a treatment for substance use disorders would likely benefit from larger samples.

Unfortunately, due to the blunted acute effects of acute cocaine following self-administration, the effects of ketamine pretreatment could not be conclusively evaluated. While no effect of ketamine pretreatment on cocaine-induced changes to FC was observed following the self-administration period, it is not possible from the present data to determine what impact ketamine may have had given a more potent effect of cocaine. Further investigation is warranted given the robust attenuation of the effects of acute cocaine following ketamine pretreatment when tested prior to the period of self-administration.

#### **4.7 Conclusions**

Acute i.v. cocaine infusion robustly decreases FC at the whole-brain level and between the dlPFC and NAcc regions specifically. The impact of cocaine on connectivity between those regions is correlated with the reinforcing effects of cocaine, as measured by response rates during self-administration. Chronic cocaine self-administration and acute administration of cocaine both reduce FC at the whole-brain level and between the dlPFC and NAcc specifically.

While the results following self-administration were inconclusive, pretreatment with sub-anesthetic ketamine was found to robustly attenuate the neural effects of cocaine in the initial scans, suggesting that ketamine may be efficacious as a treatment for cocaine use disorder.

**Table 4-1** Experimental timeline of scanning and drug administration.

<i>Initial scans</i>	Two-month period of SA, then three days of abstinence	Saline scan	One week of abstinence, then three consecutive days of SA, then three days of abstinence	Cocaine scan	One week of abstinence, then three consecutive days of SA, then one day of abstinence	Ketamine infusion day, then one more day of abstinence	KetCoc scan
----------------------	---	-------------	--	--------------	---	--	-------------

**Table 4-2** Details of cocaine self-administration.

<i>Subject</i>	<b><i>RRy7</i></b>	<b><i>RMm7</i></b>	<b><i>RJz6</i></b>
<i>Previous cocaine self-administration</i>	no	no	yes
<i>Age (years)</i>	17	17	18
<i>Unit dose of cocaine (mg/kg/inj)</i>	0.1	0.03	0.03
<i>Total cocaine intake (mg/kg)</i>	23.38	20.55	27.38
<i>Overall response rate (res/sec)</i>	0.18	0.69	2.25
<i>Final 10-session response rates (res/sec)</i>	0.23	1.02	2.7

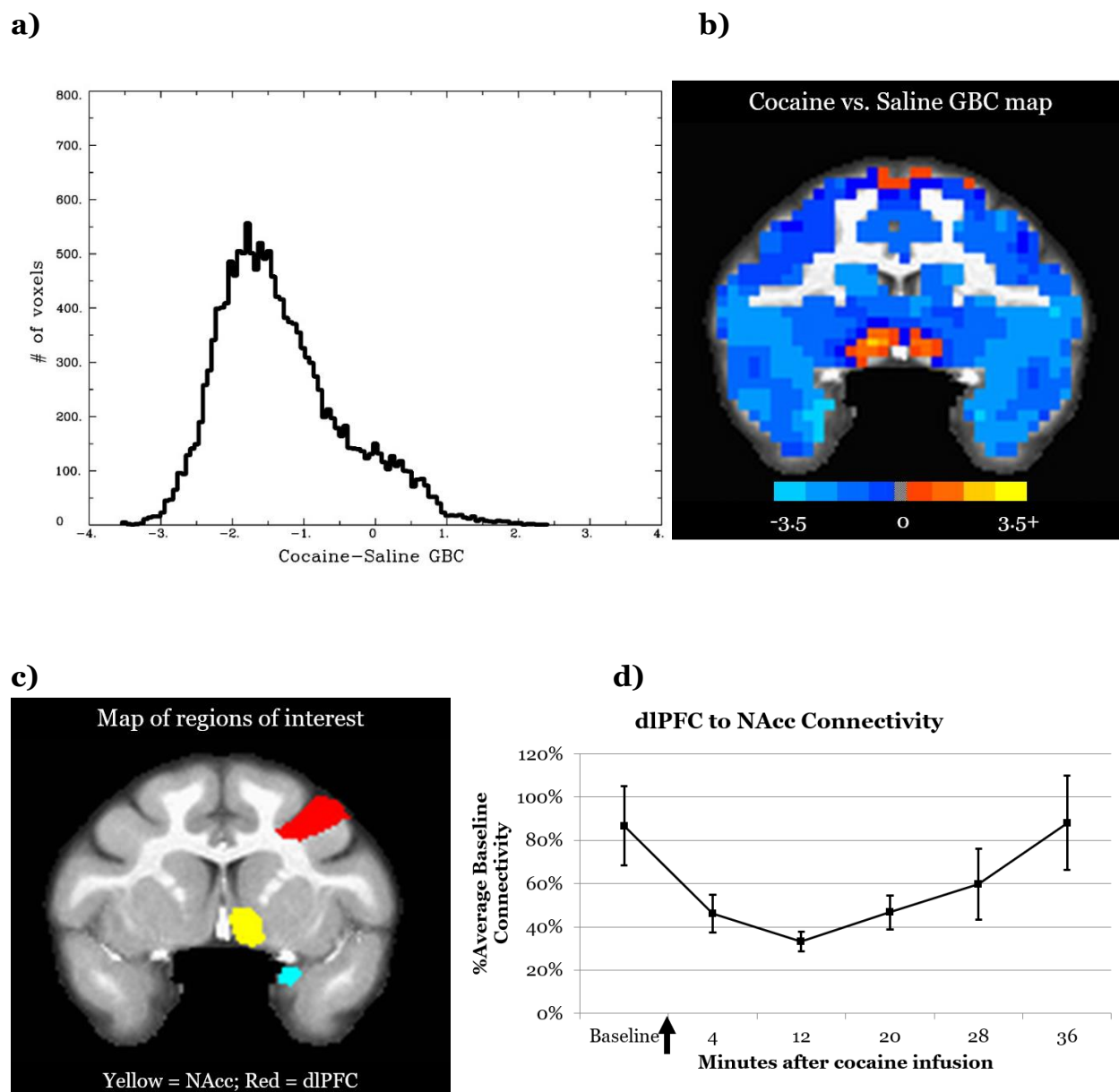


**Figure 4-1** Pre-SA effects of acute administration of cocaine on FC: **(a)** Histogram showing the distribution of voxel-wise contrast in GBC values for cocaine vs. saline for all gray matter voxels. The leftward shift indicates cocaine GBC < saline GBC for most gray matter voxels ( $p < 0.05$ ); **(b)** Coronal section with voxels colored by contrast in z-score of GBC values for cocaine vs. saline. Voxels with cocaine GBC < saline GBC are blue, while voxels with cocaine GBC > saline GBC are orange-yellow; **(c)** Same coronal section shown in (b), but with regions of interest highlighted. Yellow = NAcc; Red = dlPFC; Blue = Amygdala **(d)** Plot of Pre-SA normalized group-average dlPFC-NAcc FC over time during cocaine scan.



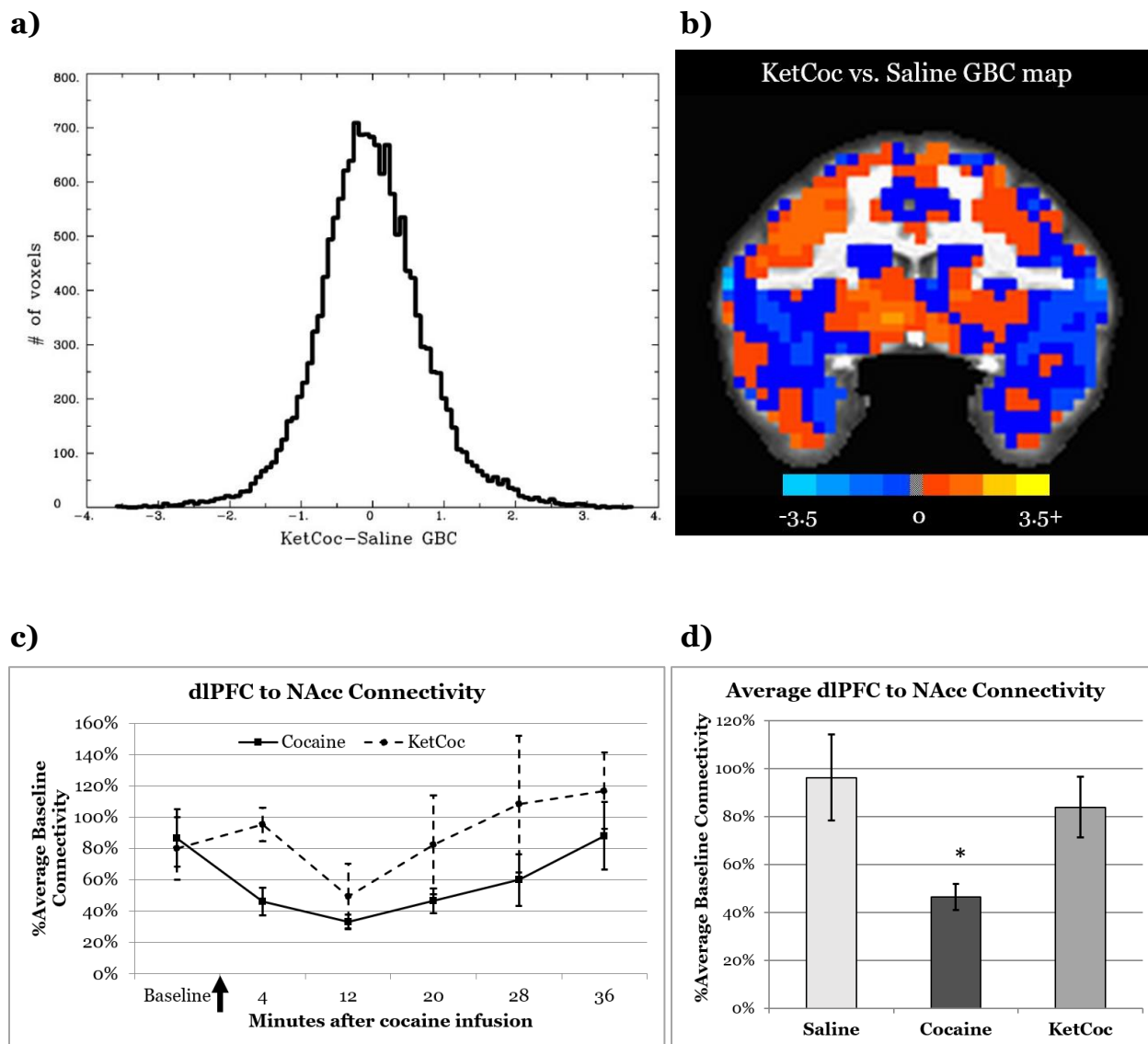


**Figure 4-2** Pre-SA effects of acute administration of cocaine following ketamine pretreatment (KetCoc) on FC: **(a)** Histogram showing the distribution of voxel-wise contrast in GBC values for KetCoc vs. saline for all gray matter voxels. The normal distribution indicates not a significant difference in KetCoc GBC vs. saline GBC at the whole-brain level; **(b)** Coronal section with voxels colored by contrast in z-score of GBC values for KetCoc vs. saline. Voxels with KetCoc GBC < saline GBC are blue, while voxels with KetCoc GBC > saline GBC are orange-yellow; **(c)** Pre-SA normalized group-average dlPFC-NAcc FC over time is plotted for cocaine and KetCoc scans; **(d)** Chart comparing Pre-SA dlPFC-NAcc FC averaged over 0-32 minutes after drug infusion for saline, cocaine, and KetCoc scans. FC is reduced for cocaine compared to both saline ( $p < 0.05$ ) and KetCoc ( $p < 0.05$ ). FC does not significantly differ between saline and KetCoc.

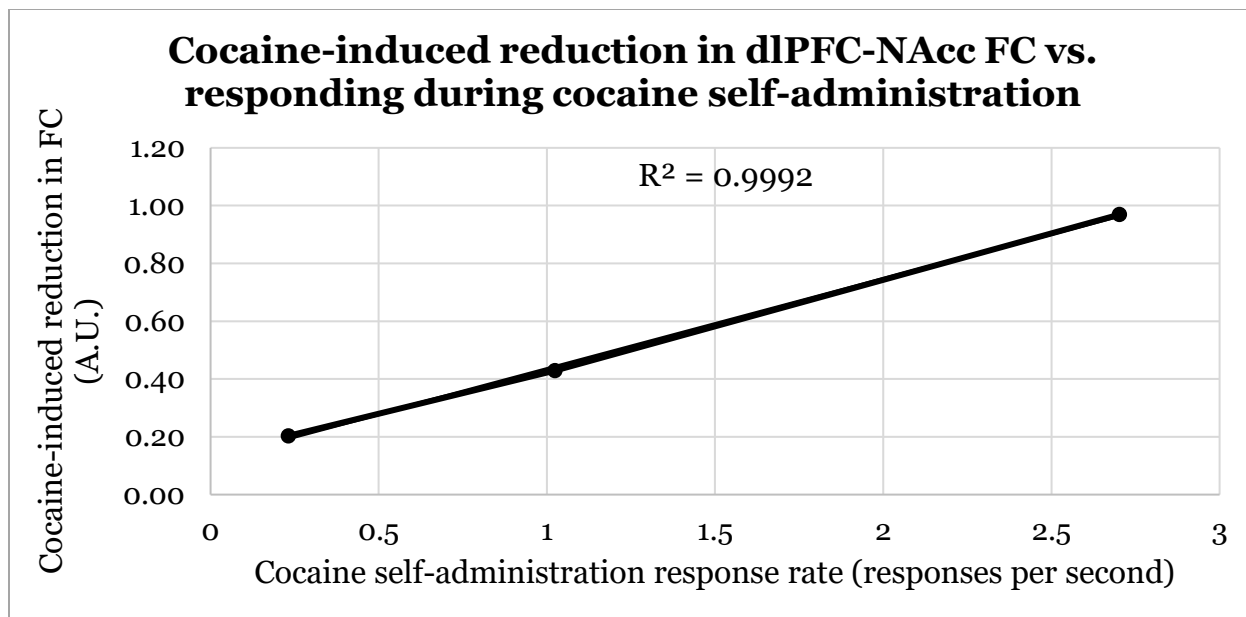


**Figure 4-3** Plot of cocaine-induced reduction in dlPFC-NAcc FC during Pre-SA cocaine scan vs. response rate during cocaine self-administration. A significant ( $p < 0.05$ ) linear relationship is demonstrated. Cocaine-induced reduction in FC is calculated as the difference in FC between the within-scan baseline and the time period 8-16 minutes after infusion when the peak effects of cocaine were observed.

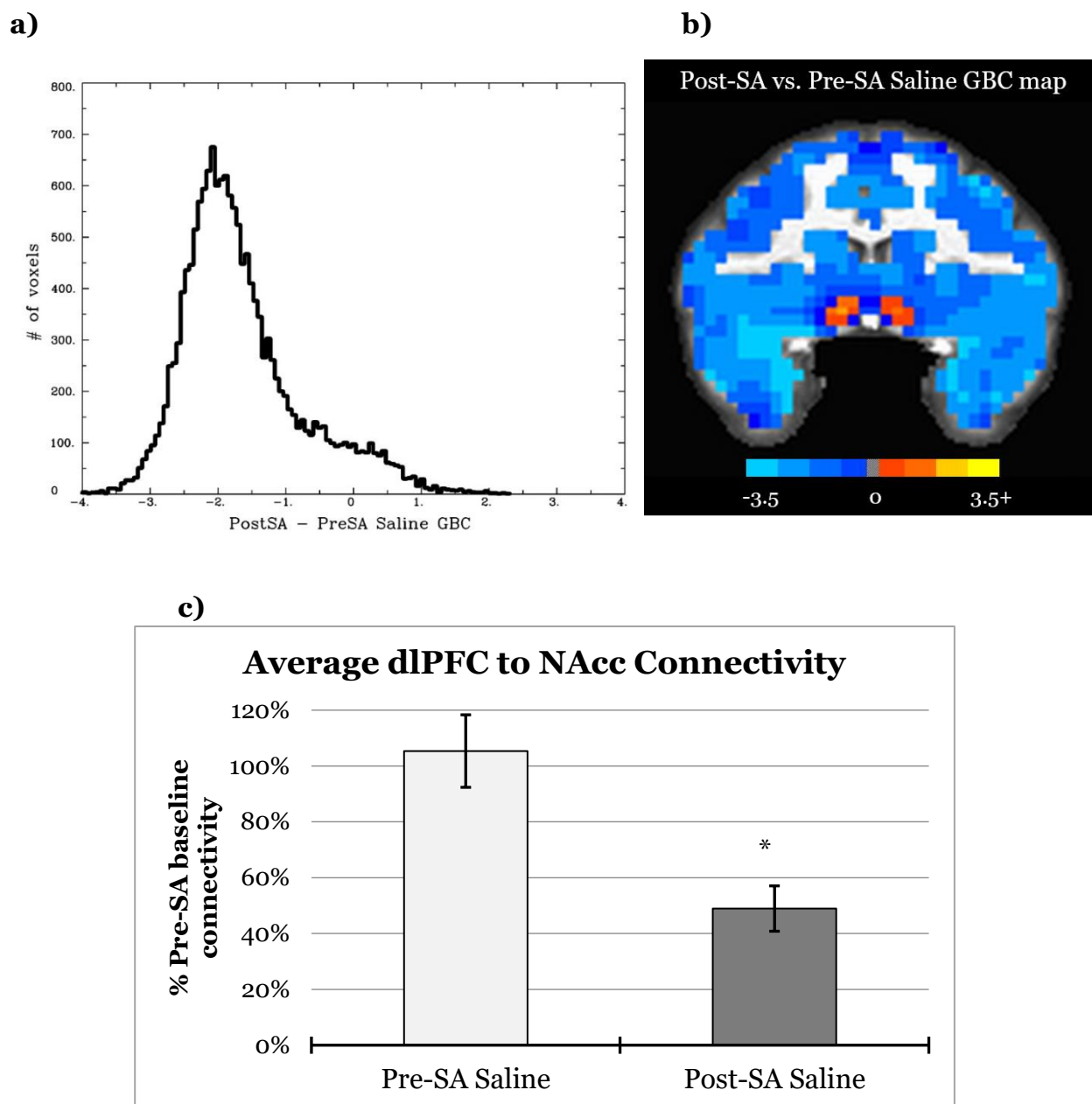


**Figure 4-4** Effects of chronic cocaine self-administration on FC: **(a)** Histogram showing the distribution of voxel-wise contrast in GBC values for Post-SA vs. Pre-SA saline scans for all gray matter voxels. The leftward shift indicates Post-SA saline GBC < Pre-SA saline GBC for most gray matter voxels ( $p < 0.05$ ); **(b)** Coronal section with voxels colored by contrast in z-score of GBC values for Post-SA vs. Pre-SA saline scans. Voxels with Post-SA saline GBC < Pre-SA saline GBC are blue, while voxels with Post-SA saline GBC > Pre-SA saline GBC are orange-yellow; **(c)** Chart comparing Pre-SA dlPFC-NAcc FC averaged over the full 48-minute scan including both baseline and saline infusion for both Pre-SA and Post-SA saline scans. FC is reduced for the Post-SA saline scan compared to Pre-SA saline scan ( $p < 0.05$ ).

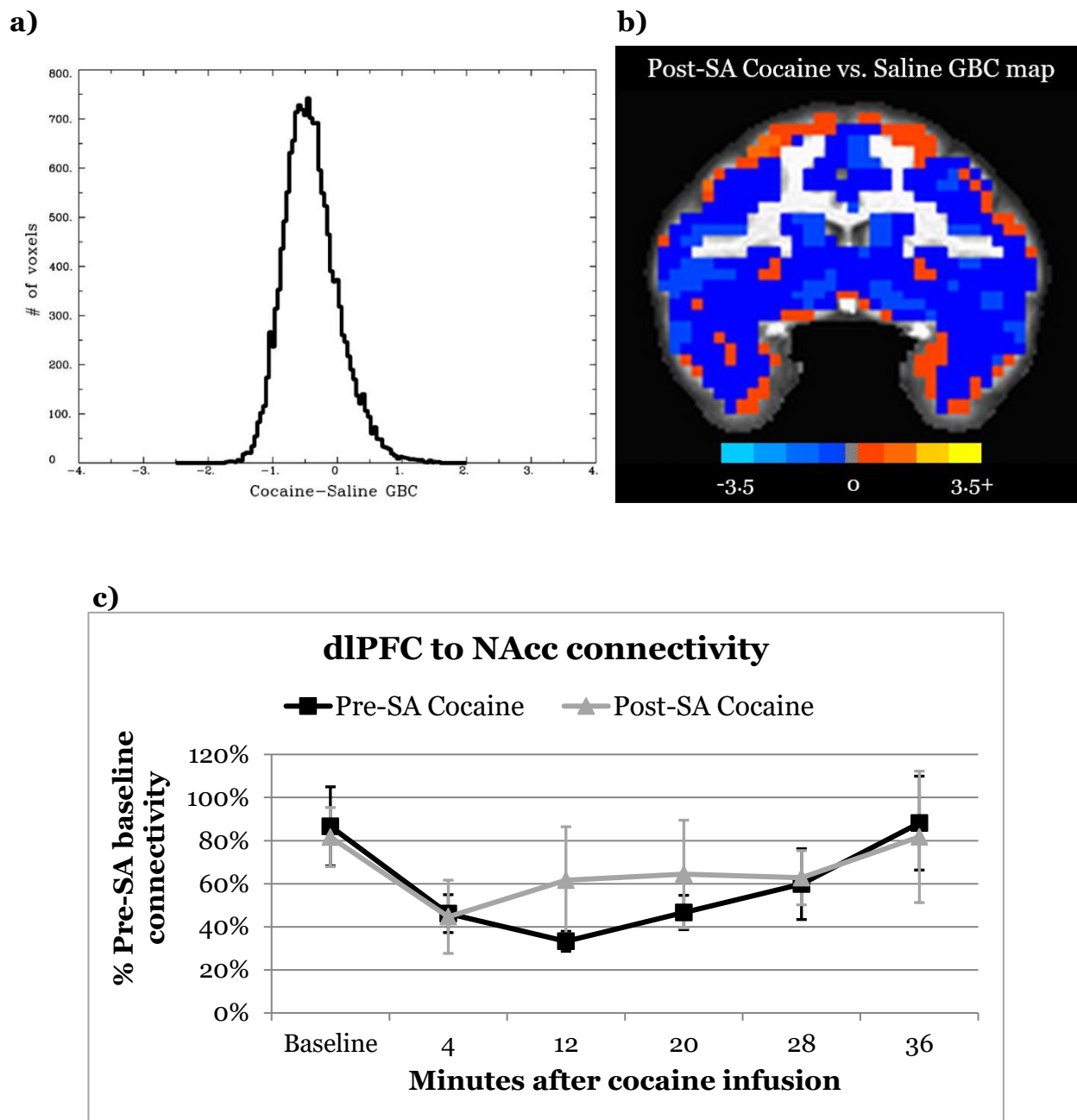


**Figure 4-5** Post-SA effects of acute administration of cocaine on FC: **(a)** Histogram showing the distribution of voxel-wise contrast in GBC values for Post-SA cocaine vs. Pre-SA saline for all gray matter voxels. There is a non-significant leftward shift indicating Post-SA cocaine GBC < Pre-SA saline GBC for some gray matter voxels; **(b)** Coronal section with voxels colored by contrast in z-score of GBC values for Post-SA cocaine vs. Pre-SA saline. Voxels with Post-SA cocaine GBC < Pre-SA saline GBC are blue, while voxels with Post-SA cocaine GBC > Pre-SA saline GBC are orange-yellow; **(c)** Normalized group-average dlPFC-NAcc FC over time is plotted for Pre-SA and Post-SA cocaine scans.

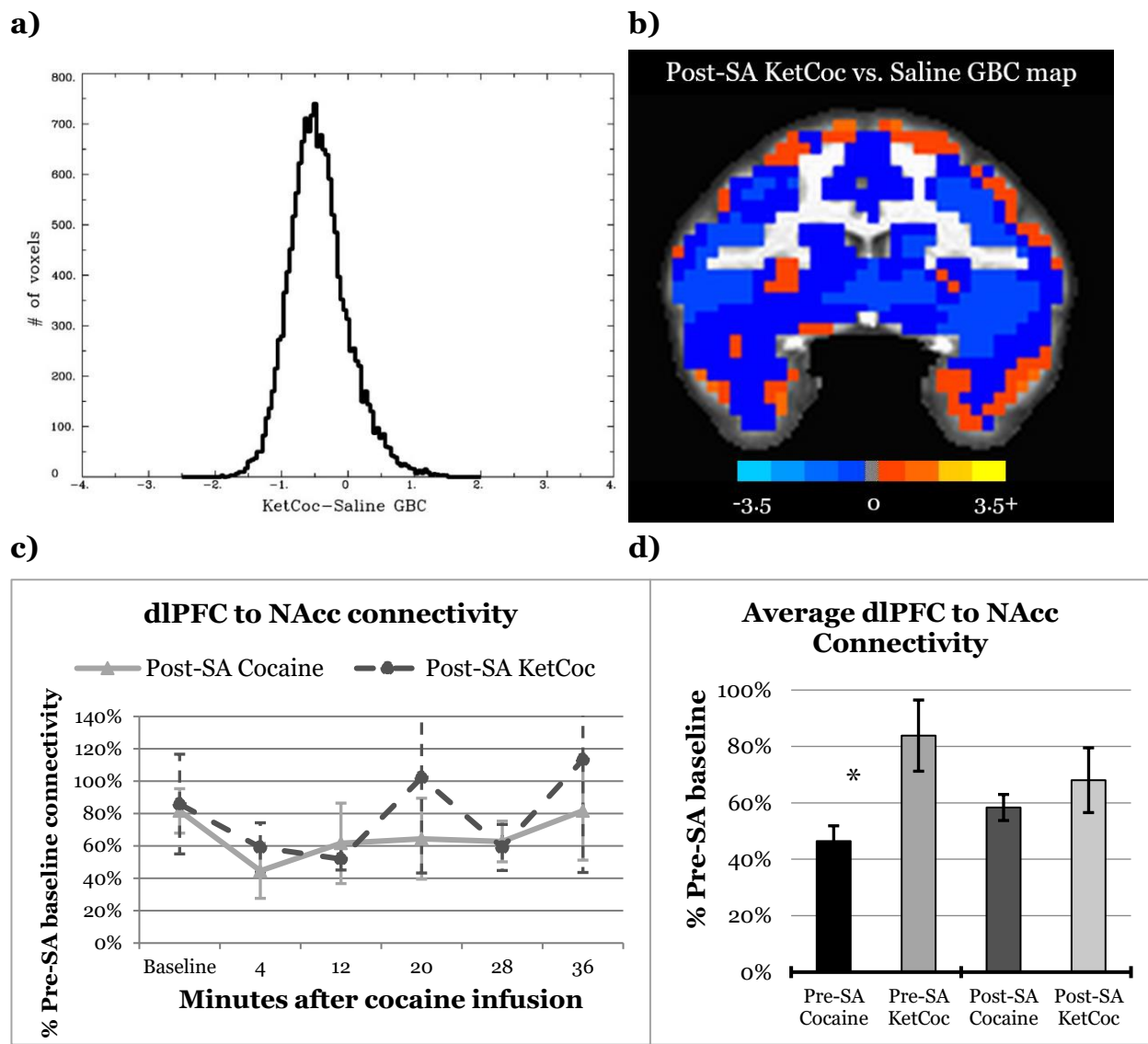


**Figure 4-6** Post-SA effects of acute administration of cocaine following ketamine pretreatment (KetCoc) on FC: **(a)** Histogram showing the distribution of voxel-wise contrast in GBC values for Post-SA KetCoc vs. Pre-SA saline for all gray matter voxels. There is a non-significant leftward shift indicating Post-SA KetCoc GBC < Pre-SA saline GBC for some gray matter voxels; **(b)** Coronal section with voxels colored by contrast in z-score of GBC values for Post-SA KetCoc vs. Pre-SA saline. Voxels with Post-SA KetCoc GBC < Pre-SA saline GBC are blue, while voxels with Post-SA KetCoc GBC > Pre-SA saline GBC are orange-yellow; **(c)** Post-SA normalized group-average dlPFC-NAcc FC over time is plotted for cocaine and KetCoc scans; **(d)** Chart comparing Pre-SA and Post-SA dlPFC-NAcc FC averaged over 0-32 minutes after drug infusion for cocaine and KetCoc. FC does not significantly differ between Post-SA cocaine and Post-SA KetCoc.

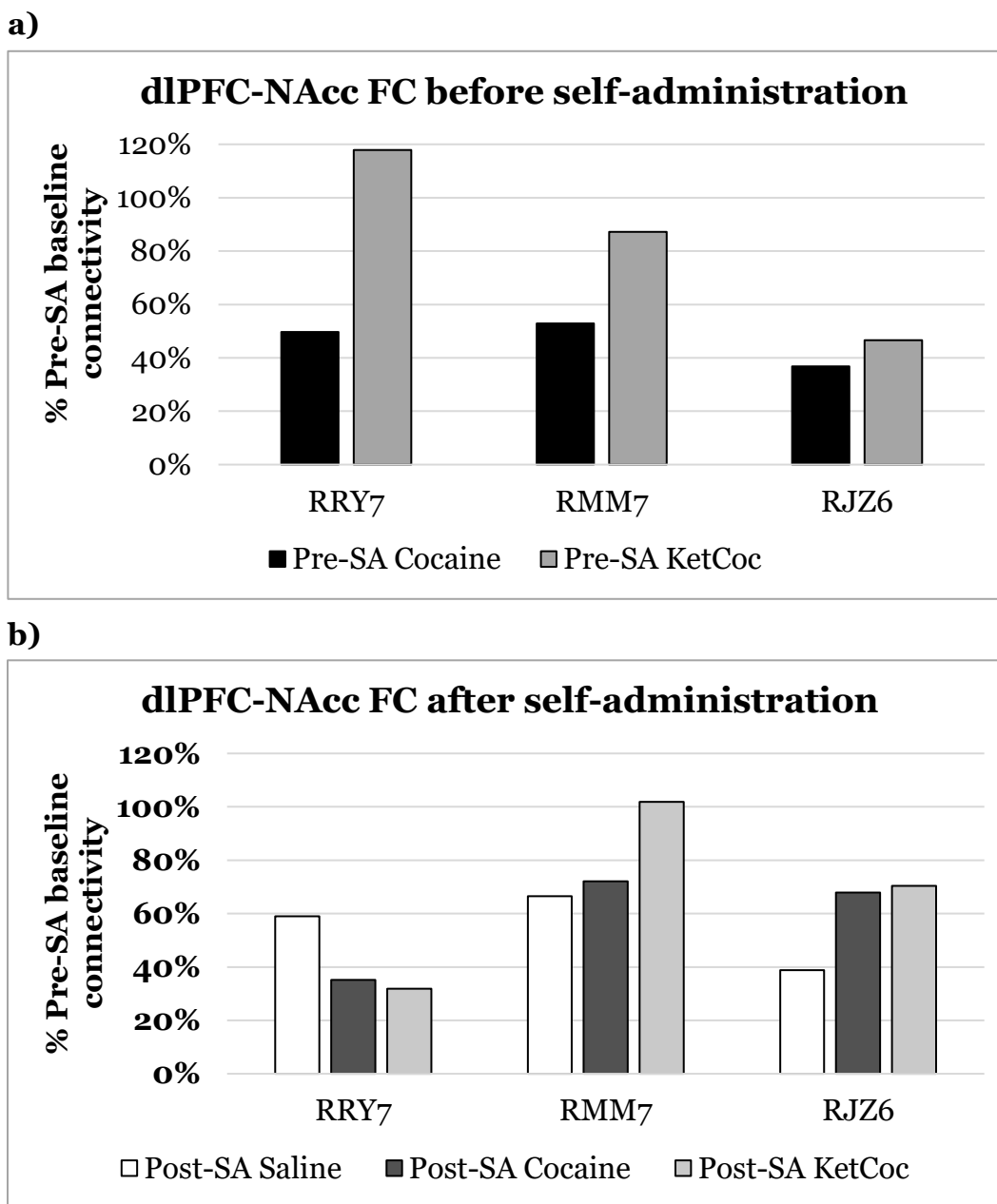


**Figure 4-7** Effects of cocaine on dlPFC-NAcc FC in individual subjects: **(a)** Chart comparing dlPFC-NAcc FC averaged over 0-32 minutes after drug infusion for Pre-SA cocaine and Pre-SA KetCoc in individual subjects. The effects of cocaine are similar across subjects, while effects of ketamine pretreatment are larger for the two previously drug-naïve subjects, RRY7 and RMM7, than for the subject with a history of cocaine self-administration, RJZ6; **(b)** Chart comparing dlPFC-NAcc FC averaged over the full 48-minute Post-SA saline scan and averaged over the 0-32 minutes after drug infusion for Post-SA cocaine and Post-SA KetCoc. Following chronic self-administration, dlPFC-NAcc FC is reduced in all subjects, while ketamine pretreatment is only effective in one of three subjects, RMM7.

**Chapter 5: Investigating the effects of ketamine treatment on  
reinstatement and reacquisition of cocaine self-administration in rhesus  
monkeys**

## **5.1 Context, Author's Contribution, and Acknowledgement of Reproduction**

The following chapter investigates the behavioral relevance of imaging findings presented in the previous chapters by evaluating the efficacy of ketamine treatment for modulating drug-seeking behavior. All surgeries were performed by Juliet Brown. The dissertation author received methods training from Drs. Lais Berro and Maylen Perez-Diaz before performing the behavioral experiments presented. The following unpublished manuscript was written in its entirety, and all experiments were designed, performed, and analyzed by the dissertation author under the guidance of Dr. Leonard Howell.

## **5.2 Abstract**

**Rationale:** The functional imaging studies presented in the previous chapters indicated that sub-anesthetic ketamine infusion attenuates the effects of cocaine on brain functional networks.

**Objective:** The current study was designed to test the behavioral relevance of these imaging findings by evaluating the efficacy of ketamine treatment for modulating drug-seeking behavior.

**Methods:** Five adult rhesus macaques (4 female) were trained to self-administer cocaine (0.1 mg/kg; i.v.) on a second-order schedule of reinforcement during daily one-hour sessions. Subsequently, cocaine was replaced with saline until responding was extinguished. Cocaine-prime + cue-induced reinstatement tests were then performed 48-hours before, and 48-hours after, treatment with either ketamine or vehicle. Ketamine treatment consisted of a bolus injection (i.v.) followed by a one-hour constant infusion (i.v.). Two doses were tested: 0.345 mg/kg bolus + 0.256 mg/kg/hr and 0.69



mg/kg + 0.512 mg/kg/hr. In addition to reinstatement, the effect of ketamine treatment on reacquisition of cocaine self-administration was examined.

**Results:** Treatment with the low, but not the high, dose of ketamine significantly attenuated reinstatement responding relative to vehicle treatment ( $p < 0.05$ ). No significant difference was observed between the two ketamine doses. There was no effect of ketamine treatment on reacquisition of cocaine reinforced responding, even after repeated treatments.

**Conclusions:** The results indicate that sub-anesthetic ketamine infusion produces lasting effects that reduce drug-seeking behavior up to 48-hours after treatment. However, the lack of an effect on reacquisition of cocaine self-administration may indicate that ketamine does not modulate the reinforcing properties of cocaine.

### 5.3 Introduction

Psychostimulant dependence presents a substantial burden to global public health (Degenhardt et al., 2014). However, despite a clear need, no pharmacotherapies are currently approved by the FDA for treating dependence to cocaine or other abused psychostimulants.

Substance use disorders are chronic illnesses (McLellan et al., 2000), characterized by repeated relapse and an inability to control use despite negative consequences (Hasin et al., 2013). The transition from initial use to compulsive use (Everitt and Robbins, 2005; Kalivas and O'Brien, 2008) is related to a loss of control over drug seeking and intake (George and Koob, 2010; Jentsch and Taylor, 1999) that has been attributed by imaging studies to the dysfunction of the prefrontal cortex (Goldstein and Volkow, 2011; Koob

and Volkow, 2010). Likewise, behavioral studies in rodents have shown a corresponding transition to compulsive drug seeking to be associated with deficits in synaptic plasticity in both the prefrontal cortex (DePoy and Gourley, 2015; Pitts et al., 2016) and the nucleus accumbens (NAcc) (Kasanetz et al., 2010; Martin et al., 2006). These findings have led to the hypothesis that new medications affecting neuroplasticity in prefrontal-accumbens circuitry could be beneficial for treating substance use disorders (Kalivas and Volkow, 2011). One such drug is ketamine.

Sub-anesthetic ketamine is now well known for producing rapid antidepressant effects in clinical studies (Zarate et al., 2006) and ketamine induces corresponding antidepressant-like effects in behavioral models that are mediated by neuroplastic changes in the prefrontal cortex (Kavalali and Monteggia, 2012; Li et al., 2010).

Ketamine has also been shown to increase functional connectivity (FC) between dorsolateral prefrontal cortex (dlPFC) and the NAcc (Chapter 3). Further, as shown in Chapter 4, treatment with ketamine 48-hrs prior to cocaine administration attenuates the acute effects of cocaine on FC between dlPFC and NAcc. Thus, there is strong rationale to investigate ketamine as a potential treatment for cocaine addiction.

Two recent pilot-studies in humans have studied the use of ketamine treatment in cocaine dependent subjects. Compared to active benzodiazepine control, ketamine treatment reduced cocaine craving while increasing motivation to quit (Dakwar et al., 2014) and also decreases cocaine choice (versus money) and self-reported cocaine intake (Dakwar et al., 2016). The present study further investigated the use of ketamine as a treatment for cocaine dependence. The effects of ketamine on reinstatement and

reacquisition of cocaine self-administration were examined in a translational nonhuman primate model utilizing a second-order schedule of drug reinforcement.

## **5.4 Methods**

### *5.4.1 Subjects*

Five adult (four female) individually housed rhesus monkeys (*Macaca mulatta*) weighing 8–15 kg served as subjects. All subjects had a history of exposure to psychostimulants and were well trained with cocaine self-administration protocols. The subjects were fed Purina monkey chow (Ralston Purina, St. Louis, MO), supplemented with fruit and vegetables daily and water was continuously available. Housing consisted of stainless steel home cages with environmental enrichment provided on a regular basis. An ambient temperature of  $22 \pm 2^\circ\text{C}$  at 45–50% humidity was maintained throughout the colony, and the lights were set to a 12-h light/dark cycle (lights on at 7h; lights off at 19h). All protocols and animal care and handling strictly followed the National Institutes of Health Guide for the Care and Use of Laboratory Animals (8th edition, revised 2011) and the recommendations of the American Association for Accreditation of Laboratory Animal Care, and were approved by the Institutional Animal Care and Use Committee of Emory University.

### *5.4.2 Surgery*

Each Subject was surgically implanted with chronic indwelling venous catheter attached to a subcutaneous vascular access port as described briefly in Chapter 2 and in detail by Howell and Fantegrossi (2009).

### 5.4.3 Cocaine Self-administration

Cocaine hydrochloride (National Institute on Drug Abuse, Bethesda, MD, USA) was dissolved in physiological saline and administered intravenously. Self-administration sessions lasting approximately one-hour were conducted in an operant test chamber with a controlled environment (Wilcox et al., 2005) and consisted of a second-order schedule of cocaine reinforcement, described previously (Berro et al., 2017). Briefly, following a 5-minute start-delay, a red light above the lever on the operant panel was illuminated and functioned as the discriminative stimulus. In the presence of the discriminative stimulus, after a fixed interval of 10-minutes (FI10) elapsed, completion of a fixed ratio of 20 lever presses (FR 20) within a 60s limited hold resulted in delivery of a cocaine infusion (1mL over 6s) and the illumination of a white light for 15s, and functioned as the conditioned stimulus. A 1-min timeout followed each component during which no lights were illuminated and responding on the lever had no programmed consequences. Completing 20 lever presses prior to the end of the FI10 resulted in a brief, 2s illumination of the conditioned stimulus light. Each operant session consisted of five components, and thus a maximum of five infusions could be earned during a single session. A unit dose of 0.1 mg/kg of cocaine was used for each infusion, allowing for a maximum cocaine intake of 0.5 mg/kg per session. This dose was chosen because it maintained high rates of responding in all subjects and was previously shown to produce peak rates of responding over a full dose-response in the majority of subjects (Berro et al., 2017). Response rates were calculated as the total number of lever presses in the presence of the discriminative stimulus divided by the duration of active time throughout the session.

#### 5.4.4 Ketamine treatment

Ketamine treatments were performed as described previously (Chapter 4). Two sub-anesthetic treatment doses were used in addition to vehicle (saline) treatment. The *low dose* consisted of a one-minute bolus of 0.345 mg/kg followed by a one-hour constant infusion of 0.256 mg/kg/hr. The *high dose* consisted of a one-minute bolus of 0.69 mg/kg followed by a one-hour constant infusion of 0.512 mg/kg/hr. The *low dose* is identical to what was used for experiments reported in Chapters 2-4. The *high dose* was chosen to further investigate the ketamine dose-response and produced plasma ketamine levels approximately twice that of the *low dose*, while remaining sub-anesthetic. The treatments occurred in a separate room from self-administration and in the presence of the experimenter. The order of vehicle and *low dose* treatments were counterbalanced across subjects, while all subjects received the *high dose* treatment last.

#### 5.4.5 Reinstatement

The reinstatement experiments followed the procedural schedule presented in **Table 5-1**. Subjects were initially required to maintain stable cocaine self-administration, defined as response rates that varied by <30% over 3 consecutive days. Following a stable maintenance period, behavior was extinguished by replacing cocaine with saline. The extinction criteria were operationally defined as two consecutive sessions with response rates <20% of the 3-day mean response rate for the prior maintenance period. The extinction sessions were identical to the self-administration maintenance sessions except that the conditioned stimulus (white light) was never illuminated. The day after extinction criteria were met, a baseline reinstatement test occurred. For the reinstatement test session, an experimenter-administered cocaine prime was delivered

i.v. 5-min before the start of the session and the conditioned stimulus light was illuminated upon completion of the FR20, but only saline infusions could be earned. Thus, these sessions are described as drug+ cue-induced reinstatement tests. No experiments occurred the day after the baseline reinstatement test. On the second day following the baseline reinstatement test, the subjects received a ketamine treatment (vehicle, *low dose*, or *high dose*). Two days later, a post-treatment reinstatement test session occurred that was identical to the baseline reinstatement session. Two days after the post-treatment reinstatement session the subjects were returned to maintenance conditions of cocaine self-administration. A cocaine priming dose of 0.1 mg/kg was used for all reinstatement sessions as this dose was previously shown to engender peak reinstatement response rates in the majority of the subjects (Berro 2017).

#### 5.4.6 Reacquisition

Experiments following the procedural schedule presented in **Table 5-2a** were performed to evaluate the effects of ketamine treatment on reacquisition of cocaine self-administration. Maintenance and extinction sessions were identical to those for reinstatement (described above). Following stable maintenance of cocaine self-administration, behavior was extinguished. Two days after meeting extinction criteria, subjects received a ketamine treatment (vehicle, *low dose*, or *high dose*). Subjects then underwent a maintenance session of cocaine self-administration to test response rates during reacquisition. In order to test the effects of repeated ketamine treatments on reacquisition, an extra ketamine treatment was added three days after the first treatment. Reacquisition of cocaine self-administration was then evaluated following the repeated treatments as shown in **Table 5-2b**.

#### 5.4.7 Data analysis

To evaluate the effects of ketamine treatment on reinstatement responding, the post-treatment response rates are presented as a percentage of the response rate measured for the baseline reinstatement session prior to ketamine treatment for individual subjects. Group data indicate the average of the normalized change in response rate following treatment. To examine the effects of ketamine treatment on reacquisition responding, the reacquisition response rates are presented as a percentage of the average response rate over the prior stable maintenance period. One-way repeated measures analysis of variance (ANOVA) and post-hoc Dunnett tests were used to assess the statistical significance of the effect of ketamine treatment on both reinstatement and reacquisition responding.

### **5.5 Results**

#### 5.5.1 Self-administration

The second order schedule of cocaine reinforcement maintained high, consistent rates of responding in all subjects. Subjects earned an average of 4.7 infusions per session during maintenance conditions with a range of 4.3 to 5.0 across individual subjects. Individual subjects typically met stable response criteria after the first 3 sessions. Maintenance response rates varied considerably across subjects, ranging from 0.39 to 2.15 responses per second with a group-average ( $\pm$  standard error) of  $1.0 \pm 0.3$  responses per second. This high variability in individual response rates necessitated the within-subject normalization used throughout the study. During extinction, response rates declined to below 20% of the mean maintenance rate within 1-3 sessions, with no more than 4 sessions required to achieve extinction criteria. Ketamine treatments were

well tolerated in all subjects. Treatments utilizing the *high dose* of ketamine elicited an appearance of mild sedation, drooping of the eyelids, and noticeable salivation, while *low dose* ketamine treatments were not obviously distinguishable from vehicle treatments.

### 5.5.2 Reinstatement

The effects of ketamine treatment on reinstatement responding for the group are shown in **Figure 5-1a**. Response rate following vehicle treatment was marginally increased to an average ( $\pm$  standard error) of  $116 \pm 14\%$  of the baseline response rate. Following treatment with the *low dose* of ketamine, reinstatement response rate was reduced to  $79 \pm 17\%$  of the baseline response rate. The *high dose* of ketamine was less effective than the *low dose*, leading to a group-average response rate of  $88 \pm 9\%$  of baseline levels. Overall there was a significant effect of ketamine on reinstatement responding ( $F = 4.74$  by one-way repeated measures ANOVA). Compared to the vehicle treatment, reinstatement responding was significantly attenuated after treatment ( $p < 0.05$ , by Dunnett's test) with the *low dose*, but not the *high dose* of ketamine. **Figure 1b** shows the effects of vehicle and *low dose* ketamine treatment on reinstatement responding in the individual subjects. While there was high variability in individual response rates following vehicle treatment, reinstatement responding was reduced by a consistent fraction following treatment with the *low dose* of ketamine compared to vehicle in four of the five subjects. The single subject (Rh7) that did not display lower responding after *low dose* ketamine than after vehicle, exhibited the second largest decrease in responding after the *high dose* of ketamine, dropping to 76% of the baseline response



rate. Thus, Rh7 appears to have been less sensitive to ketamine compared to the other subjects.

### 5.5.3 Reacquisition

Four out of five subjects completed the reacquisition experiments, with a subset of three subjects receiving both the *low dose* and the *high dose* ketamine treatments. Subject attrition occurred due to degradation of the indwelling catheters in two of the subjects. None of the subjects required more than a single session to reacquire response rates that were at least 70% of previous maintenance levels after any single treatment. Thus, only the first reacquisition session following treatment was used to determine the reacquisition response rate. The group-level effects of ketamine treatment on reacquisition of cocaine maintained responding are shown in **Figure 5-2a**. There were no statistically significant differences in reacquisition responding following the vehicle, *low dose*, or *high dose* treatments. **Figure 5-2b** shows the changes to reacquisition response rates in individual subjects following each treatment. Only a single subject (Rh7) showed a reduction in reacquisition responding following ketamine treatment at the *low dose*. Of the three subjects receiving the *high dose* treatment, Rh7 again showed the largest effect.

The effects of repeated ketamine treatments on reacquisition of cocaine maintained responding are shown in **Figure 5-3**. The group-level effects of two repeated treatments with either vehicle or *low dose* ketamine are displayed in **Figure 5-3a**. Following repeated vehicle treatments, the reacquisition response rate was  $82 \pm 7\%$  of the average response rate over the prior stable maintenance period. After repeated *low dose* ketamine treatments, the reacquisition response rate was  $78 \pm 13\%$  of the average

maintenance response rate for the previous stable maintenance period, and did not significantly differ from rates after repeated vehicle treatments. **Figure 5-3b** shows the effects of repeated treatments in the individual subjects. Two of the four subjects exhibited reductions in reacquisition responding following repeated treatment with *low dose* ketamine compared to vehicle with Rh7 again showing the largest effect.

## 5.6 Discussion

The major finding of the present study was that infusion of sub-anesthetic ketamine 48h-prior to reinstatement sessions attenuates drug+ cue-induced reinstatement of extinguished behavior previously maintained by cocaine. In contrast, ketamine had no effect on reacquisition of cocaine-maintained self-administration behavior, even after repeated dosing with ketamine. Together, the results indicate that effects present at least 48h post-infusion of sub-anesthetic ketamine attenuate the reinstating effects of cocaine, while not modulating the reinforcing effects of cocaine. These findings agree with the human literature (albeit limited) showing behaviorally significant effects of ketamine treatment in cocaine dependent subjects (Dakwar et al., 2016; Dakwar et al., 2014).

The results of the present study are especially significant when considered in combination with the results presented in the previous chapters. Chapter 4 showed that ketamine attenuated the connectivity deficits in functional brain networks induced by acute cocaine administration in drug naïve/abstinent subjects. However, as shown in Chapter 4 and supported by the literature, chronic cocaine exposure causes changes to brain function (Henry et al., 2010; Porrino et al., 2007). When ketamine treatment was subsequently evaluated following chronic exposure to cocaine, the results were

inconclusive (Chapter 4). Therefore, it is important to note that for the present study, the behavioral effects of ketamine were evaluated in a cohort of nonhuman primates with an extensive, multi-year history of exposure to cocaine and other psychostimulants. These results clearly demonstrate that ketamine treatment produces behaviorally relevant effects in a cohort with an extensive cocaine history.

Chapter 3 demonstrated ketamine to evoke robust increases in FC to the dlPFC from many brain regions, including the NAcc. Chapter 4 showed cocaine-induced decreases in dlPFC-NAcc FC, but this effect was attenuated following ketamine pretreatment. This fronto-striatal circuitry that was shown to be strengthened by ketamine, is known to be involved in executive control over reward-based decision making (Koob and Volkow, 2010). Behavioral studies in rodents have shown that prefrontal glutamatergic projections to the striatum are critical for reinstatement, but not maintenance, of cocaine self-administration (Kalivas, 2009). Thus, the behavioral results presented in the present chapter match expectations for the effect of strengthening fronto-striatal connections. This evidence strongly supports the mechanism of action for ketamine proposed in the previous chapters.

Ketamine is not unique in causing an attenuation of drug+ cue-induced reinstatement without altering the reinforcing effects of cocaine. Serotonin 2A (5-HT<sub>2A</sub>) receptors are highly expressed in the prefrontal cortex of nonhuman primates (Sawyer et al., 2012) and previous studies demonstrated a similar pattern of effects for a 5-HT<sub>2A</sub> receptor antagonist. The highly selective 5-HT<sub>2A</sub> receptor antagonist M100907 attenuated both drug-primed (Fletcher et al., 2002) and cue-induced (Nic Dhonnchadha et al., 2009) reinstatement, but not cocaine self-administration (Fletcher et al., 2002; Nic

Dhonnchadha et al., 2009) in rats, and also in rhesus monkeys (Murnane et al., 2013). Due in part to these behavioral effects, selective 5-HT<sub>2A</sub> receptor antagonists have been proposed as good candidates for clinical testing as potential treatments for relapse to psychostimulant use (Howell and Cunningham, 2015). The results of the present study provide evidence that ketamine may also be a good candidate for clinical evaluation as a treatment for relapse based on these criteria.

Another useful future direction for the study of ketamine as a potential treatment for substance use disorders could be the use of *in vivo* microdialysis to investigate the effects of sub-anesthetic ketamine infusion on cocaine-induced dopamine overflow in the striatum. Occupancy of the dopamine transporter in the striatum is tightly coupled with the subjective effects of cocaine (Volkow et al., 1997). The 5-HT<sub>2A</sub> receptor antagonist M100907 has been shown to attenuate cocaine-induced dopamine overflow in the caudate, but not nucleus accumbens of rhesus monkeys (Murnane et al., 2013). Given that M100907 and ketamine target separate neurotransmitter systems, but have similar effects on cocaine self-administration and reinstatement, it would be of interest to determine whether there is a convergence of the neurochemical effects in the striatum.

A second-order schedule of cocaine reinforcement and reinstatement procedures were utilized to investigate the effects of ketamine on drug-seeking behavior. Second-order schedules of reinforcement emphasize drug-associated conditioned stimuli to produce high behavioral output maintained by a limited amount of drug reinforcement, which minimizes any nonspecific disrupting effects of the drug and ensures a direct correspondence between response rate and the reinforcing effects of the drug (Howell

and Fantegrossi, 2009). Reinstatement procedures are often used as a behavioral model for relapse. While the translational validity as a model for drug relapse in humans has yet to be firmly established (Epstein et al., 2006; Katz and Higgins, 2003), reinstatement procedures are useful for measuring drug-seeking behaviors in the absence of active drug reinforcement. One limitation of the methods used in the present study is that response rates can vary markedly with little effect on cocaine intake. Future experiments under a fixed-ratio schedule of reinforcement may be useful for establishing whether ketamine treatment might reduce drug-taking.

In conclusion, sub-anesthetic ketamine infusion was shown to significantly attenuate cocaine-seeking behavior in rhesus monkeys using a potentially translational model of relapse. The neuroimaging results presented in Chapters 3 and 4 suggested ketamine may strengthen executive control and attenuate the disruptive effects of cocaine on decision making. The behavioral results shown here strongly support that hypothesis, indicating that ketamine may have therapeutic value in the treatment of substance use disorders, and relapse in particular.

**Table 5-1** Reinstatement procedure

Maintenance	Extinction	Baseline reinstatement	Off day	Treatment	Off day	Reinstatement test
-------------	------------	---------------------------	------------	-----------	------------	-----------------------

**Table 5-2****a) Reacquisition procedure with single treatment**

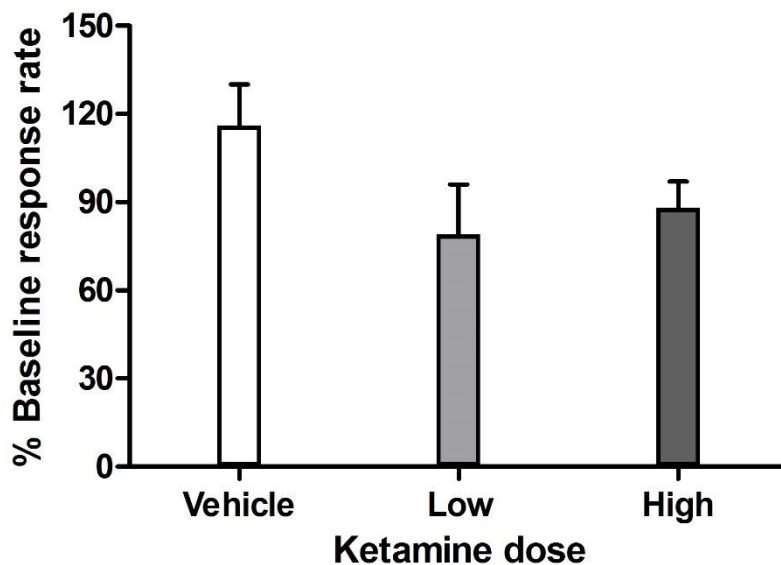
Maintenance	Extinction	Off day	Treatment	Off day	Reacquisition
-------------	------------	---------	-----------	---------	---------------

**b) Reacquisition procedure with repeated treatment**

Maintenance	Extinction	Off day	Treatment	Off day	Off day	Treatment	Off day	Reacquisition
-------------	------------	---------	-----------	---------	---------	-----------	---------	---------------

a)

### Group-average reinstatement response rate



b)

### Individual subject reinstatement response rates

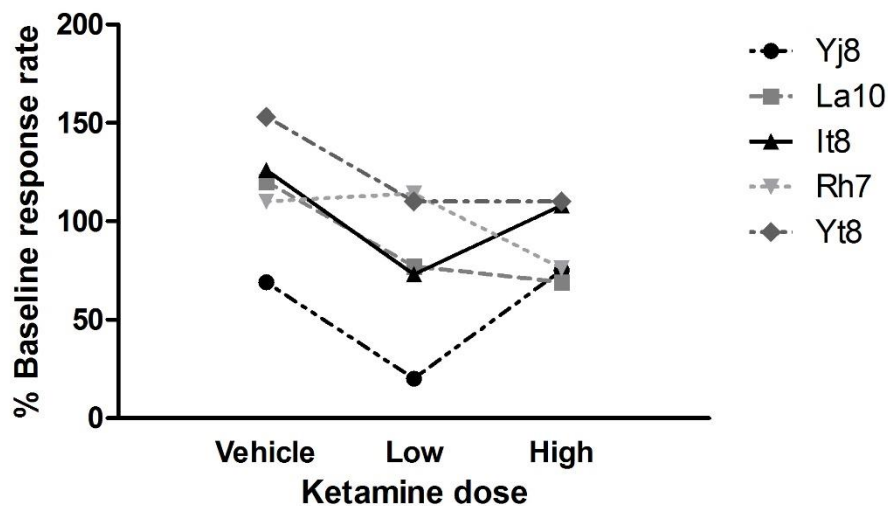
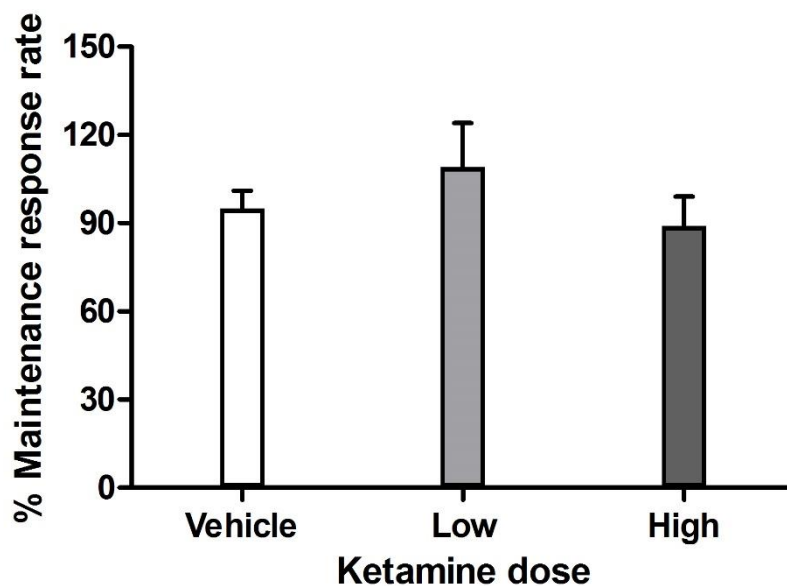


**Figure 5-1** Effects of vehicle, *low dose* (0.345 mg/kg+0.256 mg/kg/hr), and *high dose* (0.69 mg/kg + 0.512 mg/kg/hr) ketamine treatment on cocaine-prime (0.1 mg/kg) + cue-induced reinstatement responding; post-treatment reinstatement response rates as a percentage of baseline reinstatement response rate are shown for the (a) group average; and (b) individual subjects.



a)

### Group-average reacquisition response rate



b)

### Individual subject reacquisition response rates

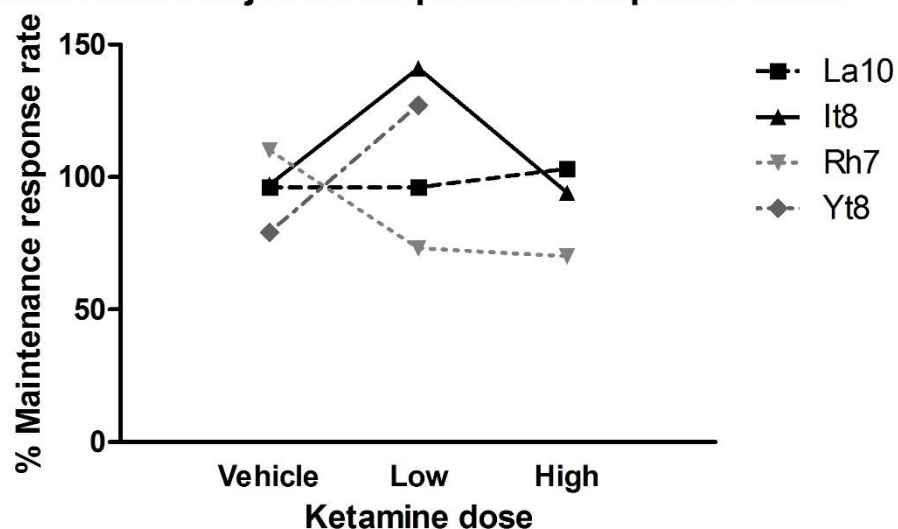
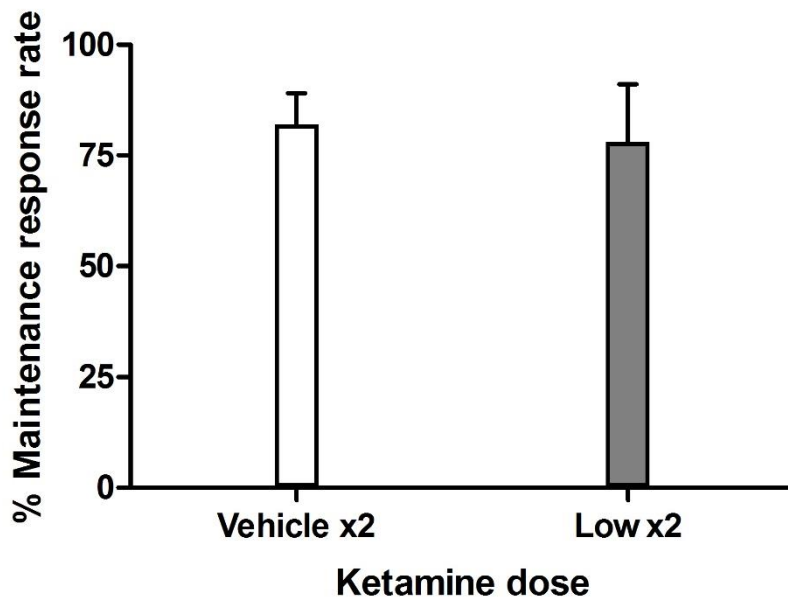


**Figure 5-2** Effects of vehicle, *low dose* (0.345 mg/kg+0.256 mg/kg/hr), and *high dose* (0.69 mg/kg + 0.512 mg/kg/hr) ketamine treatment on reacquisition of cocaine self-administration under a second-order schedule of reinforcement; response rates on the first day of reacquisition as a percentage of pre-extinction stable maintenance rate are shown for the **(a)** the group average; and **(b)** individual subjects.

a)

### Group-average reacquisition response rate



b)

### Individual subject reacquisition response rates

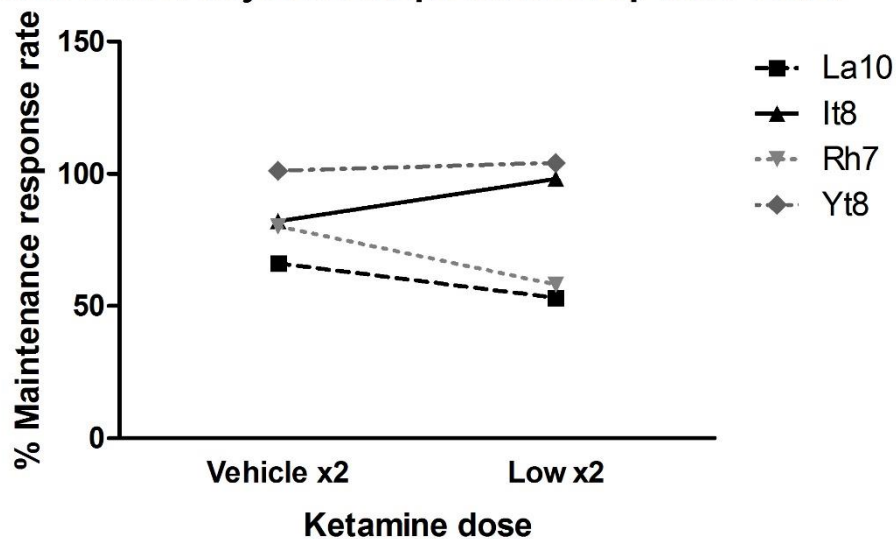


**Figure 5-3** Effects of two repeated treatments, 3-days apart, with vehicle or *low dose* (0.345 mg/kg+0.256 mg/kg/hr) ketamine on reacquisition of cocaine self-administration under a second-order schedule of reinforcement; response rates on the first day of reacquisition as a percentage of pre-extinction stable maintenance rate are shown for the **a)** group average; and **b)** individual subjects.

## **Chapter 6: Clinical use of ketamine, future directions, and limitations**

## 6.1 Results summary

The previous chapters described the effects of sub-anesthetic ketamine on brain function using phMRI in awake rhesus monkeys, demonstrating that ketamine induces robust brain activation and extensive changes to functional connectivity. Further experiments explored the use of sub-anesthetic ketamine infusion as a potential treatment for psychostimulant abuse, finding an attenuation of the acute effects of cocaine on FC and reduced responding during reinstatement of cocaine self-administration. Below is a summary of the key findings from each chapter.

Chapter 1 provided background on the effects of sub-anesthetic ketamine infusion. An introduction to the current literature examining the underlying neural mechanisms was provided and the contributions made by phMRI to understanding those mechanisms at the systems level were detailed. Further, studies correlating both the rapid antidepressant and psychotomimetic effects of ketamine with phMRI measurements were reviewed, highlighting the behavioral relevance of phMRI. Finally, the published results described in Chapters 2 and 3 were integrated to establish the basis for the investigation of sub-anesthetic ketamine as a treatment for cocaine abuse that was detailed in Chapters 4 and 5.

Chapter 2 presented data on brain activation induced by sub-anesthetic ketamine infusion in awake rhesus monkeys using phMRI. The results showed a robust and extensive BOLD response to ketamine with the greatest activation evident in the cingulate gyrus, thalamus, and SMA. Further, pretreatment with the antipsychotic drug risperidone produced a significant attenuation of the ketamine-induced BOLD activation. These findings strongly resemble those of previous studies of sub-anesthetic ketamine using

phMRI in human subjects. The latter studies found ketamine-induced BOLD activation similar in both magnitude and extent (De Simoni et al., 2013; Deakin et al., 2008), as well as a corresponding attenuation of the BOLD-response to ketamine following pretreatment with risperidone (Doyle et al., 2013). The strong concordance between the results of phMRI studies of ketamine in rhesus monkeys and humans lends validity to the use of NHPs as a translational model for studying the CNS effects of ketamine and for investigating the effects of antipsychotics in studies using ketamine as a model for psychosis.

Chapter 3 examined the effects of sub-anesthetic ketamine on FC in awake rhesus monkeys. Ketamine infusion was shown to induce extensive changes in FC, with the greatest changes occurring in FC to the dlPFC. During ketamine infusion, FC to the dlPFC was shown to increase in several cortical and subcortical regions, including the NAcc. Pretreatment with risperidone significantly attenuated the ketamine-induced changes to FC, including the increases in FC to the dlPFC.

These findings are important for several reasons. First, a strong concordance was shown to the results of FC studies in human subjects that have found ketamine-induced changes to FC at the whole-brain level (Driesen et al., 2013a) as well as to dlPFC (Grimm et al., 2015) and striatal (Dandash et al., 2015) regions specifically. Further, pretreatment with risperidone has also been shown to attenuate ketamine-induced changes to FC in human subjects (Joules et al., 2015). This lends additional validity to the use of NHP models in translational studies of ketamine and antipsychotics. Second, the dlPFC is implicated in both schizophrenia (Arnsten et al., 2012; Meyer-Lindenberg et al., 2005) and depression (Concerto et al., 2015; Dutta et al., 2014). Hence, changes to dlPFC FC could be related to

both the psychotomimetic and antidepressant effects of ketamine. Finally, the ketamine-induced increases in FC between dlPFC and NAcc were directly opposed to the decreases in dlPFC-NAcc FC shown during acute administration of cocaine (Murnane et al., 2015). This finding was an important part of the rationale motivating the investigation of ketamine as a treatment for cocaine dependence detailed in Chapters 4 and 5.

Chapter 4 provided a longitudinal investigation of the effects of cocaine on FC in awake rhesus monkeys at different stages of drug history and was the first to evaluate how sub-anesthetic ketamine infusion modulates the effects of cocaine on FC. The results replicated the previous findings (Murnane et al., 2015) that acute administration of cocaine robustly decreases FC at the whole-brain level and specifically between dlPFC and NAcc. Further, the reduction in dlPFC-NAcc FC induced by cocaine was correlated with response rates during cocaine self-administration. Murnane et al. (2015) previously found a similar association between baseline dlPFC-NAcc FC and cocaine intake using a slightly different self-administration procedure.

Further, ketamine pretreatment was shown to significantly attenuate the effects of cocaine on both whole-brain GBC and dlPFC-NAcc FC. These findings have broad implications for the treatment of stimulant use disorders, providing evidence for the potential efficacy of ketamine as a treatment and the possible use of FC as a biomarker.

Chapter 4 also showed the longitudinal effects of chronic cocaine self-administration on FC. After two-months of self-administration both whole-brain GBC and dlPFC-NAcc FC were significantly reduced. While previous longitudinal brain imaging studies in NHPs have demonstrated functional changes associated with chronic cocaine self-

administration (Henry et al., 2010; Porrino et al., 2007), this was the first to investigate changes to FC.

Chapter 5 examined the effects of ketamine pretreatment on cocaine self-administration behavior in rhesus monkeys. The data demonstrated reduced responding during cocaine-induced reinstatement occurring 48h after infusion of sub-anesthetic ketamine (compared to vehicle control). These results, indicating reduced drug-seeking behavior following ketamine pretreatment, corroborated previous findings showing ketamine treatment to reduce cocaine craving while increasing motivation to quit (Dakwar et al., 2014) and to decrease cocaine-choice and self-reported cocaine intake (Dakwar et al., 2016) in cocaine dependent human subjects. Furthermore, behavioral studies in rodents have shown that prefrontal glutamatergic projections to the striatum are critical for reinstatement, but not maintenance, of cocaine self-administration (Kalivas, 2009). Thus, the results of the behavioral experiments in Chapter 5 support the findings in the previous imaging chapters of strengthened dlPFC-NAcc FC as the mechanism of action for ketamine treatment.

Indeed, taken together the results presented in this dissertation strongly support the validity of translational models using phMRI in awake NHPs, and provide considerable evidence for the efficacy of sub-anesthetic ketamine as a treatment for substance use disorders. The remainder of this discussion will cover the clinical utility of sub-anesthetic ketamine as a treatment for drug dependence, future directions for the use of phMRI in awake NHPs as a translational model, and some of the limitations of the findings presented in this dissertation.

## 6.2 Clinical use of sub-anesthetic ketamine treatment

Ever since the rapid antidepressant efficacy of sub-anesthetic ketamine was first reported by Berman et al. (2000), the clinical use of ketamine as an off-label treatment for mood disorders has been increasing (Sanacora et al., 2017). However, further investigation is required to better establish the dose-response relationship of ketamine treatment. In Chapter 5, the lower of two ketamine doses evaluated showed greater efficacy for reducing drug-seeking behavior. Indeed, the optimal dose, infusion duration, and route of administration remain unknown. Interestingly, in a study of the optimal frequency of repeated ketamine treatments, two infusions per week showed equal efficacy to three infusions per week for treating depression (Singh et al., 2016). While ketamine treatment is typically administered i.v. in clinical settings, other routes of administration may prove more feasible for broad implementation, including intranasal ketamine for example, which has already demonstrated therapeutic efficacy (Opler et al., 2016). A systematic study of ketamine dosing regimens and routes of administration could be beneficial for optimizing the therapeutic potential of ketamine.

While the clinical evidence thus far suggests that ketamine treatments are safe and well tolerated (Perry et al., 2007; Wan et al., 2015), use of ketamine as a treatment for substance use disorders is likely to generate concerns given the abuse liability of ketamine (Morgan et al., 2012). There is at least one report of ketamine abuse extending from treatment for major depressive disorder (Schak et al., 2016). However, substance abuse is highly context dependent (Volkow and Swanson, 2003; Volkow et al., 2008b) and thus the medical context of ketamine treatments administered in the clinic combined with effective monitoring should mitigate the abuse liability (Carter and Griffiths, 2009).



Alternatives to ketamine may still be desirable and the literature indicates several related compounds that provide good candidates for further investigation as potential treatments for drug dependence. Ketamine is a chiral compound consisting of a pair of (R,S) enantiomers. While the racemic mixture is typically administered for ketamine treatments there is some evidence suggesting that R-ketamine may have greater antidepressant efficacy (Zhang et al., 2014) while also producing fewer psychotomimetic effects (Yang et al., 2015). Further, there is evidence that a specific metabolite of R-ketamine is sufficient for producing rapid antidepressant-like effects in mice without several of the side effects of racemic ketamine (Zanos et al., 2016). A higher concentration of the same metabolite has been observed in human responders compared to non-responders after ketamine treatment for both major depressive and bipolar disorders (Zarate et al., 2012). Other NMDA receptor antagonists may also warrant further examination, such as the NR2B sub-unit selective compound CP-101,606 that has been shown to produce rapid antidepressant effects with a reduced side effect profile (Preskorn et al., 2008).

### **6.3 Future directions for translational models using phMRI in awake NHPs**

The translational relevance of phMRI experiments in awake NHPs provides a powerful preclinical screening tool. Future studies should take advantage of this methodology for evaluating novel compounds, including new antipsychotic drugs and candidate treatments for drug dependence. As detailed above, several compounds that may exhibit fewer side effects and lower abuse liability have demonstrated rapid antidepressant effects analogous to ketamine. Examining each of these novel compounds using phMRI

in awake NHPs could prove a quick and effective method for determining whether any of these drugs may have efficacy for the treatment of drug dependence.

Likewise, a similar procedure may be useful for evaluating novel antipsychotic compounds. Current clinical antipsychotics typically exhibit moderate to severe side effects (Kim et al., 2007) and show limited efficacy for treating the negative and cognitive symptoms of schizophrenia (Strous et al., 2003). Identifying novel antipsychotics that feature a reduced side effect profile and successfully treat the negative or cognitive symptoms of schizophrenia should be a priority of future research and the use of phMRI in awake NHPs could provide a valuable tool for this search.

Further investigation of FC as a biomarker for cocaine dependence should be pursued. The results presented in Chapter 4 corroborate the previous finding from Murnane et al. (2015) of a correlation between dlPFC-NAcc FC and behavior during cocaine self-administration. However, both studies were underpowered for examining individual differences with each featuring a 3-subject sample size. A larger study to determine associations between FC and the behavioral response to treatment could prove valuable. Such a study could also compare the effects of ketamine to other treatments known to affect FC, such as transcranial magnetic stimulation (Hanlon et al., 2015a).

#### **6.4 Limitations**

In addition to using small sizes, another significant limitation of the data presented in this dissertation is that nearly all of the experimental subjects were female. All of the subjects of the imaging experiments performed in chapters 2-4 were female and four out of five subjects of the behavioral experiments in Chapter 5 were female. Hence, the results may not be generalizable to male subjects. Sex differences have been observed in the

sensitivity to ketamine treatment both clinically (Saland et al., 2017) and in preclinical models (Franceschelli et al., 2015). Further, notable sex differences have also been observed in substance use disorders (Andersen et al., 2012), with female subjects generally showing greater vulnerability than males (Anker and Carroll, 2011).

The therapeutic-like effects of ketamine were only demonstrated for acute treatments occurring 48h prior to experimental evaluation. While the rapid antidepressant effects of a single ketamine treatment have in some cases been shown to last more than one month (Murrough et al., 2013) and subjects have been shown to continue to respond following repeated dosing (aan het Rot et al., 2010), the time-course of the therapeutic-like effects of ketamine in the context of substance abuse remains unknown. Given the chronic, relapsing nature of substance use disorders (McLellan et al., 2000), the duration of treatment effects becomes a critical consideration.

While the findings from chapters 4 and 5 demonstrate therapeutic-like effects of ketamine treatment when evaluated in the context of cocaine use, the results may not be generalizable to other drugs of abuse. However, there is evidence from neuroimaging studies suggesting that disruption of the fronto-striatal circuits responsible for executive control over reward-based decision making leads to a general vulnerability to a wide range of substance use disorders (Volkow et al., 2012). There is even evidence to suggest a common pathology in these the neurobiological systems may be also be involved in obesity (Volkow et al., 2008a). This data from the literature implies that the therapeutic effects of ketamine may indeed be highly generalizable, given that ketamine has now been shown to bolster fronto-striatal circuitry and to attenuate the disruptive effects of cocaine. Indeed, while ketamine has not yet been evaluated for therapeutic potential in treating

the abuse of substances other than cocaine, there may be great value in doing so in the future.

## **6.5 Conclusions**

The results presented in this dissertation highlight the use of phMRI in awake NHPs as an innovative methodology for creating translational brain imaging models. The chapters above utilized this methodology to provide translational models for studying the effects of ketamine, evaluating novel antipsychotics, and examining the impact of cocaine use on the brain. A strong concordance with the human literature is demonstrated for each of these models, lending them translational validity. Sub-anesthetic ketamine infusion was shown to enhance FC in brain networks associated with executive control over decision making, in direct opposition to the effects of cocaine. Ketamine pretreatment was further shown to attenuate both the effects of cocaine on FC in these same fronto-striatal connections. Further, ketamine pretreatment reduced cocaine-seeking behavior in a pattern consistent with strengthened executive control. Thus, this dissertation has established the behavioral relevance of FC, produced consistent findings in support of a therapeutic mechanism for sub-anesthetic ketamine as a treatment of psychostimulant abuse.

**Appendix: Complete list of publications to which the author has contributed during his graduate training**

**Maltbie E**, Gopinath K, Howell L (2017). Ketamine and pharmacological imaging: use of functional magnetic resonance imaging to evaluate mechanisms of action. *Behavioural Pharmacology* **28**: 610-622.

Berro L, Perez-Diaz M, **Maltbie E**, Howell L (2017). Effects of the serotonin 2C receptor agonist WAY163909 on the abuse-related effects and mesolimbic dopamine neurochemistry induced by abused stimulants in rhesus monkeys. *Psychopharmacology (Berl)*. Epub ahead of print.

Gopinath K, **Maltbie E\***, Urushino N, Kempf D, Howell L (2016). Ketamine-induced changes in connectivity of functional brain networks in awake female nonhuman primates: a translational functional imaging model. *Psychopharmacology (Berl)* **233**: 3673-3684.

**Maltbie E\***, Gopinath K, Urushino N, Kempf D, Howell L (2016). Ketamine-induced brain activation in awake female nonhuman primates: a translational functional imaging model. *Psychopharmacology (Berl)* **233**: 961-972.

Murnane K, Gopinath K, **Maltbie E**, Daunais J, Telesford Q, Howell L (2015). Functional connectivity in frontal-striatal brain networks and cocaine self-administration in female rhesus monkeys. *Psychopharmacology (Berl)* **232**: 745-754.

\*co-first author papers with equal contribution from the first two authors

## References

aan het Rot M, Collins KA, Murrough JW, Perez AM, Reich DL, Charney DS, et al. (2010). Safety and efficacy of repeated-dose intravenous ketamine for treatment-resistant depression. *Biol Psychiatry* **67**: 139-145.

Aan Het Rot M, Zarate CA, Jr., Charney DS, Mathew SJ (2012). Ketamine for depression: where do we go from here? *Biol Psychiatry* **72**: 537-547.

Abdallah CG, Averill LA, Collins KA, Geha P, Schwartz J, Averill C, et al. (2016). Ketamine Treatment and Global Brain Connectivity in Major Depression. *Neuropsychopharmacology*.

Abel KM, Drake R, Goldstein JM (2010). Sex differences in schizophrenia. *Int Rev Psychiatry* **22**: 417-428.

Adachi Y, Osada T, Sporns O, Watanabe T, Matsui T, Miyamoto K, et al. (2012). Functional connectivity between anatomically unconnected areas is shaped by collective network-level effects in the macaque cortex. *Cereb Cortex* **22**: 1586-1592.

Adams B, Moghaddam B (1998). Corticolimbic dopamine neurotransmission is temporally dissociated from the cognitive and locomotor effects of phencyclidine. *J Neurosci* **18**: 5545-5554.

Agid O, Kapur S, Arenovich T, Zipursky RB (2003). Delayed-onset hypothesis of antipsychotic action: a hypothesis tested and rejected. *Arch Gen Psychiatry* **60**: 1228-1235.

Anand A, Charney DS, Oren DA, Berman RM, Hu XS, Cappiello A, et al. (2000). Attenuation of the neuropsychiatric effects of ketamine with lamotrigine: support for hyperglutamatergic effects of N-methyl-D-aspartate receptor antagonists. *Arch Gen Psychiatry* **57**: 270-276.

Anand A, Li Y, Wang Y, Lowe MJ, Dziedzic M (2009). Resting state corticolimbic connectivity abnormalities in unmedicated bipolar disorder and unipolar depression. *Psychiatry Res* **171**: 189-198.

Andersen ML, Sawyer EK, Howell LL (2012). Contributions of neuroimaging to understanding sex differences in cocaine abuse. *Exp Clin Psychopharmacol* **20**: 2-15.

Anker JJ, Carroll ME (2011). Females are more vulnerable to drug abuse than males: evidence from preclinical studies and the role of ovarian hormones. *Curr Top Behav Neurosci* **8**: 73-96.

Anticevic A, Brumbaugh MS, Winkler AM, Lombardo LE, Barrett J, Corlett PR, et al. (2013). Global prefrontal and fronto-amygdala dysconnectivity in bipolar I disorder with psychosis history. *Biol Psychiatry* **73**: 565-573.

Anticevic A, Corlett PR, Cole MW, Savic A, Gancsos M, Tang Y, et al. (2015). N-methyl-D-aspartate receptor antagonist effects on prefrontal cortical connectivity better model early than chronic schizophrenia. *Biol Psychiatry* **77**: 569-580.

Arnsten AF, Wang MJ, Paspalas CD (2012). Neuromodulation of thought: flexibilities and vulnerabilities in prefrontal cortical network synapses. *Neuron* **76**: 223-239.

Autry AE, Adachi M, Nosyreva E, Na ES, Los MF, Cheng PF, et al. (2011). NMDA receptor blockade at rest triggers rapid behavioural antidepressant responses. *Nature* **475**: 91-95.

Ballard ED, Ionescu DF, Vande Voort JL, Niciu MJ, Richards EM, Luckenbaugh DA, et al. (2014). Improvement in suicidal ideation after ketamine infusion: relationship to reductions in depression and anxiety. *J Psychiatr Res* **58**: 161-166.

Banks ML, Andersen ML, Murnane KS, Meyer RC, Howell LL (2009). Behavioral and neurochemical effects of cocaine and diphenhydramine combinations in rhesus monkeys. *Psychopharmacology (Berl)* **205**: 467-474.

Beck AT, Ward CH, Mendelson M, Mock J, Erbaugh J (1961). An inventory for measuring depression. *Arch Gen Psychiatry* **4**: 561-571.

Berman RM, Cappiello A, Anand A, Oren DA, Heninger GR, Charney DS, et al. (2000). Antidepressant effects of ketamine in depressed patients. *Biol Psychiatry* **47**: 351-354.

Berro LF, Perez Diaz M, Maltbie E, Howell LL (2017). Effects of the serotonin 2C receptor agonist WAY163909 on the abuse-related effects and mesolimbic dopamine neurochemistry induced by abused stimulants in rhesus monkeys. *Psychopharmacology (Berl)*.

Berton O, Hahn CG, Thase ME (2012). Are we getting closer to valid translational models for major depression? *Science* **338**: 75-79.

Bolstad I, Andreassen OA, Groote I, Server A, Sjaastad I, Kapur S, et al. (2015). Effects of haloperidol and aripiprazole on the human mesolimbic motivational system: A pharmacological fMRI study. *Eur Neuropsychopharmacol*.

Bortolozzi A, Diaz-Mataix L, Scorza MC, Celada P, Artigas F (2005). The activation of 5-HT receptors in prefrontal cortex enhances dopaminergic activity. *J Neurochem* **95**: 1597-1607.

Braga RM, Buckner RL (2017). Parallel Interdigitated Distributed Networks within the Individual Estimated by Intrinsic Functional Connectivity. *Neuron* **95**: 457-471 e455.

Bremner JD, Krystal JH, Putnam FW, Southwick SM, Marmar C, Charney DS, et al. (1998). Measurement of dissociative states with the Clinician-Administered Dissociative States Scale (CADSS). *J Trauma Stress* **11**: 125-136.

Buckner RL, Krienen FM, Yeo BT (2013). Opportunities and limitations of intrinsic functional connectivity MRI. *Nat Neurosci* **16**: 832-837.

Bullmore ET, Brammer MJ, Rabe-Hesketh S, Curtis VA, Morris RG, Williams SC, et al. (1999). Methods for diagnosis and treatment of stimulus-correlated motion in generic brain activation studies using fMRI. *Hum Brain Mapp* **7**: 38-48.

Buxton RB (2002) *Introduction to functional magnetic resonance imaging : principles and techniques*. Cambridge University Press: Cambridge, UK ; New York.

Camchong J, Macdonald AW, 3rd, Mueller BA, Nelson B, Specker S, Slaymaker V, et al. (2014). Changes in resting functional connectivity during abstinence in stimulant use disorder: a preliminary comparison of relapsers and abstainers. *Drug Alcohol Depend* **139**: 145-151.

Carr DB, Sesack SR (2000). Dopamine terminals synapse on callosal projection neurons in the rat prefrontal cortex. *J Comp Neurol* **425**: 275-283.

Carter LP, Griffiths RR (2009). Principles of laboratory assessment of drug abuse liability and implications for clinical development. *Drug Alcohol Depend* **105 Suppl 1**: S14-25.



Casey DE, Bruhwyler J, Delarge J, Geczy J, Liegeois JF (2001). The behavioral effects of acute and chronic JL 13, a putative antipsychotic, in Cebus non-human primates. *Psychopharmacology (Berl)* **157**: 228-235.

Catafau AM, Corripio I, Perez V, Martin JC, Schotte A, Carrio I, et al. (2006). Dopamine D2 receptor occupancy by risperidone: implications for the timing and magnitude of clinical response. *Psychiatry Res* **148**: 175-183.

Cato MA, Crosson B, Gokcay D, Soltysik D, Wierenga C, Gopinath K, et al. (2004). Processing words with emotional connotation: an fMRI study of time course and laterality in rostral frontal and retrosplenial cortices. *J Cogn Neurosci* **16**: 167-177.

Chai XJ, Whitfield-Gabrieli S, Shinn AK, Gabrieli JD, Nieto Castanon A, McCarthy JM, et al. (2011). Abnormal medial prefrontal cortex resting-state connectivity in bipolar disorder and schizophrenia. *Neuropsychopharmacology* **36**: 2009-2017.

Chin CL, Upadhyay J, Marek GJ, Baker SJ, Zhang M, Mezler M, et al. (2011). Awake rat pharmacological magnetic resonance imaging as a translational pharmacodynamic biomarker: metabotropic glutamate 2/3 agonist modulation of ketamine-induced blood oxygenation level dependence signals. *J Pharmacol Exp Ther* **336**: 709-715.

Chouinard G, Miller R (1999). A rating scale for psychotic symptoms (RSPS) part I: theoretical principles and subscale 1: perception symptoms (illusions and hallucinations). *Schizophr Res* **38**: 101-122.

Cohen SM, Tsien RW, Goff DC, Halassa MM (2015). The impact of NMDA receptor hypofunction on GABAergic neurons in the pathophysiology of schizophrenia. *Schizophr Res* **167**: 98-107.

Cole MW, Anticevic A, Repovs G, Barch D (2011). Variable global dysconnectivity and individual differences in schizophrenia. *Biol Psychiatry* **70**: 43-50.

Cole MW, Pathak S, Schneider W (2010). Identifying the brain's most globally connected regions. *Neuroimage* **49**: 3132-3148.

Concerto C, Lanza G, Cantone M, Ferri R, Pennisi G, Bella R, et al. (2015). Repetitive transcranial magnetic stimulation in patients with drug-resistant major depression: A six-month clinical follow-up study. *Int J Psychiatry Clin Pract* **19**: 252-258.

Contreras-Rodriguez O, Albein-Urios N, Perales JC, Martinez-Gonzalez JM, Vilar-Lopez R, Fernandez-Serrano MJ, et al. (2015). Cocaine-specific neuroplasticity in the ventral striatum network is linked to delay discounting and drug relapse. *Addiction* **110**: 1953-1962.

Cox RW (1996). AFNI: software for analysis and visualization of functional magnetic resonance neuroimages. *Comput Biomed Res* **29**: 162-173.

Cyr M, Ghribi O, Thibault C, Morissette M, Landry M, Di Paolo T (2001). Ovarian steroids and selective estrogen receptor modulators activity on rat brain NMDA and AMPA receptors. *Brain Res Brain Res Rev* **37**: 153-161.

Dakwar E, Hart CL, Levin FR, Nunes EV, Foltin RW (2016). Cocaine self-administration disrupted by the N-methyl-D-aspartate receptor antagonist ketamine: a randomized, crossover trial. *Mol Psychiatry*.

Dakwar E, Levin F, Foltin RW, Nunes EV, Hart CL (2014). The effects of subanesthetic ketamine infusions on motivation to quit and cue-induced craving in cocaine-dependent research volunteers. *Biol Psychiatry* **76**: 40-46.

Dandash O, Harrison BJ, Adapa R, Gaillard R, Giorlando F, Wood SJ, et al. (2015). Selective augmentation of striatal functional connectivity following NMDA receptor antagonism: implications for psychosis. *Neuropsychopharmacology* **40**: 622-631.

De Simoni S, Schwarz AJ, O'Daly OG, Marquand AF, Brittain C, Gonzales C, et al. (2013). Test-retest reliability of the BOLD pharmacological MRI response to ketamine in healthy volunteers. *Neuroimage* **64**: 75-90.

Deakin JF, Lees J, McKie S, Hallak JE, Williams SR, Dursun SM (2008). Glutamate and the neural basis of the subjective effects of ketamine: a pharmaco-magnetic resonance imaging study. *Arch Gen Psychiatry* **65**: 154-164.

Degenhardt L, Baxter AJ, Lee YY, Hall W, Sara GE, Johns N, et al. (2014). The global epidemiology and burden of psychostimulant dependence: findings from the Global Burden of Disease Study 2010. *Drug Alcohol Depend* **137**: 36-47.

Del Arco A, Mora F (2009). Neurotransmitters and prefrontal cortex-limbic system interactions: implications for plasticity and psychiatric disorders. *J Neural Transm (Vienna)* **116**: 941-952.

Del Arco A, Segovia G, Mora F (2008). Blockade of NMDA receptors in the prefrontal cortex increases dopamine and acetylcholine release in the nucleus accumbens and motor activity. *Psychopharmacology (Berl)* **201**: 325-338.

DePoy LM, Gourley SL (2015). Synaptic Cytoskeletal Plasticity in the Prefrontal Cortex Following Psychostimulant Exposure. *Traffic* **16**: 919-940.

DiazGranados N, Ibrahim LA, Brutsche NE, Ameli R, Henter ID, Luckenbaugh DA, et al. (2010). Rapid resolution of suicidal ideation after a single infusion of an N-methyl-D-aspartate antagonist in patients with treatment-resistant major depressive disorder. *J Clin Psychiatry* **71**: 1605-1611.

Doan L, Manders T, Wang J (2015). Neuroplasticity underlying the comorbidity of pain and depression. *Neural Plast* **2015**: 504691.

Domino EF, Domino SE, Smith RE, Domino LE, Goulet JR, Domino KE, et al. (1984). Ketamine kinetics in unmedicated and diazepam-premedicated subjects. *Clin Pharmacol Ther* **36**: 645-653.

Downey D, Dutta A, McKie S, Dawson GR, Dourish CT, Craig K, et al. (2016). Comparing the actions of lanicemine and ketamine in depression: key role of the anterior cingulate. *Eur Neuropsychopharmacol* **26**: 994-1003.

Doyle OM, De Simoni S, Schwarz AJ, Brittain C, O'Daly OG, Williams SC, et al. (2013). Quantifying the attenuation of the ketamine pharmacological magnetic resonance imaging response in humans: a validation using antipsychotic and glutamatergic agents. *J Pharmacol Exp Ther* **345**: 151-160.

Driesen NR, McCarthy G, Bhagwagar Z, Bloch M, Calhoun V, D'Souza DC, et al. (2013a). Relationship of resting brain hyperconnectivity and schizophrenia-like symptoms produced by the NMDA receptor antagonist ketamine in humans. *Mol Psychiatry* **18**: 1199-1204.

Driesen NR, McCarthy G, Bhagwagar Z, Bloch MH, Calhoun VD, D'Souza DC, et al. (2013b). The impact of NMDA receptor blockade on human working memory-related prefrontal function and connectivity. *Neuropsychopharmacology* **38**: 2613-2622.

Duncan GE, Moy SS, Knapp DJ, Mueller RA, Breese GR (1998). Metabolic mapping of the rat brain after subanesthetic doses of ketamine: potential relevance to schizophrenia. *Brain Res* **787**: 181-190.

Dutta A, McKie S, Deakin JF (2014). Resting state networks in major depressive disorder. *Psychiatry Res* **224**: 139-151.

Epstein DH, Preston KL, Stewart J, Shaham Y (2006). Toward a model of drug relapse: an assessment of the validity of the reinstatement procedure. *Psychopharmacology (Berl)* **189**: 1-16.

Everitt BJ, Robbins TW (2005). Neural systems of reinforcement for drug addiction: from actions to habits to compulsion. *Nat Neurosci* **8**: 1481-1489.

Fales CL, Barch DM, Rundle MM, Mintun MA, Snyder AZ, Cohen JD, et al. (2008). Altered emotional interference processing in affective and cognitive-control brain circuitry in major depression. *Biol Psychiatry* **63**: 377-384.

Fletcher PJ, Grottick AJ, Higgins GA (2002). Differential effects of the 5-HT(2A) receptor antagonist M100907 and the 5-HT(2C) receptor antagonist SB242084 on cocaine-induced locomotor activity, cocaine self-administration and cocaine-induced reinstatement of responding. *Neuropsychopharmacology* **27**: 576-586.

Forman SD, Cohen JD, Fitzgerald M, Eddy WF, Mintun MA, Noll DC (1995). Improved assessment of significant activation in functional magnetic resonance imaging (fMRI): use of a cluster-size threshold. *Magn Reson Med* **33**: 636-647.

Fox MD, Buckner RL, White MP, Greicius MD, Pascual-Leone A (2012). Efficacy of transcranial magnetic stimulation targets for depression is related to intrinsic functional connectivity with the subgenual cingulate. *Biol Psychiatry* **72**: 595-603.

Fox MD, Greicius M (2010). Clinical applications of resting state functional connectivity. *Front Syst Neurosci* **4**: 19.

Fox MD, Raichle ME (2007). Spontaneous fluctuations in brain activity observed with functional magnetic resonance imaging. *Nat Rev Neurosci* **8**: 700-711.

Fox MD, Snyder AZ, Vincent JL, Corbetta M, Van Essen DC, Raichle ME (2005). The human brain is intrinsically organized into dynamic, anticorrelated functional networks. *Proc Natl Acad Sci U S A* **102**: 9673-9678.

Fox PT, Raichle ME, Mintun MA, Dence C (1988). Nonoxidative glucose consumption during focal physiologic neural activity. *Science* **241**: 462-464.

Franceschelli A, Sens J, Herchick S, Thelen C, Pitychoutis PM (2015). Sex differences in the rapid and the sustained antidepressant-like effects of ketamine in stress-naive and "depressed" mice exposed to chronic mild stress. *Neuroscience* **290**: 49-60.

Frangou S (2014). A systems neuroscience perspective of schizophrenia and bipolar disorder. *Schizophr Bull* **40**: 523-531.

Frangou S, Kington J, Raymont V, Shergill SS (2008). Examining ventral and dorsal prefrontal function in bipolar disorder: A functional magnetic resonance imaging study. *Eur Psychiat* **23**: 300-308.

Frohlich J, Van Horn JD (2014). Reviewing the ketamine model for schizophrenia. *J Psychopharmacol* **28**: 287-302.

George O, Koob GF (2010). Individual differences in prefrontal cortex function and the transition from drug use to drug dependence. *Neurosci Biobehav Rev* **35**: 232-247.

Goldstein RZ, Volkow ND (2011). Dysfunction of the prefrontal cortex in addiction: neuroimaging findings and clinical implications. *Nat Rev Neurosci* **12**: 652-669.

Gopinath K, Maltbie E, Urushino N, Kempf D, Howell L (2016). Ketamine-induced changes in connectivity of functional brain networks in awake female nonhuman primates: a translational functional imaging model. *Psychopharmacology (Berl)* **233**: 3673-3684.

Goya-Maldonado R, Brodmann K, Keil M, Trost S, Dechent P, Gruber O (2016). Differentiating unipolar and bipolar depression by alterations in large-scale brain networks. *Hum Brain Mapp* **37**: 808-818.

Gozzi A, Schwarz A, Crestan V, Bifone A (2008). Drug-anaesthetic interaction in phMRI: the case of the psychotomimetic agent phencyclidine. *Magn Reson Imaging* **26**: 999-1006.

Greicius MD, Flores BH, Menon V, Glover GH, Solvason HB, Kenna H, et al. (2007). Resting-state functional connectivity in major depression: abnormally increased contributions from subgenual cingulate cortex and thalamus. *Biol Psychiatry* **62**: 429-437.

Grimm O, Gass N, Weber-Fahr W, Sartorius A, Schenker E, Spedding M, et al. (2015). Acute ketamine challenge increases resting state prefrontal-hippocampal connectivity in both humans and rats. *Psychopharmacology (Berl)* **232**: 4231-4241.

Gu H, Salmeron BJ, Ross TJ, Geng X, Zhan W, Stein EA, et al. (2010). Mesocorticolimbic circuits are impaired in chronic cocaine users as demonstrated by resting-state functional connectivity. *Neuroimage* **53**: 593-601.

Guo S, Kendrick KM, Zhang J, Broome M, Yu R, Liu Z, et al. (2013). Brain-wide functional inter-hemispheric disconnection is a potential biomarker for schizophrenia and distinguishes it from depression. *Neuroimage Clin* **2**: 818-826.

Gusnard DA, Raichle ME, Raichle ME (2001). Searching for a baseline: functional imaging and the resting human brain. *Nat Rev Neurosci* **2**: 685-694.

Haas DA, Harper DG (1992). Ketamine: a review of its pharmacologic properties and use in ambulatory anesthesia. *Anesth Prog* **39**: 61-68.

Haber SN (2003). The primate basal ganglia: parallel and integrative networks. *J Chem Neuroanat* **26**: 317-330.

Haber SN, Knutson B (2010). The reward circuit: linking primate anatomy and human imaging. *Neuropsychopharmacology* **35**: 4-26.

Hadley JA, Nenert R, Kraguljac NV, Bolding MS, White DM, Skidmore FM, et al. (2014). Ventral tegmental area/midbrain functional connectivity and response to antipsychotic medication in schizophrenia. *Neuropsychopharmacology* **39**: 1020-1030.

Haensel JX, Spain A, Martin C (2015). A systematic review of physiological methods in rodent pharmacological MRI studies. *Psychopharmacology (Berl)* **232**: 489-499.

Hakami T, Jones NC, Tolmacheva EA, Gaudias J, Chaumont J, Salzberg M, et al. (2009). NMDA receptor hypofunction leads to generalized and persistent aberrant gamma oscillations independent of hyperlocomotion and the state of consciousness. *PLoS one* **4**: e6755.

Hanlon CA, DeVries W, Dowdle LT, West JA, Siekman B, Li X, et al. (2015a). A comprehensive study of sensorimotor cortex excitability in chronic cocaine users: Integrating TMS and functional MRI data. *Drug Alcohol Depend* **157**: 28-35.

Hanlon CA, Dowdle LT, Austelle CW, DeVries W, Mithoefer O, Badran BW, et al. (2015b). What goes up, can come down: Novel brain stimulation paradigms may attenuate craving and craving-related neural circuitry in substance dependent individuals. *Brain Res* **1628**: 199-209.

Hanlon CA, Dowdle LT, Moss H, Canterberry M, George MS (2016). Mobilization of Medial and Lateral Frontal-Striatal Circuits in Cocaine Users and Controls: An Interleaved TMS/BOLD Functional Connectivity Study. *Neuropsychopharmacology* **41**: 3032-3041.

Hasin DS, O'Brien CP, Auriacombe M, Borges G, Bucholz K, Budney A, et al. (2013). DSM-5 criteria for substance use disorders: recommendations and rationale. *Am J Psychiatry* **170**: 834-851.

Henry PK, Murnane KS, Votaw JR, Howell LL (2010). Acute brain metabolic effects of cocaine in rhesus monkeys with a history of cocaine use. *Brain Imaging Behav* **4**: 212-219.

Hodkinson DJ, de Groote C, McKie S, Deakin JF, Williams SR (2012). Differential Effects of Anaesthesia on the phMRI Response to Acute Ketamine Challenge. *Br J Med Med Res* **2**: 373-385.

Holcomb HH, Lahti AC, Medoff DR, Weiler M, Tamminga CA (2001). Sequential regional cerebral blood flow brain scans using PET with H<sub>2</sub>(15)O demonstrate ketamine actions in CNS dynamically. *Neuropsychopharmacology* **25**: 165-172.

Homayoun H, Moghaddam B (2007). NMDA receptor hypofunction produces opposite effects on prefrontal cortex interneurons and pyramidal neurons. *J Neurosci* **27**: 11496-11500.

Howell LL, Cunningham KA (2015). Serotonin 5-HT<sub>2</sub> receptor interactions with dopamine function: implications for therapeutics in cocaine use disorder. *Pharmacol Rev* **67**: 176-197.

Howell LL, Fantegrossi WE (2009). Intravenous Drug Self-Administration in Nonhuman Primates. In *Methods of Behavior Analysis in Neuroscience*. ed Buccafusco J.J.: Boca Raton (FL).

Hu Y, Salmeron BJ, Gu H, Stein EA, Yang Y (2015). Impaired functional connectivity within and between frontostriatal circuits and its association with compulsive drug use and trait impulsivity in cocaine addiction. *JAMA Psychiatry* **72**: 584-592.

Hudetz AG (2012). General anesthesia and human brain connectivity. *Brain Connect* **2**: 291-302.

Hutchison RM, Gallivan JP, Culham JC, Gati JS, Menon RS, Everling S (2012). Functional connectivity of the frontal eye fields in humans and macaque monkeys investigated with resting-state fMRI. *J Neurophysiol* **107**: 2463-2474.

Jentsch JD, Taylor JR (1999). Impulsivity resulting from frontostriatal dysfunction in drug abuse: implications for the control of behavior by reward-related stimuli. *Psychopharmacology (Berl)* **146**: 373-390.

Johansen-Berg H, Gutman DA, Behrens TE, Matthews PM, Rushworth MF, Katz E, et al. (2008). Anatomical connectivity of the subgenual cingulate region targeted with deep brain stimulation for treatment-resistant depression. *Cereb Cortex* **18**: 1374-1383.

Joules R, Doyle OM, Schwarz AJ, O'Daly OG, Brammer M, Williams SC, et al. (2015). Ketamine induces a robust whole-brain connectivity pattern that can be differentially modulated by drugs of different mechanism and clinical profile. *Psychopharmacology (Berl)*.

Kalivas PW (2009). The glutamate homeostasis hypothesis of addiction. *Nat Rev Neurosci* **10**: 561-572.

Kalivas PW, O'Brien C (2008). Drug addiction as a pathology of staged neuroplasticity. *Neuropsychopharmacology* **33**: 166-180.

Kalivas PW, Volkow N, Seamans J (2005). Unmanageable motivation in addiction: a pathology in prefrontal-accumbens glutamate transmission. *Neuron* **45**: 647-650.

Kalivas PW, Volkow ND (2011). New medications for drug addiction hiding in glutamatergic neuroplasticity. *Mol Psychiatry* **16**: 974-986.

Kasanetz F, Deroche-Gamonet V, Berson N, Balado E, Lafourcade M, Manzoni O, et al. (2010). Transition to addiction is associated with a persistent impairment in synaptic plasticity. *Science* **328**: 1709-1712.



Katz JL,Higgins ST (2003). The validity of the reinstatement model of craving and relapse to drug use. *Psychopharmacology (Berl)* **168**: 21-30.

Kavalali ET,Monteggia LM (2012). Synaptic mechanisms underlying rapid antidepressant action of ketamine. *Am J Psychiatry* **169**: 1150-1156.

Kay SR, Fiszbein A,Opler LA (1987). The positive and negative syndrome scale (PANSS) for schizophrenia. *Schizophr Bull* **13**: 261-276.

Khalili-Mahani N, Niesters M, van Osch MJ, Oitzl M, Veer I, de Rooij M, et al. (2015). Ketamine interactions with biomarkers of stress: a randomized placebo-controlled repeated measures resting-state fMRI and PCASL pilot study in healthy men. *Neuroimage* **108**: 396-409.

Kim SF, Huang AS, Snowman AM, Teuscher C,Snyder SH (2007). From the Cover: Antipsychotic drug-induced weight gain mediated by histamine H1 receptor-linked activation of hypothalamic AMP-kinase. *Proc Natl Acad Sci U S A* **104**: 3456-3459.

King JA, Garelick TS, Brevard ME, Chen W, Messenger TL, Duong TQ, et al. (2005). Procedure for minimizing stress for fMRI studies in conscious rats. *J Neurosci Methods* **148**: 154-160.

Kirkland Henry P, Davis M,Howell LL (2009). Effects of cocaine self-administration history under limited and extended access conditions on in vivo striatal dopamine neurochemistry and acoustic startle in rhesus monkeys. *Psychopharmacology (Berl)* **205**: 237-247.

Koenigs M,Grafman J (2009). The functional neuroanatomy of depression: distinct roles for ventromedial and dorsolateral prefrontal cortex. *Behav Brain Res* **201**: 239-243.

Komossa K, Rummel-Kluge C, Schwarz S, Schmid F, Hunger H, Kissling W, et al. (2011). Risperidone versus other atypical antipsychotics for schizophrenia. *Cochrane Database Syst Rev*: CD006626.

Koob GF,Volkow ND (2010). Neurocircuitry of addiction. *Neuropsychopharmacology* **35**: 217-238.

Kopelowicz A, Ventura J, Liberman RP, Mintz J (2008). Consistency of Brief Psychiatric Rating Scale factor structure across a broad spectrum of schizophrenia patients. *Psychopathology* **41**: 77-84.

Kraguljac NV, White DM, Hadley JA, Visscher K, Knight D, Ver Hoef L, et al. (2016). Abnormalities in large scale functional networks in unmedicated patients with schizophrenia and effects of risperidone. *Neuroimage Clin* **10**: 146-158.

Krystal JH, D'Souza DC, Karper LP, Bennett A, Abi-Dargham A, Abi-Saab D, et al. (1999). Interactive effects of subanesthetic ketamine and haloperidol in healthy humans. *Psychopharmacology (Berl)* **145**: 193-204.

Krystal JH, Karper LP, Seibyl JP, Freeman GK, Delaney R, Bremner JD, et al. (1994). Subanesthetic effects of the noncompetitive NMDA antagonist, ketamine, in humans. Psychotomimetic, perceptual, cognitive, and neuroendocrine responses. *Arch Gen Psychiatry* **51**: 199-214.

Krystal JH, Sanacora G, Duman RS (2013). Rapid-acting glutamatergic antidepressants: the path to ketamine and beyond. *Biol Psychiatry* **73**: 1133-1141.

Langsjo JW, Kaisti KK, Aalto S, Hinkka S, Aantaa R, Oikonen V, et al. (2003). Effects of subanesthetic doses of ketamine on regional cerebral blood flow, oxygen consumption, and blood volume in humans. *Anesthesiology* **99**: 614-623.

Langsjo JW, Salmi E, Kaisti KK, Aalto S, Hinkka S, Aantaa R, et al. (2004). Effects of subanesthetic ketamine on regional cerebral glucose metabolism in humans. *Anesthesiology* **100**: 1065-1071.

Leslie RA, James MF (2000). Pharmacological magnetic resonance imaging: a new application for functional MRI. *Trends Pharmacol Sci* **21**: 314-318.

Lewis DA, Liberman JA (2000). Catching up on schizophrenia: natural history and neurobiology. *Neuron* **28**: 325-334.

Li N, Lee B, Liu RJ, Banasr M, Dwyer JM, Iwata M, et al. (2010). mTOR-dependent synapse formation underlies the rapid antidepressant effects of NMDA antagonists. *Science* **329**: 959-964.

Lodge D, Mercier MS (2015). Ketamine and phencyclidine: the good, the bad and the unexpected. *Br J Pharmacol* **172**: 4254-4276.

Lorrain DS, Baccei CS, Bristow LJ, Anderson JJ, Varney MA (2003). Effects of ketamine and N-methyl-D-aspartate on glutamate and dopamine release in the rat prefrontal cortex: modulation by a group II selective metabotropic glutamate receptor agonist LY379268. *Neuroscience* **117**: 697-706.

Luckenbaugh DA, Niciu MJ, Ionescu DF, Nolan NM, Richards EM, Brutsche NE, et al. (2014). Do the dissociative side effects of ketamine mediate its antidepressant effects? *J Affect Disord* **159**: 56-61.

Lv Q, Yang L, Li G, Wang Z, Shen Z, Yu W, et al. (2016). Large-Scale Persistent Network Reconfiguration Induced by Ketamine in Anesthetized Monkeys: Relevance to Mood Disorders. *Biol Psychiatry* **79**: 765-775.

Ma Y (2015). Neuropsychological mechanism underlying antidepressant effect: a systematic meta-analysis. *Mol Psychiatry* **20**: 311-319.

Maeng S, Zarate CA, Jr., Du J, Schloesser RJ, McCammon J, Chen G, et al. (2008). Cellular mechanisms underlying the antidepressant effects of ketamine: role of alpha-amino-3-hydroxy-5-methylisoxazole-4-propionic acid receptors. *Biol Psychiatry* **63**: 349-352.

Maltbie E, Gopinath K, Urushino N, Kempf D, Howell L (2016). Ketamine-induced brain activation in awake female nonhuman primates: a translational functional imaging model. *Psychopharmacology (Berl)* **233**: 961-972.

Martin M, Chen BT, Hopf FW, Bowers MS, Bonci A (2006). Cocaine self-administration selectively abolishes LTD in the core of the nucleus accumbens. *Nat Neurosci* **9**: 868-869.

Mason OJ, Morgan CJ, Stefanovic A, Curran HV (2008). The psychotomimetic states inventory (PSI): measuring psychotic-type experiences from ketamine and cannabis. *Schizophr Res* **103**: 138-142.

Mayberg HS (2003). Modulating dysfunctional limbic-cortical circuits in depression: towards development of brain-based algorithms for diagnosis and optimised treatment. *Br Med Bull* **65**: 193-207.

Mayberg HS, Lozano AM, Voon V, McNeely HE, Seminowicz D, Hamani C, et al. (2005). Deep brain stimulation for treatment-resistant depression. *Neuron* **45**: 651-660.

McGregor KM, Sudhyadhom A, Nocera J, Seff A, Crosson B, Butler AJ (2015). Reliability of negative BOLD in ipsilateral sensorimotor areas during unimanual task activity. *Brain Imaging Behav* **9**: 245-254.

McLellan AT, Lewis DC, O'Brien CP, Kleber HD (2000). Drug dependence, a chronic medical illness: implications for treatment, insurance, and outcomes evaluation. *JAMA* **284**: 1689-1695.

Meltzer HY, McGurk SR (1999). The effects of clozapine, risperidone, and olanzapine on cognitive function in schizophrenia. *Schizophr Bull* **25**: 233-255.

Meyer-Lindenberg A (2010). From maps to mechanisms through neuroimaging of schizophrenia. *Nature* **468**: 194-202.

Meyer-Lindenberg A, Poline JB, Kohn PD, Holt JL, Egan MF, Weinberger DR, et al. (2001). Evidence for abnormal cortical functional connectivity during working memory in schizophrenia. *Am J Psychiatry* **158**: 1809-1817.

Meyer-Lindenberg AS, Olsen RK, Kohn PD, Brown T, Egan MF, Weinberger DR, et al. (2005). Regionally specific disturbance of dorsolateral prefrontal-hippocampal functional connectivity in schizophrenia. *Arch Gen Psychiatry* **62**: 379-386.

Minzenberg MJ, Laird AR, Thelen S, Carter CS, Glahn DC (2009). Meta-analysis of 41 functional neuroimaging studies of executive function in schizophrenia. *Arch Gen Psychiatry* **66**: 811-822.

Miyamoto S, Duncan GE, Marx CE, Lieberman JA (2005). Treatments for schizophrenia: a critical review of pharmacology and mechanisms of action of antipsychotic drugs. *Mol Psychiatry* **10**: 79-104.

Moffett K, Crosson B, Spence JS, Case K, Levy I, Gopinath K, et al. (2015). Word-finding impairment in veterans of the 1991 Persian Gulf War. *Brain Cogn* **98**: 65-73.

Moghaddam B, Adams B, Verma A, Daly D (1997). Activation of glutamatergic neurotransmission by ketamine: a novel step in the pathway from NMDA receptor blockade to dopaminergic and cognitive disruptions associated with the prefrontal cortex. *J Neurosci* **17**: 2921-2927.

Montgomery SA, Asberg M (1979). A new depression scale designed to be sensitive to change. *Br J Psychiatry* **134**: 382-389.

Morgan CJ, Curran HV, Independent Scientific Committee on D (2012). Ketamine use: a review. *Addiction* **107**: 27-38.

Morgan CJ, Perry EB, Cho HS, Krystal JH, D'Souza DC (2006). Greater vulnerability to the amnestic effects of ketamine in males. *Psychopharmacology (Berl)* **187**: 405-414.

Muly EC, Votaw JR, Ritchie J, Howell LL (2012). Relationship between dose, drug levels, and D2 receptor occupancy for the atypical antipsychotics risperidone and paliperidone. *J Pharmacol Exp Ther* **341**: 81-89.

Murnane KS, Gopinath KS, Maltbie E, Daunais JB, Telesford QK, Howell LL (2015). Functional connectivity in frontal-striatal brain networks and cocaine self-administration in female rhesus monkeys. *Psychopharmacology (Berl)* **232**: 745-754.

Murnane KS, Howell LL (2010). Development of an apparatus and methodology for conducting functional magnetic resonance imaging (fMRI) with pharmacological stimuli in conscious rhesus monkeys. *J Neurosci Methods* **191**: 11-20.

Murnane KS, Winschel J, Schmidt KT, Stewart LM, Rose SJ, Cheng K, et al. (2013). Serotonin 2A receptors differentially contribute to abuse-related effects of cocaine and cocaine-induced nigrostriatal and mesolimbic dopamine overflow in nonhuman primates. *J Neurosci* **33**: 13367-13374.

Murrough JW, Iosifescu DV, Chang LC, Al Jurdi RK, Green CE, Perez AM, et al. (2013). Antidepressant efficacy of ketamine in treatment-resistant major depression: a two-site randomized controlled trial. *Am J Psychiatry* **170**: 1134-1142.

Nader MA, Daunais JB, Moore T, Nader SH, Moore RJ, Smith HR, et al. (2002). Effects of cocaine self-administration on striatal dopamine systems in rhesus monkeys: initial and chronic exposure. *Neuropsychopharmacology* **27**: 35-46.

Nic Dhonnchadha BA, Fox RG, Stutz SJ, Rice KC, Cunningham KA (2009). Blockade of the serotonin 5-HT<sub>2A</sub> receptor suppresses cue-evoked reinstatement of cocaine-seeking behavior in a rat self-administration model. *Behav Neurosci* **123**: 382-396.

Nyberg S, Farde L, Eriksson L, Halldin C, Eriksson B (1993). 5-HT<sub>2</sub> and D<sub>2</sub> dopamine receptor occupancy in the living human brain. A PET study with risperidone. *Psychopharmacology (Berl)* **110**: 265-272.

Ochsner KN, Gross JJ (2005). The cognitive control of emotion. *Trends Cogn Sci* **9**: 242-249.

Olney JW, Farber NB (1995). Glutamate receptor dysfunction and schizophrenia. *Arch Gen Psychiatry* **52**: 998-1007.

Ongur D, Lundy M, Greenhouse I, Shinn AK, Menon V, Cohen BM, et al. (2010). Default mode network abnormalities in bipolar disorder and schizophrenia. *Psychiatry Res* **183**: 59-68.

Opler LA, Opler MG, Arnsten AF (2016). Ameliorating treatment-refractory depression with intranasal ketamine: potential NMDA receptor actions in the pain circuitry representing mental anguish. *CNS Spectr* **21**: 12-22.

Papp M, Gruca P, Lason-Tyburkiewicz M, Willner P (2017). Antidepressant, anxiolytic and procognitive effects of subacute and chronic ketamine in the chronic mild stress model of depression. *Behav Pharmacol* **28**: 1-8.

Paxinos G, Huang XF, Toga AW (2000) *The rhesus monkey brain in stereotaxic coordinates*. Academic Press: San Diego, CA.

Perry EB, Jr., Cramer JA, Cho HS, Petrakis IL, Karper LP, Genovese A, et al. (2007). Psychiatric safety of ketamine in psychopharmacology research. *Psychopharmacology (Berl)* **192**: 253-260.

Phillips KA, Bales KL, Capitanio JP, Conley A, Czoty PW, t Hart BA, et al. (2014). Why primate models matter. *Am J Primatol* **76**: 801-827.

Phillips ML, Swartz HA (2014). A critical appraisal of neuroimaging studies of bipolar disorder: toward a new conceptualization of underlying neural circuitry and a road map for future research. *Am J Psychiatry* **171**: 829-843.

Pitts EG, Taylor JR, Gourley SL (2016). Prefrontal cortical BDNF: A regulatory key in cocaine- and food-reinforced behaviors. *Neurobiol Dis* **91**: 326-335.

Porrino LJ, Smith HR, Nader MA, Beveridge TJ (2007). The effects of cocaine: a shifting target over the course of addiction. *Prog Neuropsychopharmacol Biol Psychiatry* **31**: 1593-1600.

Power JD, Barnes KA, Snyder AZ, Schlaggar BL, Petersen SE (2012). Spurious but systematic correlations in functional connectivity MRI networks arise from subject motion. *Neuroimage* **59**: 2142-2154.

Preskorn SH, Baker B, Kolluri S, Menniti FS, Krams M, Landen JW (2008). An innovative design to establish proof of concept of the antidepressant effects of the NR2B subunit selective N-methyl-D-aspartate antagonist, CP-101,606, in patients with treatment-refractory major depressive disorder. *J Clin Psychopharmacol* **28**: 631-637.

Preuss TM (1995). Do rats have prefrontal cortex? The rose-woolsey-akert program reconsidered. *J Cogn Neurosci* **7**: 1-24.

Price RB, Mathew SJ (2015). Does ketamine have anti-suicidal properties? Current status and future directions. *CNS Drugs* **29**: 181-188.

Reinstatler L, Youssef NA (2015). Ketamine as a potential treatment for suicidal ideation: a systematic review of the literature. *Drugs R D* **15**: 37-43.

Rohlfing T, Kroenke CD, Sullivan EV, Dubach MF, Bowden DM, Grant KA, et al. (2012). The INIA19 Template and NeuroMaps Atlas for Primate Brain Image Parcellation and Spatial Normalization. *Front Neuroinform* **6**: 27.

Rotarska-Jagiela A, van de Ven V, Oertel-Knochel V, Uhlhaas PJ, Vogeley K, Linden DE (2010). Resting-state functional network correlates of psychotic symptoms in schizophrenia. *Schizophr Res* **117**: 21-30.

Rowland LM (2005). Subanesthetic ketamine: how it alters physiology and behavior in humans. *Aviat Space Environ Med* **76**: C52-58.

Saad ZS, Gotts SJ, Murphy K, Chen G, Jo HJ, Martin A, et al. (2012). Trouble at rest: how correlation patterns and group differences become distorted after global signal regression. *Brain Connect* **2**: 25-32.

Saland SK, Duclot F, Kabbaj M (2017). Integrative analysis of sex differences in the rapid antidepressant effects of ketamine in preclinical models for individualized clinical outcomes. *Curr Opin Behav Sci* **14**: 19-26.

Salvadore G, Cornwell BR, Colon-Rosario V, Coppola R, Grillon C, Zarate CA, Jr., et al. (2009). Increased anterior cingulate cortical activity in response to fearful faces: a neurophysiological biomarker that predicts rapid antidepressant response to ketamine. *Biol Psychiatry* **65**: 289-295.

Salvadore G, Cornwell BR, Sambataro F, Latov D, Colon-Rosario V, Carver F, et al. (2010). Anterior cingulate desynchronization and functional connectivity with the amygdala during a working memory task predict rapid antidepressant response to ketamine. *Neuropsychopharmacology* **35**: 1415-1422.

Sanacora G, Frye MA, McDonald W, Mathew SJ, Turner MS, Schatzberg AF, et al. (2017). A Consensus Statement on the Use of Ketamine in the Treatment of Mood Disorders. *JAMA Psychiatry* **74**: 399-405.

Sarpal DK, Argyelan M, Robinson DG, Szeszko PR, Karlsgodt KH, John M, et al. (2016). Baseline Striatal Functional Connectivity as a Predictor of Response to Antipsychotic Drug Treatment. *Am J Psychiatry* **173**: 69-77.

Sarpal DK, Robinson DG, Lencz T, Argyelan M, Ikuta T, Karlsgodt K, et al. (2015). Antipsychotic treatment and functional connectivity of the striatum in first-episode schizophrenia. *JAMA Psychiatry* **72**: 5-13.

Sawyer EK, Mun J, Nye JA, Kimmel HL, Voll RJ, Stehouwer JS, et al. (2012). Neurobiological changes mediating the effects of chronic fluoxetine on cocaine use. *Neuropsychopharmacology* **37**: 1816-1824.

Schak KM, Vande Voort JL, Johnson EK, Kung S, Leung JG, Rasmussen KG, et al. (2016). Potential Risks of Poorly Monitored Ketamine Use in Depression Treatment. *Am J Psychiatry* **173**: 215-218.

Schmechtig A, Lees J, Perkins A, Altavilla A, Craig KJ, Dawson GR, et al. (2013). The effects of ketamine and risperidone on eye movement control in healthy volunteers. *Transl Psychiatry* **3**: e334.

Schmid RL, Sandler AN, Katz J (1999). Use and efficacy of low-dose ketamine in the management of acute postoperative pain: a review of current techniques and outcomes. *Pain* **82**: 111-125.



Schwartzman RJ, Alexander GM, Grothusen JR, Paylor T, Reichenberger E, Perreault M (2009). Outpatient intravenous ketamine for the treatment of complex regional pain syndrome: a double-blind placebo controlled study. *Pain* **147**: 107-115.

Shaffer CL, Osgood SM, Smith DL, Liu J, Trapa PE (2014). Enhancing ketamine translational pharmacology via receptor occupancy normalization. *Neuropharmacology* **86**: 174-180.

Shively CA, Willard SL (2012). Behavioral and neurobiological characteristics of social stress versus depression in nonhuman primates. *Exp Neurol* **233**: 87-94.

Simon AB, Buxton RB (2015). Understanding the dynamic relationship between cerebral blood flow and the BOLD signal: Implications for quantitative functional MRI. *Neuroimage* **116**: 158-167.

Singh JB, Fedgchin M, Daly EJ, De Boer P, Cooper K, Lim P, et al. (2016). A Double-Blind, Randomized, Placebo-Controlled, Dose-Frequency Study of Intravenous Ketamine in Patients With Treatment-Resistant Depression. *Am J Psychiatry* **173**: 816-826.

Skoblenick K, Everling S (2012). NMDA antagonist ketamine reduces task selectivity in macaque dorsolateral prefrontal neurons and impairs performance of randomly interleaved prosaccades and antisaccades. *J Neurosci* **32**: 12018-12027.

Smith SM, Jenkinson M, Woolrich MW, Beckmann CF, Behrens TE, Johansen-Berg H, et al. (2004). Advances in functional and structural MR image analysis and implementation as FSL. *Neuroimage* **23 Suppl 1**: S208-219.

Steward CA, Marsden CA, Prior MJ, Morris PG, Shah YB (2005). Methodological considerations in rat brain BOLD contrast pharmacological MRI. *Psychopharmacology (Berl)* **180**: 687-704.

Stone JM (2011). Glutamatergic antipsychotic drugs: a new dawn in the treatment of schizophrenia? *Ther Adv Psychopharmacol* **1**: 5-18.

Strous RD, Maayan R, Lapidus R, Stryjer R, Lustig M, Kotler M, et al. (2003). Dehydroepiandrosterone augmentation in the management of negative, depressive, and anxiety symptoms in schizophrenia. *Arch Gen Psychiatry* **60**: 133-141.

Takahata R, Moghaddam B (2003). Activation of glutamate neurotransmission in the prefrontal cortex sustains the motoric and dopaminergic effects of phencyclidine. *Neuropsychopharmacology* **28**: 1117-1124.

Thompson SM, Kallarackal AJ, Kvarata MD, Van Dyke AM, LeGates TA, Cai X (2015). An excitatory synapse hypothesis of depression. *Trends Neurosci* **38**: 279-294.

van den Buuse M, Mingon RL, Gogos A (2015). Chronic estrogen and progesterone treatment inhibits ketamine-induced disruption of prepulse inhibition in rats. *Neurosci Lett* **607**: 72-76.

Veilleux-Lemieux D, Castel A, Carrier D, Beaudry F, Vachon P (2013). Pharmacokinetics of ketamine and xylazine in young and old Sprague-Dawley rats. *J Am Assoc Lab Anim Sci* **52**: 567-570.

Verma A, Moghaddam B (1996). NMDA receptor antagonists impair prefrontal cortex function as assessed via spatial delayed alternation performance in rats: modulation by dopamine. *J Neurosci* **16**: 373-379.

Volkow ND, Fowler JS, Wolf AP, Schlyer D, Shiue CY, Alpert R, et al. (1990). Effects of chronic cocaine abuse on postsynaptic dopamine receptors. *Am J Psychiatry* **147**: 719-724.

Volkow ND, Swanson JM (2003). Variables that affect the clinical use and abuse of methylphenidate in the treatment of ADHD. *Am J Psychiatry* **160**: 1909-1918.

Volkow ND, Tomasi D, Wang GJ, Fowler JS, Telang F, Goldstein RZ, et al. (2011). Reduced metabolism in brain "control networks" following cocaine-cues exposure in female cocaine abusers. *PloS one* **6**: e16573.

Volkow ND, Wang GJ, Fischman MW, Foltin RW, Fowler JS, Abumrad NN, et al. (1997). Relationship between subjective effects of cocaine and dopamine transporter occupancy. *Nature* **386**: 827-830.

Volkow ND, Wang GJ, Fowler JS, Telang F (2008a). Overlapping neuronal circuits in addiction and obesity: evidence of systems pathology. *Philos Trans R Soc Lond B Biol Sci* **363**: 3191-3200.

Volkow ND, Wang GJ, Fowler JS, Tomasi D (2012). Addiction circuitry in the human brain. *Annu Rev Pharmacol Toxicol* **52**: 321-336.

Volkow ND, Wang GJ, Telang F, Fowler JS, Logan J, Childress AR, et al. (2008b). Dopamine increases in striatum do not elicit craving in cocaine abusers unless they are coupled with cocaine cues. *Neuroimage* **39**: 1266-1273.

Vollenweider FX, Leenders KL, Scharfetter C, Antonini A, Maguire P, Missimer J, et al. (1997). Metabolic hyperfrontality and psychopathology in the ketamine model of psychosis using positron emission tomography (PET) and [18F]fluorodeoxyglucose (FDG). *Eur Neuropsychopharmacol* **7**: 9-24.

Vollenweider FX, Vontobel P, Oye I, Hell D, Leenders KL (2000). Effects of (S)-ketamine on striatal dopamine: a [11C]raclopride PET study of a model psychosis in humans. *J Psychiatr Res* **34**: 35-43.

Wan LB, Levitch CF, Perez AM, Brallier JW, Iosifescu DV, Chang LC, et al. (2015). Ketamine safety and tolerability in clinical trials for treatment-resistant depression. *J Clin Psychiatry* **76**: 247-252.

Wang HX, Gao WJ (2009). Cell type-specific development of NMDA receptors in the interneurons of rat prefrontal cortex. *Neuropsychopharmacology* **34**: 2028-2040.

Wang HX, Gao WJ (2012). Prolonged exposure to NMDAR antagonist induces cell-type specific changes of glutamatergic receptors in rat prefrontal cortex. *Neuropharmacology* **62**: 1808-1822.

Wang M, Arnsten AF (2015). Contribution of NMDA receptors to dorsolateral prefrontal cortical networks in primates. *Neurosci Bull* **31**: 191-197.

Wang M, Yang Y, Wang CJ, Gamo NJ, Jin LE, Mazer JA, et al. (2013). NMDA receptors subserve persistent neuronal firing during working memory in dorsolateral prefrontal cortex. *Neuron* **77**: 736-749.

Weiser M, Heresco-Levy U, Davidson M, Javitt DC, Werbeloff N, Gershon AA, et al. (2012). A multicenter, add-on randomized controlled trial of low-dose d-serine for negative and cognitive symptoms of schizophrenia. *J Clin Psychiatry* **73**: e728-734.

Wessa M, Kanske P, Linke J (2014). Bipolar disorder: a neural network perspective on a disorder of emotion and motivation. *Restor Neurol Neurosci* **32**: 51-62.

Wilcox KM, Kimmel HL, Lindsey KP, Votaw JR, Goodman MM, Howell LL (2005). In vivo comparison of the reinforcing and dopamine transporter effects of local anesthetics in rhesus monkeys. *Synapse* **58**: 220-228.

Willner P, Belzung C (2015). Treatment-resistant depression: are animal models of depression fit for purpose? *Psychopharmacology (Berl)* **232**: 3473-3495.

Wood J, Kim Y, Moghaddam B (2012). Disruption of prefrontal cortex large scale neuronal activity by different classes of psychotomimetic drugs. *J Neurosci* **32**: 3022-3031.

Woodward ND, Rogers B, Heckers S (2011). Functional resting-state networks are differentially affected in schizophrenia. *Schizophr Res* **130**: 86-93.

Yang C, Shirayama Y, Zhang JC, Ren Q, Yao W, Ma M, et al. (2015). R-ketamine: a rapid-onset and sustained antidepressant without psychotomimetic side effects. *Transl Psychiatry* **5**: e632.

Yang SY, Hong CJ, Huang YH, Tsai SJ (2010). The effects of glycine transporter I inhibitor, N-methylglycine (sarcosine), on ketamine-induced alterations in sensorimotor gating and regional brain c-Fos expression in rats. *Neurosci Lett* **469**: 127-130.

Young E, Korszun A (2010). Sex, trauma, stress hormones and depression. *Mol Psychiatry* **15**: 23-28.

Zanos P, Moaddel R, Morris PJ, Georgiou P, Fischell J, Elmer GI, et al. (2016). NMDAR inhibition-independent antidepressant actions of ketamine metabolites. *Nature* **533**: 481-486.

Zarate CA, Jr., Brutsche N, Laje G, Luckenbaugh DA, Venkata SL, Ramamoorthy A, et al. (2012). Relationship of ketamine's plasma metabolites with response, diagnosis, and side effects in major depression. *Biol Psychiatry* **72**: 331-338.

Zarate CA, Jr., Singh JB, Carlson PJ, Brutsche NE, Ameli R, Luckenbaugh DA, et al. (2006). A randomized trial of an N-methyl-D-aspartate antagonist in treatment-resistant major depression. *Arch Gen Psychiatry* **63**: 856-864.

Zhang J, Kendrick KM, Lu G, Feng J (2015). The Fault Lies on the Other Side: Altered Brain Functional Connectivity in Psychiatric Disorders is Mainly Caused by Counterpart Regions in the Opposite Hemisphere. *Cereb Cortex* **25**: 3475-3486.

Zhang JC, Li SX, Hashimoto K (2014). R (-)-ketamine shows greater potency and longer lasting antidepressant effects than S (+)-ketamine. *Pharmacol Biochem Behav* **116**: 137-141.